COLONY VARIATION IN *BURKHOLDERIA PSEUDOMALLEI*: A STRATEGY FOR HYPOXIC GROWTH AND PERSISTENT GASTRIC COLONIZATION

by

CHAD R. AUSTIN

B.S. Seattle Pacific University, 2006

A thesis submitted to the

Faculty of the Graduate School of the

University of Colorado in partial fulfillment

of the requirements for the degree of

Doctor of Philosophy

Microbiology Program

2014

This thesis for the Doctor of Philosophy degree by

Chad R. Austin

has been approved for the

Microbiology Program

by

Michael Schurr, Chair

Martin Voskuil, Mentor

Randall Holmes

Andrés Vazquez-Torres

Steven Dow

Date 02/21/2014

Austin, Chad R. (Ph.D., Microbiology)

Colony Variation in *Burkholderia pseudomallei*: A Strategy for Hypoxic Growth and Persistent Gastric Colonization

Thesis directed by Associate Professor Martin I. Voskuil.

ABSTRACT

Burkholderia pseudomallei is well known for its diverse colony morphologies when recovered from infected patients. We have observed that inhibition of aerobic respiration shifted populations of *B. pseudomallei* from the canonical white colony morphotype toward two distinct, reversible, yet relatively stable yellow colony variants that are referred to here as YA and YB. The yellow variants contrasted dramatically with the white form (WHT). They exhibited alternative cellular physiology in stationary phase, including gross cellular physiology, divergent gene expression profiles, production of unique excreted compounds, and excretion of a toxic substance. Most importantly, yellow variants exhibited a competitive advantage under hypoxic conditions and alkalized cultures without production of ammonia.

Since hypoxia and acidity are key characteristics of the gastric niche environment, we tested the ability of yellow variants to colonize the stomach using a *B. pseudomallei* persistent gastric colonization model. Virulence studies demonstrated that the YB variant, although attenuated in acute virulence, was the only form that colonized and persisted in the stomach. DNA staining of gastric *B. pseudomallei* YB colonies demonstrated the bacteria were associated with extracellular DNA. Furthermore, we developed an *in vitro* model that mimicked the gastric microenvironment. Investigation of YB in this *in vitro* stomach model demonstrated that the variant forms, but not the parental form produced

large amounts of extracellular DNA without indication of cell lysis. The YA and YB variants were also much more resistant to acid stress in the gastric model than the parental form. These data demonstrate that the YB variant is a unique form specifically adapted to the harsh gastric environment and necessary for persistent colonization.

Transposon mutagenesis identified a transcriptional regulator (BPSL1887) that, when overexpressed, produced a yellow colony morphology, as well as the media alkalization and eDNA production phenotypes. Deletion of *bpsl1887* stopped the shift of the white form to yellow forms under normally permissive conditions, and ablated expression of the other phenotypes. Overexpression of BPSL1887 in either a wild type or deletion background yielded colonies with yellow morphology as well as expression of the media alkalization and eDNA production phenotypes. In addition to results of the transposon mutagenesis, no genetic mutations were observed in the YA and YB forms as determined by whole genome sequencing. Taken together, these two observations suggest a model for control of colony variation in *B. pseudomallei*. We propose that BPSL1887 (YelR) is a master regulator of the various phenotypes associated with yellow colony variation and the epigenetic maintenance of the yellow colony forms.

The form and content of this abstract are approved. I recommend this publication

Approved: Martin I. Voskuil

ACKNOWLEDGEMENTS

It has been said before and I will say it again, we who push the boundaries of human understanding do so from the shoulders of giants. In acknowledgement of the giants - both intellectual and industrious I bow my head. Without the dedication and insight of innumerable individuals this work would have been impossible. From the Doctors Whitmore and Krishnaswamy - discoverers of the disease and the etiological agent, to the clinicians and doctors and engineers who have dedicated their lives to the eradication of the diseases, to the tireless scientists who have dedicated themselves to understanding the agent, I would truly be at a loss for even a starting point. More specifically, I wish to acknowledge Dr. Voskuil, my mentor, without whom I would have abandoned this project long ago and to whom I owe my drive to truly understand my research subject. I also wish to acknowledge the tenacity and insight of the Dow laboratory, especially Andrew Goodyear - without whom all of this would be simply a

jumbled mess of confusion. Yet an undertaking of this scope and scale cannot be undertaken in a vacuum. I wish to acknowledge those who have been a source of encouragement and support for me: my lab-mates Ryan, Iona, Josh, Matt, Adrienne, and Katie, for helping me to find the humor in the absurd and for the occasional help in the laboratory. My peers, for commiseration and an understanding shoulder to lean on during the hard times. My blood family: Dad, Mom, David, Brooke, and Ryan and my adopted families: the Twifords and the Bromstrups for reminding me that there is more to life than work. To Scott, thank you. To those who have given me a chance in the dating world and to my friends outside of work, to everyone who has a hand in this undertaking, I thank you.

CONTENTS

TABLES

TABLE

FIGURES

FIGURE

CHAPTER I

BACKGROUND AND INTRODUCTION

Burkholderia pseudomallei

Burkholderia pseudomallei is a Gram-negative environmental bacterium, saprophyte, and opportunistic pathogen. Found in soil, mud, and freshwater between latitudes of 20° North and South worldwide,[1–3] it is frequently found several centimeters below the surface of standing water and moist soil of a broad pH range: 2-8. *B. pseudomallei* also tolerates temperatures as low as 2-5°C for periods of up to one month, can survive over winter in soil achieving 0°C, and can tolerate salinity of up to 2.5% (w/v). Although it is a robust environmental organism, optimal growth conditions are reported to be a mildly acidic pH (~6.8), elevated temperatures of 20-40°C, and salinity of no more than 0.4% (w/v).[4–6] The organism can be found in ecological niches matching these parameters year-round, especially in Southeast Asia and Northern Australia, where

it is most frequently found. The bacteria become markedly more abundant during the rainy season each year[7] and it is during this time that cases of melioidosis also dramatically increase.[8–10]

Melioidosis

Melioidosis is the term for infection by *B. pseudomallei* which, as mentioned, is an opportunistic pathogen. First described in 1912 by Drs. Whitmore and Krishnaswamy working in Rangoon,[11] the disease has long been known to be highly endemic in Northern Australia and Northeast Thailand where it is a serious burden on public health. In fact, melioidosis can account for up to 20% of all community-acquired septicemias in these locations. It is a lesser burden on public health in neighboring countries, but sporadic and increasingly frequent reports from other countries in the regions have established that Southeast Asia and Oceania are endemic regions for melioidosis.[12–16]

Epidemiology

Melioidosis is not restricted to Southeast Asia by any means. Reports of sporadic, apparently autochthonous cases from places as geographically diverse as northern Brazil[17], Ecuador, Madagascar, Turkey,[18] the states of Arizona[19] and Oklahoma[20] in the U.S.A., Iran,[21] and an epidemic caused by animals imported to France,[22] have demonstrated that melioidosis is an emerging infectious disease. They also highlight the fact that *B. pseudomallei* may be spreading in its endemicity, and that the organism is capable of dissemination in other geographical locations apart from Southeast Asia. The organism certainly finds no challenge surviving in other geographical regions as long as the right niche is available. With the relatively recent increase in the popularity of rapid

international travel and globalization of trade, melioidosis should soon be on the list of differential diagnoses for many physicians worldwide.

Risk Factors

Although an increasing number of individuals are at risk for exposure to *B. pseudomallei,* only diabetic individuals, thalassemic individuals, chronic alcoholics and other individuals compromised in innate immunity are at particular risk for melioidosis.[14] Immunocompetent individuals are not at risk for infection from casual exposure to the organism. Healthy individuals may develop melioidosis after percutaneous inoculation with the organism or aspiration of contaminated water.[23,24] However, the vast majority of healthy individuals exposed to *B. pseudomallei* do not develop disease. Resistance of healthy individuals to infection by *B. pseudomallei* is evidenced by an 80% seroprevalence rate by 4 years of age in highly endemic areas;[25] as well as decades of laboratory work at Biosafety Level 2 with only two documented incidences of laboratory-acquired melioidosis.[26,27]

Routes of Exposure

This level of seroprevalence is quite shocking and clearly indicates that exposure to the agent does not automatically result in disease. This is vexing because *B. pseudomallei* is very well known for the ability to cause gross pathology in essentially every niche of the human body, from the CNS, to soft tissue, to hard tissue, and in every organ.[16,23,28–39] Clearly, there is little tissue tropism for the organism and very little tissue restriction. In fact, the only site not reported to have gross or histologic pathology in melioidosis patients is the gastrointestinal tract.[40–42]

If the GI tract is tolerant of the organism, exposure via ingestion could explain the high seropositivity and relatively low disease rates. It might also help explain the especial sensitivity of diabetics and alcoholics to the disease. Diabetic and chronic alcoholic individuals are known to develop achlorhydria — a loss of hydrochloric acid in production the stomach.[43,44] Some diabetics are also known to develop gastroparesis — a condition in which stomach emptying times are increased.[45] Achlorhydria, with its associated increase in resting pH, and increased stomach emptying times are all risk factors for opportunistic enteric pathogens.[46]

Unfortunately, ingestion has largely been ignored as a route of exposure, and most efforts in the field have focused on inoculation and inhalation as routes of exposure to the agent. However, definitive inoculation events account for only approximately 20% of melioidosis cases.[24] If the portion of melioidosis cases with unknown exposure is due to unnoticed skin wound exposure, we would expect to see a correlation of exposure with apparent skin lesions because rodent models using percutaneous inoculation develop self-evident primary skin lesions at the sites of exposure.[47] However, human melioidosis patients typically only present with disseminated skin lesions after presentation of initial systematic symptoms.[12] Furthermore, since *B. pseudomallei* does not have the capacity to invade through desquamated epithelium, casual skin exposure cannot explain seropositivity rates.

The next most frequently posited route of inoculation is through the mucous membranes of the upper respiratory or gastrointestinal (GI) tracts via inhalation or aspiration of contaminated particles. However, only approximately 20% of infections are attributed to aspiration of contaminated water. Inhalation of the agent and invasion

through the upper respiratory tract or lungs seems plausible, and is of great concern for weaponization of *B. pseudomallei*, but there is a paucity of evidence for airborne soil particles being infectious. There is also little evidence that exposure to an airborne agent can result in a subclinical infection, as most animal models using aerosolized *B. pseudomallei* as inocula result in an acute infection.

In light of the 80% seroprevalence for the organism, it is fair to say that the route of exposure must not be especially uncommon. In addition to the lack of pathology in GI tracts of melioidosis patients, very strong molecular epidemiology shows that drinking water sources harbor *B. pseudomallei*. The same *B. pseudomallei* strains were also identified in outbreaks of melioidosis.[48–52] Not only have contaminated water sources been identified as reservoirs of infectious *B. pseudomallei*, the agent has also been isolated from the feces of infected individuals, as well as their intestinal contents and gastric fluids.[8,47,53] All of these observations are highly suggestive of ingestion as the natural route of exposure to *B. pseudomallei.*

Clinical Presentation

Regardless of route of exposure, primary symptoms of melioidosis are protean. However, once a productive infection is established, progression of the disease frequently results in pneumonia, septicemia, or both. These severe diseases are major contributors to the extremely high mortality rate, which can approach 15% even with a rapid and accurate diagnosis, and application of timely and effective antimicrobial chemotherapy.[16] Without timely and appropriate antibiotic treatment, mortality rates can climb as high as 68%.[14]

Select Agent Designation

As indicated by the high mortality rate, even in the face of harsh antibiotic therapy,[14] the agent — and therefore the disease — is inherently tolerant to antibiotics. In fact, different clinical isolates have demonstrated different profiles of drug resistance.[54–57] Drug resistance, in combination with lack of protection from prior infection and the pursuant difficulties in developing a protective vaccine, are the primary challenges in developing an effective public health approach to the disease. The severe mortality rate and lack of effective public health strategies for dealing with melioidosis have compelled the Centers for Disease Control and Prevention to declare *B. pseudomallei* a Tier 1 Select Agent — a microorganism with great capacity for weaponization.[58]

Colony Variation

Whatever the route of infection, *B. pseudomallei* recovered from infected hosts is well-noted for its highly variable colony morphology.[14,35,47,59–66] Colony variation is not a phenomenon unique to *B. pseudomallei* though; many species of numerous genera of bacteria produce different colony morphologies.[67] Colony variation is most frequently due to the variance in expression of discrete outer membrane moieties such as outer membrane proteins, lipopolysaccharide (LPS), or exopolysaccharide (EPS) which, in turn, affect the way bacteria are organized in the colony, and thus the appearance of the colony. Properties of different outer membrane moieties, such as the presence or absence of hydroxyl groups, can also affect the appearance of a colony; for instance, an exopolysaccharide capsule can give a glistening or "wet" appearance.

Colony Variation: Examples and Molecular Mechanisms

Since the outer membrane of a bacterium is the first collection of antigens exposed to the immune system by any bacterial invader, colony variation frequently impacts the virulence of pathogens. For example, two phase variants of *Streptococcus pneumoniae* exist: the opaque phase and the translucent phase. Opaque phase variants are more virulent in systemic infection, whereas translucent phase variants are more efficient at colonization of the nasopharynx. This variability in appearance is due to variable expression of capsular polysaccharide.[68,69] Expression of capsular polysaccharide is dependent upon expression of a functional *cap3A* gene product. Spontaneous recombination within the *cap3A* gene results in a premature stop codon, and thus no functional gene product, and therefore loss of opacity.[70]

Similarly to *S. pneumoniae*, the opportunistic pathogen *Haemophilus influenzae* type b strains present as opaque, intermediate, or translucent colony types. The molecular foundation of these phenotypes is the expression of recombinant forms of capsular polysaccharide and lipopolysaccharide. The different colony types vary in pathogenic behaviors, such as nasopharynx colonization and serum resistance.[71] Variable expression of the genes responsible for these moieties is due to changes in number of units of short polynucleotide repeat tracts within the coding sequences of these genes. Subunits of the repeat are typically 4 nucleotides in length, thus insertion or deletion of any number of repeats not divisible by 3 shifts the reading frame of the expressed gene. This frame-shift will frequently insert premature stop codons into coding sequences of these genes. Insertion or deletion of repeat subunits is attributed to slip-stream mispairing (SSM)

wherein Okazaki fragments melt and re-anneal with poor fidelity during chromosomal replication.[67]

Primary cultures of the dental pathogen *Actinobacillus actinomycetemcomitans* from subgingival plaques will also produce a strongly adherent, rough phase colony variant. The roughness of the colony is due to expression of fimbriae.[72] Loss of expression from this locus is due to the accumulation of deleterious mutations in the regulatory region of the operon.[73]

The respiratory pathogen *Bordetella pertussis* will regulate expression of its fimbriae using a SSM mechanism. In contrast, though, *Escherichia coli* will regulate its type 1 fimbriae through site-specific and enzyme-mediated recombination, or "inversion" of a specific DNA sequence that either places a promoter 5' to the *fimA* gene, or removes the promoter.[67]

As one can surmise from the above examples, the vast majority of colony variation is due to the expression of genetic mutation. However, not all changes in colony morphology are due to genetic variation. *Salmonella enterica* Serovar Typhimurium regulates its fimbriae by methylation of specific DNA sequences in the regulatory regions of the *pef* operon by the DNA adenine methyltransferase (Dam) enzyme. When the methylation sites contain methyl groups, binding of a DNA-binding regulatory protein is blocked, and expression of the gene is also blocked.

"Phase variation" is the phrase used to describe a unique pattern of phenotype expression. Phase variation is defined as the inheritable, binary expression of a phenotype which manifests and reverts at rates higher than would be expected from random genetic mutation.[67] Much of colony variation is considered phase variation, but not all phase

variation is colony variation; the definition of phase variation also applies to antigenic variation, which may or may not influence colony morphology. Neither is all colony variation phase variation; some instances of colony variation are due to random mutation. This is apparently the case with Small Colony Variants (SCVs), and is often the case with mucoid colonies.

SCV's are so named for their small size when grown on nutrient agar, and are frequently explained by development of auxotrophies, or reduced growth rates. SCVs from numerous bacterial species are excellent at causing persistent infection and can develop novel drug resistances.[74] Of the many bacterial species known to produce SCVs, small, rough, strongly self-adherent colony morphology variants of *Pseudomonas aeruginosa* have been isolated from biofilms,[75] and Staphylococci SCVs have been isolated from chronic infections.[76]

Mucoid *Pseudomonas aeruginosa* and *Burkholderia cepacia* complex (Bcc) can be isolated from lungs of Cystic Fibrosis (CF) patients.[77,78] Mucoid colonies are so named because they excrete abundant amounts of an exopolysaccharide (EPS). In *P. aeruginosa*, the EPS is alginate; in Bcc, the EPS is variable. These colonies appear "slimy," or mucoid, when grown on solid agar. Mucoid colonies are more persistent colonizers of the lungs of CF patients, and are associated with poorer disease outcomes than their non-mucoid counterparts.[79] Mucoidy in *P. aeruginosa* is due to accumulation of genetic mutations that remove negative regulation from the σ^E-like transcriptional regulator *algU*.[77]

Colony Variation in *B. pseudomallei*

Prior descriptions of *B. pseudomallei* colony variants have been numerous. One study described the isolation of *B. pseudomallei* SCVs from both *in vitro* conditions and experimental melioidosis.[60] These authors observed that addition of various classes of drugs could enhance the emergence of SCVs, and that SCVs are inherently more drug resistant than their parental counterparts.[60] Another publication discussed the diversity in colony morphologies of Malaysian isolates of *B. pseudomallei,* and observed that various morphotypes correlated with altered levels of drug resistance and attenuation in an animal model.[61] Yet another report described the isolation of yellow colony variants that could be enriched by serial passage in mice.[66] The most comprehensive investigation describing colony variation in *B. pseudomallei* identified seven statistically unique colony morphologies or morphotypes isolated from melioidosis patients.[59] These types were identified and characterized on Ashdown's agar, the harsh selective medium used in clinical work,[65] and were typed according to several colony characteristics including: diameter, color, translucency, intensity of color, surface texture of colony center and margin, and overall surface shape. Of these seven, the most common morphotypes (I, II, & III) showed variant-specific pathogenicity in cell culture and animal models. The authors also observed variant-specific expression of virulence factors, including production of elastase, protease, and lipase as well as biofilm formation, swarming motility, and swimming motility.

However, no particular role in infection has been shown for *B. pseudomallei* colony variants, and no particular niche in infection has been identified for any specific colony variant. Of the animal models tested to date using iso-phenotypic colony variants

as inocula, none have described a statistically significant difference in virulence for colony variations. The inability to identify a role for *B. pseudomallei* colony variants in infection may be explained by the use of irrelevant animal models, use of unnatural routes of infection, or an incomplete appreciation for *B. pseudomallei* as an extracellular pathogen. Regardless, it has been unclear what role, if any, colony variants of *B. pseudomallei* play in infection. Furthermore, no molecular mechanisms have been identified that explain the reversible and varied morphotypes of *B. pseudomallei* colonies.

I have consistently isolated colony variants of *B. pseudomallei* under conditions that limit aerobic cellular respiration. These variants express a broad array of unique physiological changes relative to the parental type. They also express unique phenotypic behaviors, including colonization and virulence in a clinically relevant animal model. This body of work sought to delineate the unique behaviors of *B. pseudomallei* colony variants in contrast with their parental form, as well as identify some of the underlying molecular mechanisms and describe their roles during infection.

CHAPTER II

MATERIALS AND METHODS

Bacterial Strains and Growth Conditions

Except where noted, the clinical isolate *B. pseudomallei* strain K96243 was used in these studies. Strain K96243 was isolated from a diabetic woman, aged 34 in Khon Kaen Hospital in Northeast Thailand who presented with acute septicemia and, sadly, did not survive the infection.[80,81] White type bacteria of K96243 are abbreviated as "WHT", type A yellow variants are denoted as YA, and type B yellow variants are denoted as YB. *In vitro* experiments with the bacteria were performed in the Select Agents–approved BSL-3 Voskuil laboratory at the University of Colorado, Denver, with all manipulations occurring in an annually certified Class II B2 Biosafety Cabinet (BSC), and complying with the Biosafety for Microbiological and Biomedical Laboratories (5th ed.) handbook.[82] For *in vitro* experiments, bacteria were, unless otherwise noted, struck for

isolation from freezer stock onto nutrient agar plates and grown at 37°C for 3 days. Plates were kept for no longer than a week and were kept at 25°C after the initial incubation at 37°C. The growth medium of choice in the Voskuil laboratory for propagation of *B. pseudomallei* and most *in vitro* work was Luria-Bertani – Lennox (10 g/L Tryptone, 5 g/L Yeast Extract, 5 g/L Sodium Chloride) (LB). Liquid cultures of bacteria were made in LB broth prepared at pH 7.0 or 5.0 unless otherwise noted. Liquid media pH was adjusted with NaOH or HCl as needed, and filter-sterilized before use. Overnight cultures of bacteria were grown in 15 mL conical bottom Bio-Reaction tubes (CellTreat Scientific Products – Shirley, MA) which feature a vented screw-cap lid lined with a 0.2 µm hydrophobic membrane to allow for gas exchange without escape of bacteria from the container. Planktonic experimental cultures and outgrowth cultures were grown in plastic 125 mL vented, screw-cap, Erlenmeyer flasks (Corning Life Sciences – Tewksbury, MA) also sealed with 0.2 µm hydrophobic membranes. Cultures were grown at 37° C unless otherwise noted. Shaken cultures were shaken at 275 rpm unless otherwise noted.

For *in vivo* experiments in the Dow laboratory at Colorado State University (CSU), overnight cultures of WHT, YA or YB strains were grown in their growth medium of choice: Luria-Bertani – Miller (LB-M) broth pH 7.0 (BD Biosciences, San Jose, CA) (10 g/L Tryptone, 5 g/L Yeast Extract, 10 g/L Sodium Chloride) at 37°C with shaking at 250 rpm in 125 mL Erlenmeyer flasks fitted with a 0.2 µm filter for aeration (BD Biosciences). Stationary phase cultures were harvested, 20% v/v sterile glycerol (Fisher Scientific, Pittsburgh, PA) was added, and 1 mL aliquots were frozen at -80°C.

Other bacteria used in this work include *B. pseudomallei* strain 1026b and *B. thailandensis* strain E264, both received from Herbert Schweizer at CSU. *Pseudomonas*

aeruginosa strain PAO1, received from Mike Schurr at the University of Colorado Denver (UCD); *Salmonella enterica* Serovar Typhimurium strains 140825 and LT2, received from Andrés Vázquez-Torres at UCD, *Bacillus cereus* strain MM1 received from Ron Gill at UCD, and *Escherichia coli* strain MG1655 substrain DH5α purchased from Promega® as competent cells and stocked for use in cloning and other experiments.

Emergence of Yellow Variants under Hypoxic Conditions

A single white colony of the wild type *B. pseudomallei* was used to inoculate a 5 mL overnight culture in LB at pH 7. Cultures were shaken overnight (16-20 hr) at 37° C. The next morning, cultures were assayed for optical density at 600 nm (OD_{600}) using a spectrophotometer. Cultures were normalized to an OD_{600} of 0.1 in fresh LB at pH 5.0, and 3.0 mL of normalized culture was placed in a sterile 20 mm x 125 mm threaded top glass tube, containing a sterile 12 x 7 mm octagonal magnetic stir bar, and fitted with a phenolic-mesh screw cap. The cultures were placed in a hypoxia chamber (Coy Laboratories - Grass Lake, MI) equilibrated to 0.2% O_2, and set atop a Wheaton 4-plate magnetic stirrer. The stirrer was set to 200 rpm and the entire apparatus was placed inside a water-jacketed incubator set to 37°C. Tubes had their caps loosened after placement in the incubators to allow for gas exchange. Cultures were sampled at 6, 12, 24, 48, 72, and 96 hours. Aliquots of culture were serially diluted, and 100 µL of appropriate dilutions were plated on 10 cm LB agar plates then spread over the surface of the plate with 4 mm glass beads. Once plates had dried, beads were removed, and plates were incubated at 37°C for a minimum of 3 days until colony morphologies were easily distinguished. Once grown, plates were counted and typed. Data reported is the average of one technical replicate performed in biological triplicate.

Growth Rate Determination

A single colony of the either the YA- or YB-type *B. pseudomallei* K96243 was used to inoculate a 5 mL overnight culture of LB at pH 7.0. Overnight cultures were diluted 1:100 in fresh LB pH 7 the following morning and incubated at 37°C for at least 3 hours to allow the bacteria to enter logarithmic growth. Once outgrowth of starter cultures was complete, each culture was assayed for OD_{600}, and then normalized to an OD_{600} of 0.10 in fresh, warm, LB pH 7. Normalized cultures were returned to the shaking incubator, and allowed to grow for 12 hours to enter early stationary phase. At 12 hours of growth, each culture was again sub-cultured to an OD_{600} of 0.1 in fresh, warm LB pH 7 and returned to the incubator. At 20 minute time intervals, each flask was assayed for OD_{600} out to approximately 200 minutes. Growth rate (*G*) was calculated according to the following formula, where *F* is the final optical density, *I* is the initial optical density, and ΔT is the difference in time.

$$G = \Delta T \div \frac{\log(F)/\log(I)}{\log 2}$$

The growth rate constant *g* was calculated by dividing ln(2) by *G*. Data reported is the average of three biological replicates ± the standard deviation. Statistical significance of doubling time (G) was determined by Student's T-test under non-parametric presumptions. Statistical significance of growth rate constants was determined by Analysis of Variance (ANOVA).

Reversion Rate Determination

A single colony of the either the YA- or YB-type *B. pseudomallei* K96243 was used to inoculate a 5 mL overnight culture in LB at pH 7.0. Cultures were grown

overnight (16-20 hr) at 37° C, with shaking. The next morning, cultures were assayed for OD_{600} and were normalized to an OD_{600} of 0.1 in fresh LB at pH 5.0. Two experimental set-ups were used, one for hypoxia and one for aerobic growth. For hypoxic cultures, 3.0 mL of normalized culture was placed in a sterile 20 mm x 125 mm threaded top glass tube containing a sterile 12 x 7 mm octagonal magnetic stir bar and fitted with a phenolic-mesh screw cap. For aerobic cultures, 25 mL of normalized culture was placed in a 125 mL vented, screw-cap Erlenmeyer flask. Two incubation set-ups were used; for hypoxic growth, the inoculated glass tubes were placed in a hypoxia chamber equilibrated to 0.2% O_2. The hypoxia chamber was set atop a Wheaton 4-plate magnetic stirrer. The stirrer was set to 200 rpm and the entire apparatus was placed inside a water-jacketed incubator set to 37°C. Tubes had their caps loosened after placement in the incubators to allow for gas exchange. Cultures were sampled at 6, 12, 24, 48, 72, and 96 hours in this hypoxic stirred culture model. For aerobic growth, 25 mL of culture was grown under well-aerated conditions. Cultures were prepared as for growth rate determination with the exception that cultures were shaken at 315 rpm to ensure the best penetration of atmospheric gases into the culture medium, and, after entrance into log phase and sub-culture to OD_{600} of 0.10, cultures were sampled at 0, 2, 4, 6, and 8 hours and assayed for percent composition of colony type. At least 1,000 colonies per replicate per data point were counted and typed from plates with a density of 300-500 colonies per plate. Conversion rates were calculated according to the following formula described earlier,[83] where ΔN_R is the change in number of reverting or white colonies, ΔN_T is the change in total number of bacteria and R is the Reversion Rate. R is reported in the percent chance of the switching event occurring per cell per generation. Values reported

are the mean of three biological replicates ± the standard deviation. Statistical significance determined by the Student's T-test.

$$R = \frac{\Delta N_R / \Delta N_T}{\ln 2}$$

Competitive Advantage of Yellow Colony Variants under Hypoxic Growth Conditions

To determine any competitive advantage of yellow colony variants under hypoxic or aerobic growth conditions, YA, YB, or WHT cultures were mixed with a white-type *xylE*$^+$ culture at 1:100 (test strain to control strain) and then incubated under 0.2% O_2, or under atmospheric O_2. Cultures were sampled at several points during incubation and assayed for percent distribution of both genotype and phenotype.

To achieve this, single colonies of wild type WHT, YA, or YB-type or *xylE*$^+$ white-type colonies were used to inoculate 5 mL overnight cultures in LB pH 7 with shaking at 37°C. The next morning, cultures were diluted to an OD_{600} of 0.1 in fresh, warm, LB pH 5.0 and verified empirically. One percent of normalized *xylE*$^+$ culture was removed by pipetting and replaced with an equal volume of either: WHT, YA, or YB-type culture at the same OD_{600}. For hypoxic competitions, 3.0 mL of mixed culture was placed in the stirred tube model described for emergence of yellow variants under hypoxia and sampled at 0, 6, 12, 24, and 48 hours for percent distribution of both genotype and phenotype. For aerobic competitions, 25 mL of mixed culture was placed in a 125 mL Erlenmeyer flask and grown at 37°C with fast shaking (315 rpm) then sampled at 0, 2, 4, 6, and 8 hours for percent distribution of both genotype and phenotype. Later time points were not included because beginning at approximately 10-12 hours of aerobic

growth in LB, *B. pseudomallei* will achieve cell densities that induce hypoxia due to cellular respiration regardless of shaking speed and will also begin to enter growth arrest, which yellow variants respond to differently than the white type.

Determination of both genotype and phenotype was accomplished by plating an aliquot of dilute culture onto a 10 cm LB agar plate and spreading the inoculum over the surface of the plate in the same manner as for Reversion Rate calculation and emergence of yellow variants under hypoxic growth conditions. Approximately 300-500 colonies per plate was the target colony density and at least 1,000 colonies per data point per replicate were counted. Once colonies were grown, counted, and typed for phenotype, plates were sprayed with pyrocatechol as described for identification of pMo130 integrated merodiploids.[84] Colonies were counted a second time to record genotype.

Data reported is the average genotype distribution for three biological replicates ± the standard deviation at each time point. Statistical significance was determined by comparison of percent *xylE*$^-$ colonies in YA- and YB- mixed cultures against WHT-mixed cultures at the same time point using the two-tailed, unpaired, Student's T test.

pH Shift and Ammonia Production

Single colonies of either WHT-, YA- or YB-type colonies were used to inoculate 5 mL overnight cultures in LB at pH 7. Cultures were shaken overnight (16-20 hr) at 37° C. Overnight cultures were normalized to an OD_{600} of 0.1 in 25 mL fresh LB at pH 5.0 and placed in 125 mL vented, screw-cap Erlenmeyer flasks. Culture flasks were placed in rotary, forced-air incubators set to 37° C, and 275 rpm, then sampled at 3, 6, 12, 24, and 48 hours for OD_{600}, CFU/mL, and pH. Culture pH was determined using a 7-Easy pH Meter (Mettler-Toledo) and an In Lab Versatile Pro™ pH electrode (Mettler-Toledo). At

the 48 hour experimental end-point, 10 mL of each culture was clarified by centrifugation for 15 minutes at 4,000 rpm (3220 x *g*) then filter-sterilized twice by passage through a 0.2 µm cellulose-acetate disk filtration device. Once sterile, samples were removed to the BSL-2 where they were assayed for ammonia content using an ammonia ion-selective electrode (Mettler-Toledo) as described previously.[85] Ammonia content in un-inoculated LB after 48 hours of incubation at 37°C was determined and the abiotic background ammonia was deducted from ammonia values reported for all three colony variants. Data reported is the average of three biological replicates ± the standard deviation. Statistical significance of ammonia levels was determined by the Student's T test.

Mice

Female BALB/c mice were purchased from Jackson Laboratories (Bar Harbor, ME). All mice used in experiments were housed under pathogen-free conditions in micro-isolator cages, and mice were 9 to 36 weeks of age at the time of infection. All experiments involving animals were approved by the Institutional Animal Care and Use Committee at Colorado State University. All *in vivo* experiments involving *B. pseudomallei* were performed in a Biosafety Level 3 (BSL-3) facility, in accordance with approved Select Agent protocols in place at Colorado State University.

Animal Infections

Animal infections were performed by members of the Dow lab: Andrew Goodyear, Ediane Silva, and Marjorie Sutherland as described previously.[42] Briefly, bacterial stocks in LB-M + 20% glycerol stored at -80°C were thawed and diluted in sterile phosphate buffered saline (PBS) (Sigma-Aldrich, St. Louis, MO). Infectious doses

for each experiment were determined by plating serial dilutions of each inoculum on LB-M agar (BD Biosciences). Oral (p.o.) inoc-ulations were performed using a stainless steel 22 gauge gavage needle (Roboz Surgical Instrument Co., Gaithersburg, MD) and mice were inoculated using a total volume of 100 µl.

Quantification of Tissue Bacterial Burden and Fecal Shedding

Bacterial burdens were assessed by members of the Dow laboratory listed above in the manner described previously.[86] Briefly, mice were humanely euthanized, and organs (lung, liver, spleen, stomach, intestines and colon) and feces were placed in 4 ml sterile PBS. Prior to homogenization, stomach and cecum tissues were cut into ~1-2 cm^2 sections, and small intestine and colon tissues were cut open longitudinally, and then cut into 2-3 cm lengths. Lungs, livers, spleens, stomachs, intestines, colons, and feces were homogenized using a Stomacher 80 Biomaster (Seward, Davie, FL) and serially diluted 10-fold in sterile PBS. Lung, liver and spleen were plated on LB-M agar plates (BD Biosciences). Stomach, small intestines (SI), cecum, and colon homogenates were plated on NAP-A agar.[42,64] NAP-A medium was developed for the sole purpose of isolating *B. pseudomallei* from the complex microbiological milieu of the gastrointestinal tract.[64] Agar plates were incubated at 37°C for 48 hours and colonies were counted. The limit of detection in the stomach and distal GI tract was 1 CFU/organ as the entirety of each organ was homogenized and plated. For lung, liver and spleen, the limit of detection was 10 CFU/organ.

For quantification of fecal shedding, fecal pellets were collected and processed as described previously.[42] Briefly, pellets were collected from individual mice in plastic containers and transferred to sterile PBS at a concentration of ~0.1 g/mL. Fecal pellets

were homogenized by mechanical disruption in a Whirl-Pak stomacher bag (Nasco, Fort Atkinson, WI) and 10-fold serial dilutions were prepared in sterile PBS. Serial dilutions were plated on NAP-A agar plates, incubated at 37°C for 48 hours, and colonies were counted. The limit of detection in feces was 10-60 CFU/gram, depending on the number of fecal pellets plated.

Fluorescent In Situ Hybridization

Fluorescent in situ hybridization (FISH) was performed by the Dow laboratory as described previously, with slight modifications.[42] Briefly, antisense ssDNA probes were purchased from Integrated DNA Technologies (San Diego, CA). Probes used in this study included the *B. pseudomallei* specific probes Bpm427 and Bpm975, as well as the Eub338 probe (Table B.1), which recognizes a sequence present in all bacteria, and the irrelevant control probe Non338. All probes were 5' labeled, Bpm427 and Bpm975 with Cy3, Eub338 with Alexa Fluor 488, and Non338 with Cy3 or Alexa Fluor 488. Stomach tissues were fixed in 10% neutral buffered formalin (NBF) (Sigma-Aldrich) for 48 hours, and then transferred to 70% ethanol for 7 days (Fisher Scientific, Pittsburgh, PA). Tissues were then embedded in paraffin, and sectioned. Tissue sections were baked onto slides for 1 hour at 60°C. Sections were then deparafinized with Histoclear® (National Diagnostics, Atlanta, GA) and re-hydrated in solutions with decreasing ethanol concentration (Fisher Scientific). Sections were post-fixed in 4% paraformaldehyde (Electron Microscopy Science, Hatfield, PA) in PBS for 15 minutes at room temperature and washed in PBS. Tissue sections were then permeabilized by heating in 10 mM citrate buffer pH 6.1 (Dako Cytomation, Carpinteria, CA) at 90°C for 12 minutes, and allowed to cool gradually at room temperature over 40 minutes. After water washing,

tissues were treated with 0.3% Triton X-100 in PBS (Sigma-Aldrich, St. Louis, MO) for 6 minutes at room temperature, and washed in PBS. Next, tissue sections were hybridized with ssDNA probes diluted in hybridization buffer consisting of 4X saline sodium citrate (SSC) (Fisher Scientific), 200 mg/ml dextran sulfate (Sigma, St. Louis, MO), 20% formamide (Sigma), 0.25 mg/ml PolyA (Sigma), 0.25 mg/ml salmon sperm DNA (Life Technologies, Carlsbad, CA), 0.25 mg/ml tRNA (Life Technologies), and 0.5X Dendhart's solution (Sigma). Tissues were hybridized with a cocktail of the Bpm427, Bpm975, and Eub338 probes each used at a final concentration of 1 µg/ml, or the Non-338 probe conjugated to Cy3 at a final concentration of 2 µg/ml and the Non338 probe conjugated to Alexa Fluor 488 at 1 µg/ml. Probes were hybridized with tissue sections in a humidified chamber at 37°C for 3 hours. Following hybridization, sections were washed to remove non-specific probe binding. Washes included, one 15 minute wash in 1X SSC at 37°C, one 15 minute wash in 1X SSC at 54°C, one 15 minute wash in 0.5X SSC at 54°C, and one 10 minute wash in 0.5X SSC at room temperature. Slides were then stained with 100 ng/ml DAPI (Sigma) in 2X SSC for 10 minutes at room temperature, washed in 2X SSC and dH_2O, air dried, and mounted with Pro-Long gold (Life Technologies, Carlsbad, CA).

Fluorescent microscopy was performed on a Leica DM4500 fluorescent microscope (Leica Microsystems Inc., Buffalo Grove, IL) with DAPI (Set A4; Ex. 360/40 nm; Dichroic 400 nm; Em. 470/40 nm), FITC (Set L5; Ex. 480/40 nm; Dichroic 505 nm; Em. 527/30 nm), and Cy3 (Set N3; Ex. 546/12 nm; Dichroic 565 nm; Em. 600/40 nm) filter cubes (Leica Microsystems Inc., Buffalo Grove, IL). Images were captured with a Retiga-2000R camera (Q-Imaging, Surrey, BC, Canada) utilizing QCapture Pro software

version 5.1 (Q-Imaging, Surrey, BC, Canada). Image overlays were created in Photoshop CS3 software (Adobe, San Jose, CA) as described previously.[42] Briefly, when necessary images captured at different focal planes were combined using layer masks in Photoshop software. All other manipulations were applied to globally, and settings used on images from sections hybridized with Bpm427, Bpm975, and Eub338 probes were obtained from images captured from sections hybridized with Non338 probes.

eDNA Quantification and CFU Determination in an *in vitro* Stomach Model

Single colonies of either WHT-, YA- or YB-type colonies were used to inoculate 5 mL overnight cultures in LB broth at pH 7.0. Cultures were grown overnight (16-20 hr) in a 37° C forced-air incubator with shaking at 275 rpm. The next morning, cultures were assayed for OD_{600} using a spectrophotometer. Cultures were normalized to an OD_{600} of 0.1 in fresh LB broth at pH 5.0. Five hundred microliters (500 µL) of each culture was placed in a single well of a mucin-coated 24-well plate. At 4, 8, 12, 16, 20, and 24 hours, one well per morphotype was used to determine both CFU per well and eDNA content per well. This was accomplished by addition of 1.0 mL PBS to each well and aggressive agitation by pipetting. The 1.5 mL volume of each well was then transferred to a 2.0 mL screw-cap microcentrifuge tube fitted with an O-ring, sealed tightly, and vortexed at maximum speed (setting 10) for at least 30 seconds. A 20 µL aliquot of the resulting suspension was then serially diluted and plated for CFU, and the remainder was clarified by centrifugation at maximum speed for a minimum of 5 minutes. The supernatant was removed to two 2.0 mL tubes in 750 µL aliquots, and 750 µL of tris-saturated phenol: chloroform: isoamyl alcohol (25:24:1) was added to each aliquot. Phenol-chloroform extractions were mixed aggressively for 10 seconds by hand, and then intermittently for 2

minutes, then separated by centrifugation at 13,200 rpm (16,168 x *g*) in a microcentrifuge for 15 minutes. The aqueous phase was then removed to a fresh 1.5 mL microcentrifuge tube. After verification that the aqueous phase was sterile, it was removed to the BSL-2 where 15 µL aliquots of each sample were loaded into an 8 mm thick 0.8% agarose gel and ran at 110 V for 60 minutes. Gels were then stained for 1 hour with 1 µg/mL ethidium bromide in 1xTAE. Gels were visualized on a Bio-Rad ChemiDoc XRS gel imaging station, and bands of fluorescence were quantified with ImageLab software (Bio-Rad) using 0.3 µg of GeneRuler 1KB Plus quantitative DNA ladder (Fermentas Life Sciences) as a standard (r^2 minimum of 0.90). For samples generating migration artifacts when separated by electrophoresis (due to overabundance of DNA), aliquots of samples were needle-sheared using a 27½ gauge needle with 12 passages and reassessed using the in gel quantification method described above.

Mucin-coated plates were prepared as described earlier,[87] with the modification that the mucin was sterilized before use as described,[88] and 500 µL of suspended mucin was added per well to 24-well plates. Data reported is the average of 3 biological replicates, ± the standard deviation. Statistical significance determined by ANOVA.

Synthetic Gastric Fluid Protection Assay

Settled cultures of WHT, YA, and YB were prepared as described for the eDNA analysis. Briefly, mucin-coated 24 well plates were inoculated with 0.5 mL of culture at OD_{600} of 0.1 and grown in the hypoxia chamber at 2% O_2 for 24 hours. At 24 hours of growth, multi-well plates were removed and 0.5 mL pre-warmed Synthetic Gastric Fluid (SGF) at pH 2.0 was carefully added to each well, making sure not to disturb the ultrastructure of the bacterial community. Multi-well plates were returned to the hypoxia

chamber and incubated at 37°C for 2.5 hours. After incubation in the presence of SGF for 2.5 hours, multi-well plates were removed and 0.5 mL sterile-filtered 0.5% (w/v) sodium bicarbonate was carefully added to each well. The bicarbonate was allowed to neutralize the acid in SGF for 15 minutes at room temperature without agitation. After acid was neutralized, the contents of each well were homogenized by aggressive pipetting, and 20 µL of each well was assayed for CFU per mL.

SGF was prepared according to Beumer, et al.[89] with the following minor modifications: the final pH of SGF was adjusted to pH 2.0 instead of 1.5, and instead of autoclaving, nutrient media was sterilized by vacuum filtration. Finally, the proteolytic enzymes lysozyme and pepsin were measured into aliquots as dry powder, reconstituted immediately before use, and added to SGF immediately before addition of SGF to cultures.

Percent survival was calculated using known bacterial titers for each condition (prior to addition of SGF). Data reported is the mean of three biological replicates, ± the standard deviation. Statistical significance determined by the unpaired two-tailed Student's T test comparing each variant percent survival to WHT percent survival.

Swimming Motility

Swimming motility was determined by inoculating a single strain at the bottom of the center of a single 10 cm petri dish filled with swimming agar. A 27½ gauge hypodermic needle was dipped in culture and the inocula were place at the bottom of the agar. Plates were incubated for 24 hours at 37°C at which point zones of swimming motility were measured. In the event of asymmetric zones of swimming, the largest diameter was reported. Overnight cultures of bacteria were prepared as described above,

with the exception that overnight cultures were standardized to an OD_{600} of 2.0 for swimming agar inoculation. Swimming agar was prepared by separately autoclaving 0.6% Bacto Agar and 40 g/L LB broth adjusted to either pH 5.0 or 7.0, then mixing the selected media with the melted agar at 1:1, and then pouring plates. Plates were allowed to solidify overnight and used the following day. Data reported is the average ± the standard error of the mean of 4 biological replicates with a minimum of 5 technical replicates per condition, per biological replicate. Statistical significance was determined by the unpaired, two-tailed Student's T test.

Microscopy

White and yellow-variant bacteria were grown in the same manner as for growth rate determination. At 7 and 24 hours of growth, samples were harvested by centrifugation and resuspended in PBS. Aliquots of each sample were placed on a glass microscope slide previously coated with poly-L-lysine. Glass coverslips were applied and sealed using nail polish. After drying, slides were moved to a Nikon Eclipse TE200-U inverted microscope using a 100x oil immersion objective lens, a phase contrast filter and a 10x projection lens. Pictures were taken with a Nikon DS-Fil diagnostic instrument 1.0x camera and were collected and processed with the MetaVue software suite.

Observation of Yellow Variant Toxicity

Growth curves of WHT and YA were performed by Amanda Stewart and Martin Voskuil. Briefly, cultures of both forms of bacteria were allowed to enter logarithmic growth phase then normalized for density by OD_{600}. Resulting cultures were incubated at 37°C with shaking and assayed for CFU/mL every hour for 24 hours and then again at 48

hours. Data reported is the average of two replicates ± the standard deviation. Statistical significance was not determined because of variability in repetitions with some growth curves showing total sterilization of cultures.

Growth Medium Dependency of Yellow Variant Toxicity

To determine if yellow variant toxicity was specific to LB, yellow variants YA and YB were grown in the following media with the indicated formulations and assayed for CFU/mL at 12, 24, and 48 hours: Lennox Broth (LB) (10.0 g/L casitone, 5.0 g/L Yeast Extract, 5.0 g/L sodium chloride, pH 7). Brain-Heart Infusion broth (7.7 g/L Calf Brain Infusion from 200 g, 9.8 g/L Beef Heart Infusion from 250 g, 5.0 g/L sodium chloride, 2.5 g/L disodium phosphate, pH 7). Trypticase Soy Broth (17.0 g/L Pancreatic Digest of Casein, 3.0 g/L Papaic Digest of Soybean, 5.0 g/L sodium chloride, 2.5 g/L dipotassium phosphate, pH 7). Liver Infusion broth (20.0 g/L Beef Liver Infusion from 500 g, 10.0 g/L Proteose Peptone, 5.0 g/L sodium chloride, pH 7). LB + 0.5% (w/v) pyruvate + 0.5% (w/v) succinate, pH 7. Bacterial viability was assessed by CFU typically at approximately 12, 24, and 48 hours of growth.

Yellow Variant Toxicity Stabilization and Ablation

To determine if yellow variant toxicity could be stabilized or ablated, preliminary transcriptional profiling of YA grown planktonically was performed relative to WHT using microarray analysis. Differential gene expression was observed for glycolysis and gluconeogenesis as well as Tricarboxylic Acid (TCA) cycle gene expression (Figure B.3 and B.4 and Tables B.3 and B.4) suggesting that mutually exclusive approaches to central metabolism were occurring in yellow variants relative to white. Hypothesizing that we

could stabilize the yellow variant phenotype of toxicity production by addition of metabolites feeding directly into either glycolysis or the TCA cycle, we developed modified rich growth media including combinations of: glucose, glycerol, pyruvate, or succinate. Colony variants were then grown in the modified media and monitored for survival by CFU. Data reported is the result of one experiment for LB+Glc, LB+Gly, LB+Pyv, and LB+Scc.

To determine if the effect was repeatable, colony variants were grown in LB + 0.5% pyruvate + 0.5% succinate in biological triplicate. Data reported is the average of three biological replicates of LB+Pyv+Scc ± the standard deviation. Statistical significance of death in LB+Pyv+Scc was determined by two-way ANOVA with the Bonferroni post test for multiple comparisons.

Contact-Dependence of Yellow Variant Toxicity

To determine if toxicity of yellow variant *B. pseudomallei* had activity against the WHT form, an experimental growth model was developed, allowing simultaneous growth of both yellow type bacteria in the presence of the WHT type. Overnight cultures of WHT, YA-, and YB-type were grown in LB pH 7 and sub-cultured at 1:100 in 25 mL LB pH 7 the following morning. After sub-culture, bacteria were grown for approximately 4 hours at 37°C then sub-cultured again in 25 mL of culture for WHT, and 150 mL of LB plus 0.5% pyruvate plus 0.5% succinate for YA and YB to an OD_{600} of 0.10 and grown for 10 hours. Growth in LB plus succinate and pyruvate was determined to stabilize toxicity of YA and YB (Figure 4.4). At 10 hours of growth, cultures were assayed for CFU/mL and 3 mL of WHT culture was loaded into a 10 KDa MWCO Slide-A-Lyzer dialysis cassette (Pierce) using a syringe and hypodermic needle. The cassette was

washed twice with sterile 70% isopropanol, and then three times with sterile PBS. Once washed, the loaded cassette was placed in a sterile 2 L plastic beaker containing a sterile 10 cm octagonal stir bar, and the 150 mL of yellow variant culture was added. The beaker was covered with tin foil, placed in proper secondary containment, and moved to a Wheaton 4-plate stirrer set to 200 rpm for 48 hours. The stirrer was located inside a water–jacketed incubator set to 37°C. At 48 hours of incubation, the outer culture was assayed for CFU/mL, the cassette was rinsed 3 times with PBS, and the contents extracted with a syringe and hypodermic needle, then assayed for CFU/mL. Percent survival was calculated, and data reported is the average of 5 repetitions plus the standard deviation for WHT exposure to YA or YB. Statistical significance determined by the unpaired, two-tailed Student's T test.

To determine spectrum of toxicity of live yellow variant YB, *P. aeruginosa* strain PAO1, *Bacillus cereus* strain MM1, *Salmonella enterica* Serovar Typhimurium strains LT2 and 140285, *E. coli* strain MG1655 substrain DH5α, *B. thailandensis* strain E264, or *B. pseudomallei* strain 1026b were used inside the dialysis cassette. Data reported for *E. coli*, *P. aeruginosa, S. enterica,* and *B. cereus* is the result of one experiment, no repetition. Data reported for *B. thailandensis* is the average of 4 repetitions and *B. pseudomallei* 1026b the average of 3 repetitions. No statistical analysis was performed because we wished to isolate a toxin in purity before determining total spectrum and kinetics of toxicity.

Toxicity Assays: Spectrum and Relative Susceptibility

Toxicity of yellow variant supernatant (SNT) was assayed by addition of freshly harvested YA or YB SNT to live cells in either logarithmic growth or collected from

stationary phase. To prepare cells for logarithmic phase growth, overnight cultures were made from single colonies of the following bacterial strains and forms: *B. pseudomallei* strain K96243 phases WHT, YA and YB, *B. thailandensis* strain E264, *P. aeruginosa* strain PAO1, *S. enterica* serovar Typhimurium strain 140285, and *B. cereus* strain MM1. Overnight cultures were then sub-cultured the following morning at 1:100 in warm LB pH 7 and grown for a minimum of 3 hours, then sub-cultured again to an OD_{600} of 0.10 and grown for 6 hours. At 6 hours of growth, approximately 5 OD units of log phase and 5 OD units of overnight culture in stationary phase were collected by centrifugation, rinsed twice with PBS, and then suspended in yellow variant SNT or WHT form SNT. Bacterial survival was assayed by determination of CFU/mL at 1, 2, 4, 6, 12, and 24 hours after continuous exposure to the SNT. Percent survival was calculated relative to CFU counts at time 0. Data reported for Figures 4.8 and 4.9 are the result of one experiment, Data reported for Figure 4.10 is the average of three experiments ± the standard error of the mean. No statistical analysis was performed as we wished to isolate a toxin in purity before thoroughly determining kinetics and spectrum of toxicity.

SNT of WHT, YA- or YB- form bacteria were prepared as for the growth rate determination, with the exception that experimental cultures were allowed to grow with shaking in LB plus 0.5% pyruvate plus 0.5% succinate at pH 6.6 until 48 hours of incubation. Growth in media with added pyruvate and succinate was preferred as pyruvate and succinate were observed to stabilize toxicity of the yellow variants (Figures 4.4 and 4.5). At 48 hours, SNT from all cultures was harvested by centrifugation at 4,000 rpm for 20 minutes, and then sterilized by vacuum filtration using 0.2 µm PES membrane vacuum filtration devices. SNT was then mixed 1:1 with either fresh LB for log-phase

experiments, or with the non-toxic WHT SNT for stationary phase experiments. SNT was timed to be ready when bacterial cultures were ready for testing.

Development a Semi-Defined Medium for Toxin Isolation and Purification

Middlebrook 7H9 broth was adapted to *B. pseudomallei* for use as a semi-defined medium. Two g/L casein hydrolysate was added to Middlebrook 7H9 (0.5 g/L ammonium sulfate, 0.5 g/L L-glutamic acid, 0.1 g/L sodium citrate, 1.0 mg/L pyridoxine, 0.5 mg/L biotin, 2.5 g/L disodium phosphate, 1.0 g/L monopotassium phosphate, 0.04 g/L ferric ammonium citrate, 0.05 g/L magnesium sulfate, 0.5 mg/L calcium chloride, 1.0 mg/L zinc sulfate, 1.0 mg/L copper sulfate, 2.0 g/L Casein Hydrolysate, pH 7) (7HB), then growth and toxicity were assayed in the medium (data not shown). Once it was observed that 2 g/L casein hydrolysate was not sufficient to support toxin production (data not shown), the formulation of 7HB was modified to include the same percent solute (w/v) as LB (i.e. a total of 15 g/L added solute) (Table 2.1). To investigate the relative effects of pyruvate, succinate, glucose, and glycerol, balanced combinations of the four were prepared (Table 2.1). Yellow and white variants were grown in the media and their survival was assayed by CFU/mL. Data reported is the average of 1 experiment; no statistical analysis was performed because the intent of the work was to replicate the toxicity phenotype observed for LB in a semi-defined medium that would be amenable for analysis and purification by chromatography.

Table 2.1 Formulation of Derivatives of 7H9-based Media

	Casein Hydrolysate (g/L)	Pyruvate (g/L)	Succinate (g/L)	Glucose (g/L)	Glycerol (mL/L)	7H9 mix (g/L)	Σ (g/L)
7HB	10.3	0	0	0	0	4.7	15.0
7HB/F	5.15	2.575	2.575	0	0	4.7	15.0
7HB/F/G	3.43	1.716	1.716	1.716	1.716	4.7	15.0
7HF	0	5.15	5.15	0	0	4.7	15.0
7HG	0	0	0	5.15	5.15	4.7	15.0

Small Molecule Isolation and Activity Assays

Attempts were made to isolate unique compounds from supernatants of YA and YB. Briefly, cultures of WHT, YA, or YB were grown overnight in LB, then sub-cultured the following day at 1:100 in LB. Sub-cultured bacteria were allowed to grow for 3-4 hours and were then sub-cultured again to a standard OD_{600} of 0.1 in LB + 0.5% pyruvate + 0.5% succinate, or 7HBF and allowed to grow for 12, 24, or 48 hours. After growth was complete, the bacteria were collected from the culture by centrifugation at 4,000 rpm (max speed) for 25 minutes then the supernatant was decanted through a 0.2 µm vacuum filtration devices. The supernatant was sterilized twice by vacuum filtration then removed to the BSL-2 where it was lyophilized from frozen 25 mL aliquots. Lyophilized samples were suspended in $^{1}/_{100}{}^{th}$ of the initial volume using water and then extracted with an equal volume of Folch wash (chloroform: methanol 2:1). Organic or aqueous fractions were collected and spotted onto silica gel-coated Thin Layer Chromatography plates. Loaded plates were typically run in a solvent system consisting of n-butanol: acetic acid: water (3:3:1) or n-butanol: acetic acid (3:1) then visualized with exposure to iodine crystals, UV light at 212 or 360 nm, or ninhydrin and heat. Unique bands were marked in pencil and scraped into clean tubes for repeated extraction and testing for antibacterial activity.

Plasmids and Strain Construction

Unless otherwise noted, cloning using the pMO130 construct as a backbone was carried out in *E. coli* JM109. All other plasmid backbones used *E. coli* DH5α as the host. All *E. coli* were grown in LB broth at 30°C and, when needed, antibiotics were added at the following concentrations: ampicillin – 100 μg/mL, kanamycin – 50 μg/mL, and gentamicin – 30 μg/mL. For selection in *B. pseudomallei*, kanamycin was used at 200 μg/mL, in addition to zeocin at 50 μg/mL, to abolish background resistance. For maintenance of plasmids in *B. pseudomallei*, kanamycin was used at 100 μg/mL without addition of zeocin.

The over-expression vector pHERD was generated from pHERD-30T and pMO130[84,90] by digesting pHERD-30T with *Bsr*G I and *Acl* I to remove the gentamicin resistance marker. The kanamycin resistance marker from pMO130 was PCR-amplified using primers Kan_F2-BsrGI and Kan_R3-AclI (Table C.1), TA-cloned into pGEM-T easy™, and then sub-cloned into pHERD-30T backbone sans gentamicin marker.

The over-expression vector pHERD::BPSL1887 was generated for this study using primers BPSL1887OEX_F1-EcoRI and BPSL1887OEX_R1-HindIII (Table C.1) to amplify the coding sequence for BPSL1887. PCR conditions were as follows: 20 μL reaction volume, 1.0 μL template K96243 genomic DNA (10 ng/μL), 1.0 μL forward primer (10 mM), 1.0 μL reverse primer (10 mM), 0.4 μL dNTPs (10 mM), 4.0 μL Phusion GC buffer (5X), 1.0 μL DMSO (100%), 0.2 μL Phusion high fidelity DNA-dependent DNA polymerase. PCR cycling parameters were based on "touchdown" PCR,[91] and for the first stage used an initial annealing temp of 65°C, decreasing in regular intervals for 20 cycles to a final annealing temp of 43°C. The second stage of 10

cycles used the specific annealing temp of 45°C. Both stages used an extension temperature of 72°C for 35 sec. PCR products were gel-extracted and then cloned into the pGEM-T easy™ (Invitrogen) vector using the manufacturer's protocol for TA cloning PCR products lacking endogenous 3' A overhangs. Colonies with disruptions in *lacZα* were stocked, plasmids harvested, and mini-prepped using the QIAGEN Mini-Prep Kit. Plasmids were screened by restriction digest using *Hin*D III and *Sac* II. Appropriate size fragments were gel-extracted, digested with EcoR I, and sub-cloned into pHERD-Km prepared by digestion with *Eco*R I and *Hin*D III.

The *xylE*-integrating vector pCA001 was generated from pMO130 by inserting two adjacent blocks of chromosomal homology into the two restriction sites flanking the *xylE* marker. This design allowed the plasmid to integrate into the chromosome at the orphaned transposase *bpss1519,* and then remove all but the marker upon resolution. The 5' and 3' blocks of chromosomal homology were prepared by PCR amplification from wild-type, white-type K96234 genomic DNA using the following primers: BPSS1519_USF1-ApaI and BPSS1519_USR1-NheI, BPSS1519_DSF3-BamHI and BPSS1519_DSR2-XbaI (Table C.1) in two respective PCR reactions. 20 µL reaction mixes were prepared as follows: 1.0 µL forward primer (10mM), 1.0 µL reverse primer (10mM), 1.0µL of K96243 genomic template (10 ng/µL), 0.4 µL dNTPs (10 mM), 4.0µL Phusion GC buffer (5X), 1.0 µL DMSO (100%), 11.4 µL water, 0.2 µL Phusion high fidelity DNA-dependent DNA polymerase. PCR cycling parameters were based on "touchdown" PCR, and for the first stage used an initial annealing temp of 65°C, decreasing in regular intervals for 20 cycles to a final annealing temp of 55°C. The second stage of 10 cycles used the specific annealing temp of 58°C. Both stages used an

extension temperature of 72°C for 30 sec. PCR products were gel-extracted and then cloned into the pGEM-T easy™ (Invitrogen) vector using the manufacturer's protocol for TA cloning PCR products lacking endogenous 3' A overhangs, and ligations were transformed into chemically competent *E. coli* DH5α. Colonies with disruptions in *lacZα* were stocked, plasmids harvested, and then mini-prepped using the QIAGEN Mini-Prep Kit. Plasmids were screened by restriction digest using *Apa* I and *Nhe* I for the 5' region, and *Bam*H I and *Xba* I for the 3' region. Appropriate size fragments were gel-extracted and used in subsequent cloning steps. The vector pMO130 was digested with *Apa* I and *Nhe* I for receipt of the 5' fragment. The 5' fragment was cloned into pMO130 and ligations were transformed into chemically competent JM109 *E. coli*. Positive clones were identified by restriction digest and prepared for the 3' fragment by digestion with *Bam*H I and *Xba* I. The 3' fragment was cloned into the partially completed vector and transformed also into JM109 *E. coli*. Positive colonies were identified by restriction digest and verified by screening for XylE activity with pyrocatechol as described earlier.[84] A positive integration vector was transformed into electrically-competent *E. coli* S17-1, and 3 positively-selected colonies were stocked and mated with wild-type *B. pseudomallei* K96243 as described earlier,[84] with the minor modification the matings were performed directly on the agar surface without the use of analytical filtration devices. Positive co-integrants were selected on LB agar + 200 μg/mL kanamycin + 50 μg/mL zeocin and identified by screening with pyrocatechol. Single colonies were resolved of the plasmid as described earlier.[84] Clones retaining the *xylE* marker were identified by screening with pyrocatechol and verified for loss of the remainder of the plasmid by verifying sensitivity to kanamycin.

The BPSL1887 knockout vector pMo130::BPSL1887KO was generated from pMo130 using primers BPSL1887KOF1, BPSL1887KOR2, BPSL1887KOF3, and BPSL1887 KOR4 (Table C.1). Primers 1 and 2 were used in one PCR, and Primers 3 and 4 in a second PCR to amplify regions of chromosomal homology for concatenation and insertion into pMo130. PCR conditions are as follows — reaction mix (20 µL reaction volume): 1.0 µL reverse primer (10 mM), 1.0µL template DNA (10 ng/µL), 0.4 µL dNTPs (10 mM), 7.6 µL H_2O, 4.8µL betaine (5M), 4.0µL Phusion HF Buffer (5X), 1.0µL forward primer (10 mM), 0.2µL Phusion high fidelity DNA-dependent DNA polymerase. PCR cycling parameters were based on "touchdown" PCR,[91] and for the first stage used an initial annealing temp of 65°C, decreasing in regular intervals for 20 cycles to a final annealing temp of 55°C. The second stage of 14 cycles used the specific annealing temp of 54.4°C for the 5' region of homology amplified by primers 1 and 2, or 58.4°C for the 3' region of homology amplified by primers 3 and 4. Both stages used an extension temperature of 72°C for 1 min. PCR products were gel-extracted and then mixed in a third "overlap extension PCR" reaction[92] using the following conditions (20µL reaction volume): 10µL Failsafe Buffer J (epicenter) (2x), 1.0µL 5' fragment (30ng/µL), 1.0µL 3' fragment (30ng/µL), 1.0µL primer 1 (10mM), 1.0µL primer 4 (10mM), 5.8µL H2O, 0.2µL Phusion high fidelity DNA-dependent DNA polymerase. Cycling conditions were as follows: 52.2°C for 30 sec, 72°C for 10 min, 98°C for 3 min, 32 cycles of: 98°C for 20 sec, 53.2°C for 30 sec, 72°C for 70 sec, and then 72°C for 10 min and hold at 4°C. Overlap products of appropriate size were gel-extracted and cloned into the pGEM-T easy™ (Invitrogen) vector using the manufacturer's protocol for TA cloning PCR products lacking endogenous 3' adenosine overhangs. Ligations were transformed into

chemically competent *E. coli* DH5α. Colonies with disruptions in *lacZα* were stocked and screened by restriction digest for the appropriate size insert using Not I. Appropriate-sized inserts were sub-cloned into pMO130 prepared by digestion with *Not* I. Colonies positive for the appropriate insert identified by *Not* I digestion were electroporated into *E. coli* S17-1 and the resulting strain used to mate the knockout construct into wild-type, white *B. pseudomallei* K96243. The knockout strain was derived as previously described.[84] The Δ*flgK* mutant was described previously.[84]

The Transposon pTBurk1 was generated from pMar2xT7[93] and pHBurk1[94] by Nick Vitko. The Temperature-sensitive *ori* and kanamycin resistance marker from pHBurk1 were PCR-amplified using primer pairs: pMrT7F and pMrT7R, pMrT7IntF, and pMrT7IntR, respectively (Table C.1). Plasmid pMar2xT7 was digested with restriction enzymes *Bst*Z171 and *Sal* I to remove the ampicillin resistance cassette and replace it with the temperature-sensitive *ori* (oriTS) from pHBurk1, now flanked with *Bst*Z171 and *Sal* I restrictions sites. The subsequent plasmid was then digested with *Sal* I and *Bst*Z171 to remove the gentamicin resistance cassette and replace it with the kanamycin resistance cassette. Sequences of the newly inserted portions of the plasmid were verified by Sanger sequencing at the University of Colorado Cancer Center DNA Sequencing Core.

Transposon Mutagenesis

Transposon mutagenesis was performed as described for pHBurk1[94] with minor modifications. Briefly, an overnight culture of wild-type *B. pseudomallei* K96243 was diluted 1:10 in fresh media and grown for 3 hours at 42°C. Ten milliliters of culture were then pelleted by centrifugation and washed three times with 1.0 mL of 0.3 M filter-sterile

sucrose. Cells were suspended in 100 μL 0.3 M sucrose to which were added 10 ng pTBurk1 prepared by Mini-Prep (QIAGEN). The suspension was mixed briefly, placed into a 2 mm gap electroporation cuvette, and electroporated (25μF, 200 Ω, 2.5 KV). After electroporation, 900 μL of fresh LB was added to the mixture and cells were allowed to recover in outgrowth for exactly 30 minutes at 30°C, at which point they were then diluted 1:5 or 1:10 and spread onto selection agar (LB + 200 μg/mL kanamycin + 50 μg/mL zeocin), and incubated at 37°C until colonies appeared (usually 2-3 days).

Transposon Library Construction

The transposon library used in High-Throughput Insertion Tracking by Deep Sequencing (HITS) was prepared by collecting approximately 25,000 transposon mutants that were mutagenized according to the above procedure. Each transposon mutant was patched from initial selection agar onto a second 10 cm selection agar plate to eliminate background contamination, as satellite colonies that do not passage on selection agar could be isolated on primary selection agar. This is most likely due to the inefficiency of kanamycin for negative selection in *B. pseudomallei*. The patch plates were made at a density of 140 patches per plate. After 48 hours of growth at 37°C, the transposon mutants from each patch plate were collected by scraping. Briefly, 5 mL LB+15% glycerol was added to the surface of the plate and patches were gently scraped with a sterile cell scraper. Once cells were largely suspended and no longer adhered to the surface of the agar, the suspension was pipetted into a 15 mL conical tube. The scraping procedure was repeated and the resulting 10 mL of suspension was vortexed at maximum speed for a minimum of 60 seconds to homogenize the suspension. Each suspension was then pelleted by centrifugation for 15 minutes at max speed. The supernatant was

removed and the resulting pellet was resuspended in 2 mL LB+15% glycerol and placed in a 2 mL cryo vial, then frozen at -80°C until the entire library of 180 lots was collected in an identical manner. Electroporation and selection were repeated as necessary to achieve the complete library, as only a limited number of mutants could be processed before the plates became too old to use.

Once the library was collected, each lot was thawed, and 0.5 mL from one lot was combined into one of 20 modules, with each module containing 0.5 mL each from 9 lots. Each module was then split into two 2 mL aliquots, and 0.5 mL from one aliquot of each module was mixed into a final library containing all mutants. The modules were frozen, and an aliquot of the final library was diluted to an OD_{600} of 0.10 with LB + 15% glycerol, and aliquots of 1.0 mL were frozen as single use aliquots.

Clonal Transposon Site Insertion Identification

Transposons that were starkly yellow after initial selection were struck for isolation on a fresh selection agar plate and stocked. The site of transposon insertion for isolated yellow transposons was determined by Arbitrary PCR (ARB PCR) adapted from an unpublished protocol for *P. aeruginosa* for use with pTBurk1 – see Appendix A.

ARB PCR products were Sanger-sequenced by the University of Colorado Cancer Center DNA Sequencing Center at UCD Anschutz using the ARB PCR primer pTBurk1 ARBseq. Flow-grams returned were trimmed for quality and converted to nucleotide sequence, then used as a query in a BLAST search against the *B. pseudomallei* K96243 genome on http://www.burk-holderia.com. Transposon junctions were identified from returned sequence by manual sequence comparison.

High-Throughput Insertion Tracking by Deep Sequencing (HITS)

HITS was performed by Adrienne Zweifel according to a protocol described earlier.[95] Briefly, total genomic DNA (gDNA) from input and output libraries were collected using the QIAGEN DNeasy Blood & Tissue Kit with minor modifications as described above. Sequencing libraries were prepared by first shearing total gDNA using a Covaris focused ultrasonicator to achieve a target fragment size of 200 bp. Fragment ends were repaired using NEBNExt® End Repair Module (New England Biolabs), cleaned using the PCR Purification kit (QIAGEN), and then 3' polyadenylated using Klenow fragment Exo (New England Biolabs). Polyadenylated products were cleaned using PCR Purification kit (QIAGEN), and then ligated to adapter oligonucleotides Read 1 Adapter and Read 2 Adapter (Table C.1) using T4 DNA ligase. Both adapters contained a phosphorothioate bond and a phosphate group indicated with an asterisk (Table C.1). Adapter-ligated fragments of appropriate size were selected by agarose gel electrophoresis and gel extraction for fragments of 200-300 bp in size. Sites of transposon insertion were then enriched by PCR using primers PE PCR 1.0 and HITS PCR 2.0-Indexx 1, 2, 3, 4, or 5 (Table C.1) to allow for multiplex sequencing of multiple libraries. Final sequencing libraries were then purified by AMPureXP® magnetic beads, according to manufacturer's directions.

Sequencing libraries were quantified using the Agilent Bioanalyzer DNA7500 chip, multiplexed, cluster amplified, and sequenced on the Illumina MiSeq platform. High quality sequencing reads containing the Himar1 IR sequence and the adjacent TA were selected from the raw fastq file for analysis. The Internal Repeat sequence was removed from each sequence read, and the processed reads were then mapped onto the *B.*

pseudomallei K96243 reference genome using the program Bowtie2, with local alignment settings and a *k* value of 1.[96] Annotation of TA sites was accomplished using Seqanno — a publically available set of custom Python scripts (https://git-hub.com/brwnj/seqanno) used to characterize specific genomic sequences. Seqanno scripts were used to quantify reads over a given sequence, compile those counts at the gene level, compare results between samples, and add functional annotation using a UniProt flat file for *B. pseudomallei*.

Microarray Analysis

Microarray analysis was performed as described earlier.[85] RNA used in microarray analysis was extracted from WHT and YA cells incubated at 37°C planktonically with shaking for 12 hours post-normalization by OD_{600} to 0.10. Microarray analyses and RNA isolations were performed in triplicate.

RNAseq Analysis

RNA for RNAseq was collected from the *in vitro* stomach model at 24 hours of hypoxic growth from both WHT and YB in triplicate. RNAseq was performed by the Genomics and Microarray Core at the University of Colorado Denver. Samples were pre-processed to remove ribosomal RNA using the MICROB*Express*™ Bacterial mRNA Enrichment Kit (Ambion,® Grand Island, NY) according the manufacturer's instructions. RNA was then precipitated by the same protocol used to precipitate RNA for microarray analysis and the pellet sent to the Genomics and Microarray Core. At the core, samples were processed for 50 cycle, single read analysis (1x50) according to the Illumina TruSeq protocol for indexing and single end read analysis, skipping the steps of the protocol that

call for poly-dT pull-down of mRNAs, as prokaryotic mRNAs are not polyadenylated. Indexed and processed samples were pooled and sequenced on an Illumina GAIIX. Data was analyzed by DNASTAR's ArrayStar software suite, using Reads per Kilobase per Million mapped (RPKM) normalization, excluding reads for ribosomal RNA and transfer RNA. Data reported is the linear-normalized read count ± the standard deviation per gene as determined by ArrayStar.

Whole Genome Sequence Analysis

Genomic DNA from YA, YB, and two WHT revertants of YA: YAr3.1 and YAr4.1 was collected by phenol: chloroform extraction and purified by Cesium chloride density gradient ultracentrifugation. DNA was precipitated, washed, and resuspended in TE pH 8. 0. Purified genomic DNA was sent to the Keim laboratory at Northern Arizona University for high throughput sequencing on the Roche 454 platform. Data was returned and analyzed by Gareth Highnam in the Mittelman laboratory at Virginia Tech using the -*mpileup* command in the genome sequence analysis software package, SAMtools.[97] Phred-linked p-values (*PL* values) were converted to probability values (*p* values) using the following formula: $p = 100 * 10^{-PL/10}$. *P* values greater than or equal to 90% were considered high quality, statistically significant genotype identities. Lower quality PL values were discarded. Because SAMtools does not consider haplotype genotypes, heterozygous genotype identifications were treated as indicative of mixed populations of mutant and reference genomic sequence at the identified site. Indel mutations in homopolymeric repeat tracts were manually filtered out as 454 sequencing analysis does not reliably distinguish mutations in homopolymeric repeat tracts. Remaining mutations were analyzed for correlation with phenotype, assuming YA would be mixed in sequence

(heterozygous alternate), YB would be completely mutant sequence (homozygous alternate), and the revertants would be completely reference sequence (homozygous reference). When no mutations were identified that correlated with phenotypes, polar mutations were considered as alternate explanations for variant and revertant phenotypes.

CHAPTER III

A COLONY VARIANT OF *B. PSEUDOMALLEI* IS RESPONSIBLE FOR PERSISTENT GASTRIC COLONIZATION IN CHRONIC MURINE MELIOIDOSIS

Introduction

Colony variants of *B. pseudomallei* are most frequently isolated from infected patients; however they can also be isolated from *in vitro* conditions. Previously reported methods for *in vitro* isolation of colony variants called for weeks-old settled cultures of bacteria. A settled growth model is a model system with several uncontrolled variables. Possible contributors to emergence of variant phenotypes in this model include, but are not limited to: nutrient starvation, hypoxia, progressive expression of motility and/or pellicle formation, or accumulation of metabolic waste products. Utilizing a hypoxic growth system model, we demonstrate isolation of colony variants from relatively young,

agitated cultures wherein the primary limiting factor was the capacity for aerobic respiration.

Further complicating a thorough understanding of *B. pseudomallei* colony variants is the lack of any significant differences observed to date in virulence when tested in animal models. Utilizing an oral infection model for chronic murine melioidosis, we demonstrate that one of the variants displayed a significant difference in virulence. This variant also had the capacity to establish a persistent colonization of mouse stomachs without overt signs of disease. Making use of an *in vitro* model growth system, we describe some of the possible mechanisms employed by the colony variant used to establish gastric colonization.

Isolation of Colony Variants

We observed that respiration-limiting conditions allow for emergence of yellow colony variants from cultures in which only white colony morphotype bacteria could initially be observed (Figure 3.1). Other stresses, such as addition of antibiotics, heat shock, inhibition of cell wall synthesis by antibiotics, nutrient starvation, or iron starvation did not allow for conversion of white to yellow type or expansion of yellow type bacteria (data not shown).

When a population of predominately white phase bacteria was placed under hypoxic conditions, yellow colony variants were isolated in increasing frequency as cultures were continually exposed to low oxygen conditions (Figure 3.1). However, the kinetics of variant emergence varied with technical repetition of the experiment: up to 48 or 72 hours or longer (data not shown), indicating that although the physiological changes that manifested as altered colony morphology provided an extreme advantage under

hypoxia, lack of oxygen was not the primary environmental signal or trigger for induction of the phenotype. This observation also indicated that the initial switch to the yellow forms was likely a stochastic event and the amount of time for significant yellow variant emergence was likely determined by the number of yellow variants in the original inocula.

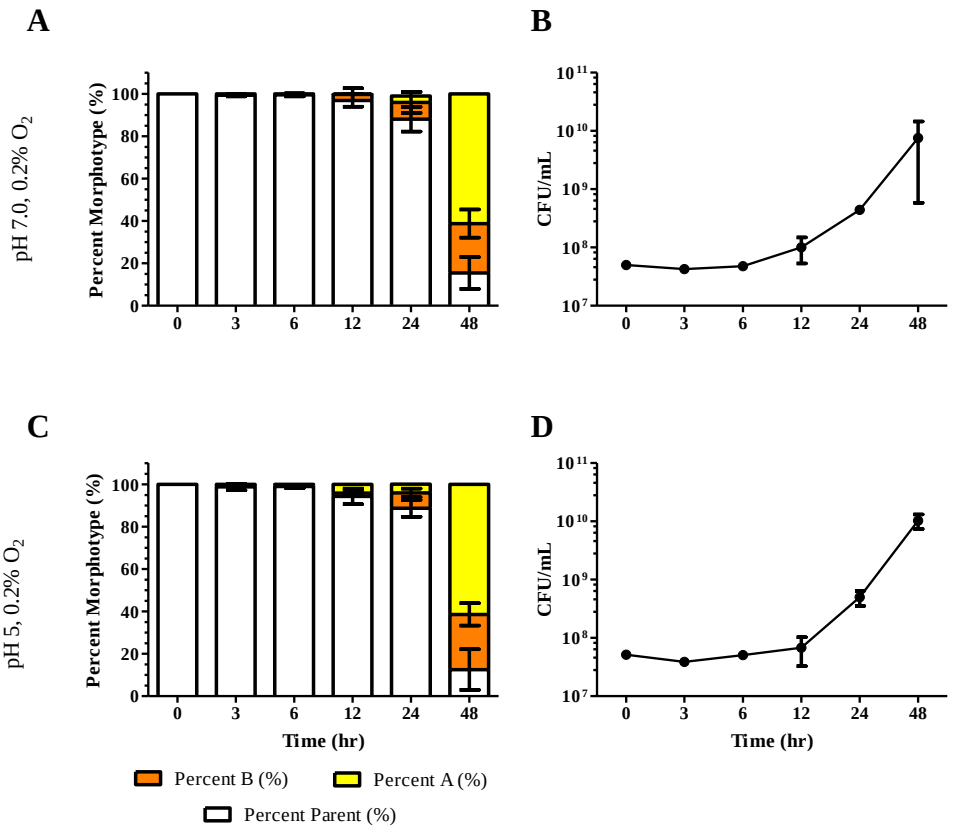

Figure 3.1 Emergence of Yellow Variants under Hypoxic Conditions
White-type, wild-type *B. pseudomallei* K96243 was used to inoculate LB at pH 7.0 or 5.0 at an OD_{600} of 0.1. Each culture was placed in a glass tube fitted with a stir bar, vented, and placed in a hypoxia chamber with oxygen tension set to 0.2%. At 3, 6, 12, 24, and 48 hours following entrance into a hypoxic environment, colony type distribution in the culture was determined (A and C) and CFU/mL calculated (B and D).

Yellow Variant Reversion Kinetics and Colonial Morphology

Identification and characterization of yellow variants revealed significant changes in bacterial physiology relative to parental type bacteria. Beginning only with the parental white colony morphotype, we isolated two colony variants and both were yellow on LB agar (Figure 3.2) — one with a smooth, domed, glistening surface, a moderate yellow pigmentation — termed YA, and a relatively high median rate of reversion under well-aerated logarithmic growth conditions (0.15 ± 0.05 changes per cell per generation), and under hypoxic conditions a lower rate of reversion (median 0.06 ± 0.04 changes per cell per generation) (Table 3.1). The second, termed YB, was darker in pigmentation, had a mounded, umbonate center, a clearly defined margin (Figure 3.2), a lower rate of reversion (0.005 ± 0.06 changes per cell per generation) under highly aerated conditions and 0.012 ± 0.03 changes per cell per generation under hypoxic conditions (Table 3.1) These representative colony types were isolated *in vitro* under conditions of respirative stress: hypoxia and nitric oxide stress described in previous publications.[85,98]

YA and YB had moderately slower maximum doubling times under aerobic conditions relative to the parental form. YA had a median doubling time of 70.4 minutes, YB had a median doubling time of 69.9 minutes, and the white form had a median doubling time of 63.6 minutes (Table 3.1) ($p < 0.05$ for both pairwise comparisons).

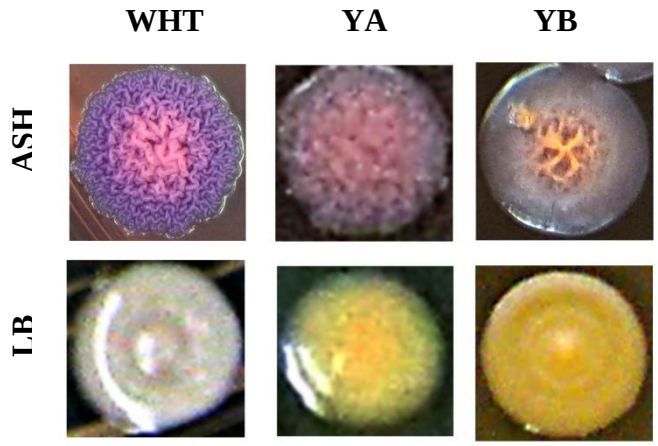

Figure 3.2 Photographs of Representative Colony Variants.
White (left), YA (center), and YB (right) on Ashdown's Agar (top) or LB agar (bottom) grown for 72 hours at 37°C.

Yellow Variant Growth Advantage under Hypoxic Growth Conditions

Since yellow variants were initially isolated under conditions of limited respiration, we sought to determine if they possessed a competitive advantage under growth conditions limited for oxygen. Because yellow colony variants revert at relatively high rates, obtaining accurate competition kinetics without an integrated genomic marker would not have been possible. To overcome this, a white-type strain of *B. pseudomallei* with an integrated genomic copy of the visual marker *xylE* was generated. Competitions with the white, *xylE*$^{+}$ strain were performed with WHT, YA, or YB and the mixture was placed under hypoxic conditions in acidified growth medium (pH 5.0). We observed that predominance in the culture by yellow variants YA and YB increased from 1% of the population at the beginning of the experiment to over 40% by 48 hours under hypoxic conditions (Figure 3.3, top). This increase in percent yellow variant was significant: $p = 0.0002$ (***) for YA compared to WHT at 48 hours, $p = 0.0038$ (**) and at 24 hours, $p = 0.017$ (*) at 12 hours. For comparisons of YB to WHT, $p = 0.029$ (*) at 48 hours, $p = 0.013$ (*) at 24 hours, and $p = 0.04$ (*) at 12 hours. The diminished significance in YB

competitions is due to the larger standard deviation measured in these experiments. The increase in yellow variants was always due to an expansion of the original yellow variant minority except when the *xylE*$^{+}$ strain was mixed with the parental white strain – in that scenario, yellow variants arose from white *xylE*$^{+}$ bacteria that were the primary variant in the culture; white *xylE*$^{-}$ bacteria were not present in sufficient number to observe emergence of variants in this model. There was no competitive advantage for YA, YB, or the unmarked white-type bacteria under well-aerated conditions and no competitive advantage for the *xylE*-marked or unmarked white-type bacteria under hypoxic and acidic conditions (Figure 3.3, bottom).

Table 3.1 Reversion Rates of Colony Variants in Two Model Growth Systems

Colony Type	Doubling Time (min) (aerobic model)	Growth Rate Constant (*g*) (aerobic model)	Reversion Rate (aerobic model)	Reversion Rate (hypoxic model)
White	63.6	0.013 ± 0.0020	-	N/A
YA	70.4	0.011 ± 0.0017	0.15 ± 0.05	0.041 ± 0.02
YB	69.9	0.011 ± 0.0016	0.0049 ± 0.059†	0.008 ± 0.03†

†YB bacteria revert to YA bacteria

Yellow Variant Media Alkalization

In addition to the hypoxic growth advantage, we observed that planktonic cultures of YA and YB became alkaline late in stationary phase, whereas the parental white type remained at a neutral pH throughout its growth cycle (Figure 3.4). Hypothesizing that this shift in pH by the yellow variants could provide an advantage under acidic conditions such as the stomach, we chose to investigate the phenomenon. WHT-, YA-, and YB-type colonies were grown planktonically in moderately acidified rich media (LB, pH 5.0) and

observed that YA and YB neutralized the acid in the culture and alkalized the culture to pH 8.6 by 48 hours of growth (Figure 3.4 B) whereas the white morphotype shifted the pH only to approximately 6.5 within the same time frame (Figure 3.4 B). This difference was significant: comparison of YA to WHT at experimental endpoint by the unpaired, two-tailed Student's T test shows $p < 0.001$, and $p < 0.001$ for YB compared to WHT at the same time as well.

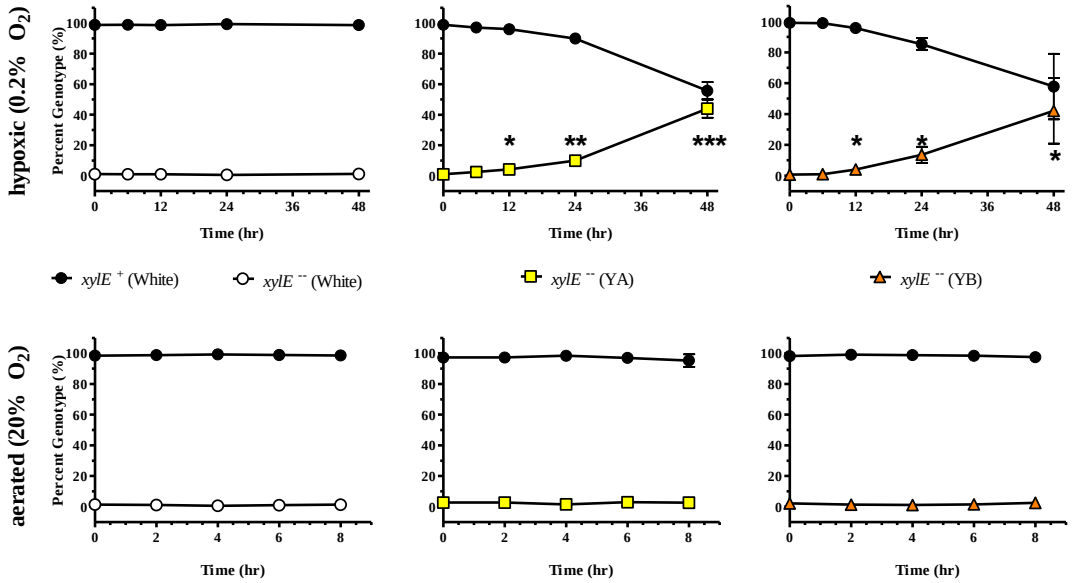

Figure 3.3 Competitive Advantage of Yellow Variants under Hypoxic Conditions
Wild-type WHT (○), YA (□), or YB-type (△) bacteria were added to a *xylE*-marked WHT strain (●) at 1% of the population. Cultures were grown under hypoxic (top), or aerobic (bottom) conditions and percent composition of the mixtures by genotype was determined at 0, 6, 12, 24, and 48 hours for the hypoxic cultures and 0, 2, 4, 6, and 8 hours for the aerobic cultures. Statistical significance was determined by comparing percent genotype of yellow variant competitions against white variant competitions at each time point using the unpaired, two-tailed Student's T test. *(YA, 12 hr) $p = 0.0168$, *(YB, 12 hr) $p = 0.0397$, *(YB, 24 hr) $p = 0.0397$, *(YB, 48 hr) $p = 0.0292$, **(YA, 24 hr) $p = 0.0038$, *** (YA, 48 hr) $p = 0.0002$, $n = 3$ for all.

Ammonia is a common byproduct of bacterial growth on amino acid-rich media, and its production is a mechanism for acid neutralization employed by other stomach-tolerant bacteria.[99] If present in supernatants of cultures of yellow variants, it could potentially explain the observed increase in the culture pH of yellow variants. Because of this, we measured ammonia levels at experimental end-points and observed that white morphotype cultures produced large amounts of ammonia as a byproduct of growth on rich medium – to 73.9 (± 5.8) mM NH_3 (Figure 3.4 C). Unexpectedly, the yellow variants produced significantly less ammonia under the same conditions with YA producing 21.3 (± 2.5) mM NH_3 and YB producing 23.0 (± 2.6) mM NH_3 (Figure 3.4 C) above a background level of 1.8 ± 0.1 mM NH_3 produced abiotically in un-inoculated LB. This effect was significant: comparison of ammonia levels in WHT supernatant compared to YA by the unpaired, two-tailed Student's T test produced $p = 0.0001$ for the comparison of WHT to YA and $p = 0.002$ for the comparison of WHT to YB. YA and YB were capable of producing ammonia to the same degree as the white morphotype bacteria when grown in defined media using amino acids as the only carbon and nitrogen source (data not shown), indicating that yellow variant bacteria were not deficient in ammonia production or growth on amino acids via deamination/deamidation.

Oral Infection Animal Model: Animal Survival and Bacterial Burden

Since both hypoxia and acid stress are hallmarks of the stomach niche environment, and the stomach is one of very few sites in healthy individuals with both selective pressures, we chose to determine if yellow colony variants of *B. pseudomallei* were forms capable of establishing chronic gastric colonization in an ingestion model of chronic murine melioidosis. WHT, YA, or YB (approximately $1x10^4$ CFU of each) were

used to infect BALB/c mice orally (n = 10) (Figure 3.5 A). Mice were monitored for 66 days and mice reaching the pre-determined morbidity were euthanized. Infection with the WHT morphotype produced severe acute disease and mortality in 50% of mice by day 12. Infection with the YA morphotype produced a trend towards more severe acute disease resulting in 70% of mice dying by 12 days post infection (p = 0.34) (Figure 3.5 A). In contrast, infection with the YB morphotype typically resulted in a latent colonization and delayed presentation of melioidosis with only 2 in 9 mice developing acute disease and these relatively late in the model with one mouse succumbing at day 14 (Figure 3.5 A), another at day 28 and with one mouse exhibiting signs of systemic melioidosis at the experimental endpoint (Figure 3.5 A). This difference in acute lethality for YB was significant compared to the YA strain (p = 0.01), and a trend was observed compared to the WHT strain (p = 0.14).

To identify sites of bacterial persistence following oral infection, bacterial burdens in mice surviving to day 66 or 71 (n = 3-5 per strain) were determined. All tissues from survivors infected with the WHT or YA morphotype were negative for colonies of *B. pseudomallei* (Figure 3.5 B). Three of the six surviving mice infected with the YB morphotype were positive for colonies of *B. pseudomallei* in both stomach and feces; one animal also yielded a liver colonization of 20 CFU (Figure 3.5 B). If the infected animals are considered in two groups: infected with YB and infected with a strain that is not YB, and the number of animals developing chronic GI carriage and shedding are counted (i.e. 0/20 for those not infected with YB, and 3/9 for those infected with YB), YB is statistically more significant at achieving chronic GI carriage and shedding (p = 0.044, Fisher's exact test). Colonies recovered from YB-infected animals

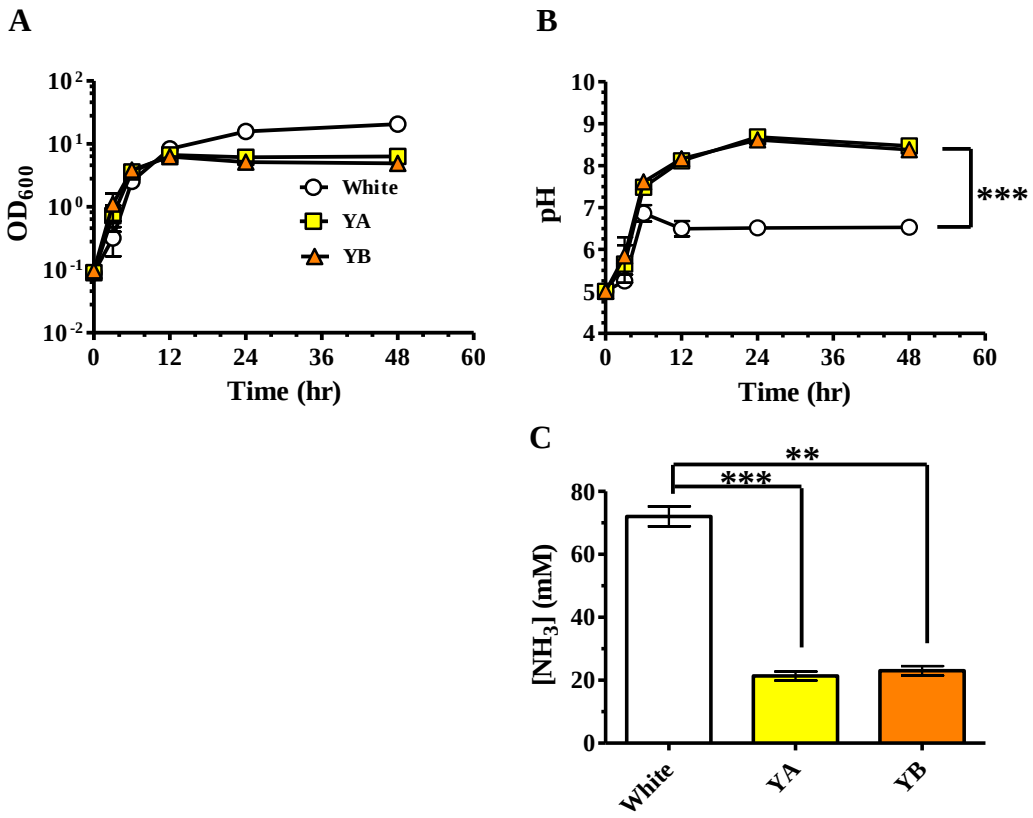

Figure 3.4 Media Alkalization by Yellow Variants without Ammonia Production. WHT (○), YA (□), or YB-type (△) bacteria were grown planktonically in LB pH 7.0 and sampled at 0, 3, 6, 12, 24, and 48 hours for OD_{600} (A) and pH (B). Cultures at experimental end-points were harvested and assayed for ammonia content using an ion-selective electrode (C). Statistical significance for (B) and (C) was determined using the unpaired, two-tailed Student's T test comparing values for yellow variants against values for the white variant. ***$p < 0.001$, $n = 3$ for (B), **$p = 0.002$ and ***$p = 0.0001$ for (C), $n = 3$ for all.

also displayed YB morphology when sub-cultured on LB Agar plates. In summary, changes in colony morphology were associated with changes in virulence and strains which became less acutely virulent were more efficient at persistent colonization, specifically within GI tissues.

Visualization of Infection Foci in YB-Infected Mice

To verify stomach colonization by YB bacteria, stomachs from two mice infected with YB were collected following euthanasia due to development of chronic disease (day 30 and day 66) and washed. Washed tissues were fixed, sectioned, and stained with FISH probes and inspected by fluorescence microscopy (Figure 3.6 A and B). Four different sites in the stomach – one in the antrum and three in the corpus of the two animals were identified by FISH as positive for *B. pseudomallei* (Figure 3.6 D). Bacteria appeared to be grouped together in a microcolony. This community was observed to be lumenal to the gastric mucin layer and loosely associated with the gastric epithelium (Figure 3.6). The bacterial community was also observed to be surrounded by a blue fluorescent signal indicating the presence of a DAPI staining–material. DAPI is highly specific for DNA, thus the presence of extracellular DNA (eDNA) in association with the bacteria (Figure 3.6). Antisense FISH probes did not yield fluorescence signal (Figure 3.6 C) indicating that fluorescence signal from the proper sense probes was, in fact, due to them binding their target sequences and not non-specific binding.

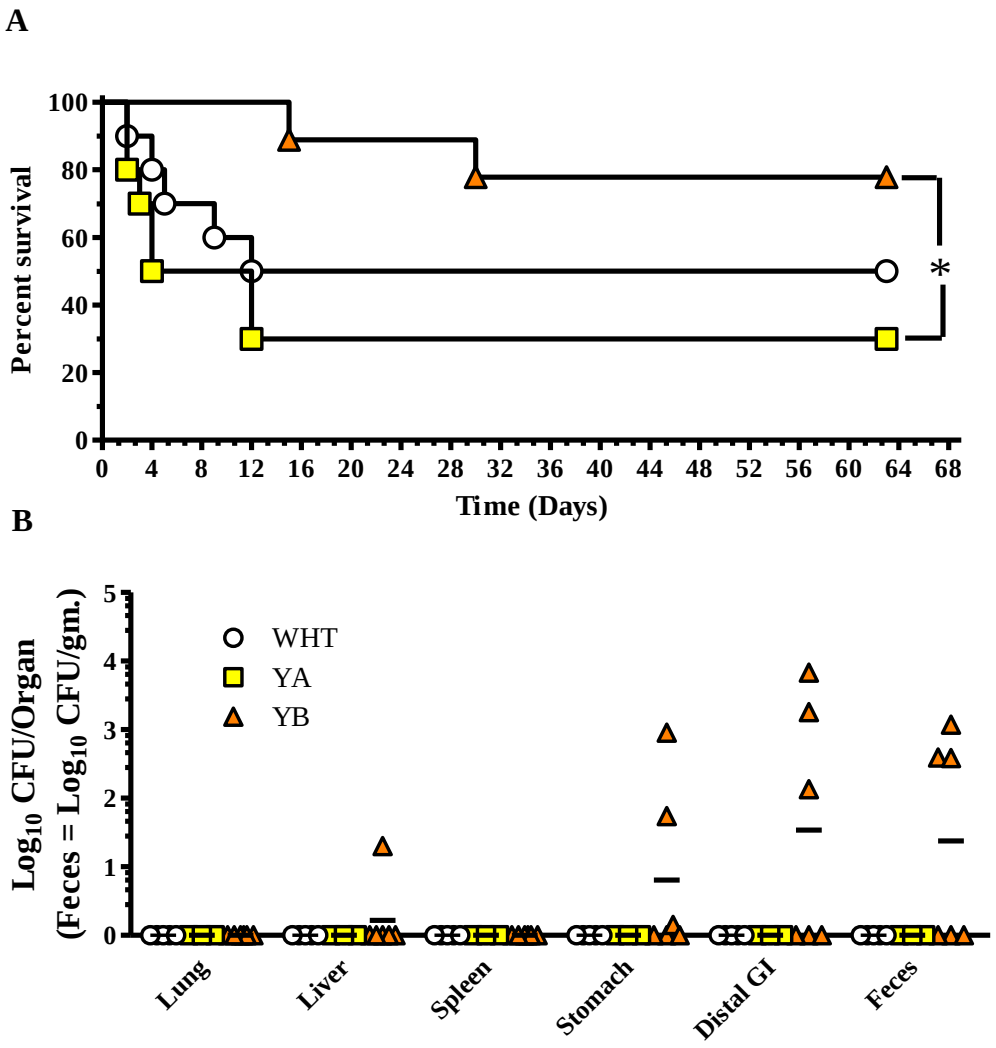

Figure 3.5 Oral Infection, Animal Survival and Bacterial Burden
A) BALB-c mice (n = 10 per group) were infected with ~10^4 CFU *B. pseudomallei* orally (WHT 2.2×10^4 CFU (○); YA 8.3×10^3 CFU (□); YB 5.7×10^3 CFU (△)) by the Dow laboratory at Colorado State University. Mice were monitored for survival and humanely euthanized upon reaching a pre-determined morbidity. Statistical differences were determined using log rank analysis. The Bonferroni correction for multiple comparisons was applied, and p values ≤ 0.017 were considered significant. Data were pooled from two independent experiments. *p = 0.01 between YA and YB. (B) Bacterial burdens were determined in mice surviving to day 66 or 71 post infection (WT n = 5; YA n = 3; YB n = 6). Data were graphed as individual values with bars representing the mean $\log_{10}$ CFU/organ titer (Feces = $\log_{10}$ CFU/gram).

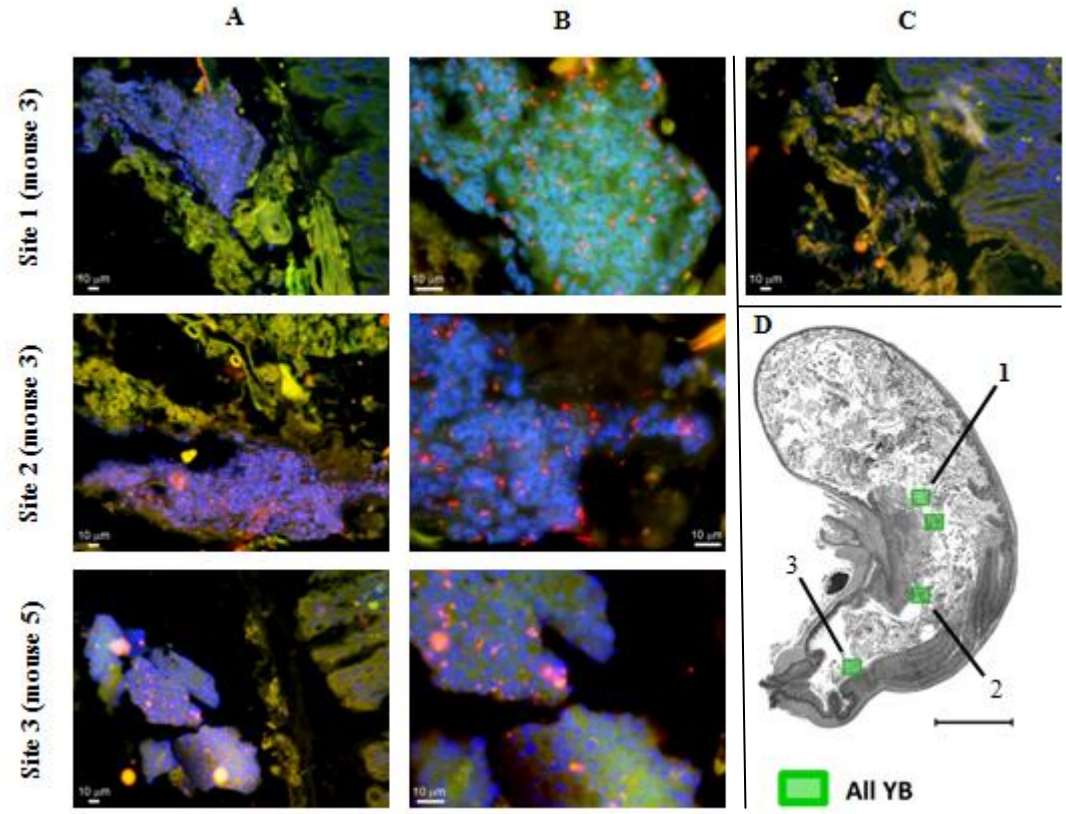

Figure 3.6 FISH Analysis of YB-Infected Mouse Stomachs.
BALB-c mice infected with YB variant *B. pseudomallei* orally, and were euthanized upon reaching a pre-determined morbidity endpoint (day 66 for mouse 3 and day 30 for mouse 5). Stomach tissues were fixed in 10% NBF, embedded in paraffin, sectioned, and all sections stained with FISH probes by the Dow laboratory. Four sites in two animals were positive for *B. pseudomallei*, labeled red (Bpm427 and Bpm975 probes). Enteric bacteria were labeled green (Eub338 probe), and DNA was stained blue (DAPI). Column (A): images at 200X final magnification. Column (B): images at 1000X final magnification. Panel (C): control image stained with the anti-sense FISH probe (green and red), and DAPI (blue), and captured at 200X final magnification. (D) Sites of *B. pseudomallei* colonization are outlined in green on a representative stomach image generated from merged FISH images. In all fluorescent images the scale bar represents 10 microns; in the representative stomach image the scale bar represents 2 mm.

In vitro Production of eDNA

Many different extracellular polymers can comprise the matrices of different microbial communities but two observations indicated that YB established a microcolony by production of an eDNA matrix: one, the FISH observations revealed eDNA in the microcolony matrix (Figure 3.7), and two: settled *in vitro* cultures of YB (and to a lesser extent, YA) in the presence of the glycoprotein, mucin, were observed to be highly viscous during manipulations. Viscosity in this system was abolished with the enzyme DNase I suggesting the foundation of the extracellular matrix produced by YB was eDNA.

An *in vitro* stomach model was established to investigate the behaviors of colony variants under conditions approximating a mouse stomach at the peak of a meal. This model consisted of gastric mucin-coated multi-well plates, a moderately acidic (pH 5.0) rich growth medium (LB), 2.0% oxygen tension, and settled (un-agitated) growth of the bacteria. Production of eDNA by YB in this model was apparently dependent on attachment, as viscosity was not observed in naked wells uncoated with mucin and inoculated with YB (data not shown). The supernatant of well contents was analyzed by extracting supernatant from each well with phenol:chloroform, and analyzing the extracted aqueous phase by agarose gel electrophoresis and ethidium bromide staining. In this analysis, bands from all colony types were observed (Figure 3.7 C, top half). These bands were degraded with addition of DNase I, further confirming the presence of extracellular DNA in the *in vitro* stomach model (Figure 3.7 C, bottom half).

Accumulation of eDNA in coated wells inoculated with YB was significant relative to wells inoculated with WHT. At 24 hours, WHT-inoculated wells had

accumulated an average 1,200 ng eDNA whereas YB-inoculated wells had accumulated 20,700 ng eDNA (Figure 3.7 B). At 48 hours, WHT-inoculated wells had accumulated an average of 500 ng eDNA, but YB-inoculated wells had accumulated an average 33,500 ng eDNA (Figure 3.7 B). The bulk of eDNA accumulation in YB-inoculated wells occurred between 16 and 24 hours (Figure 3.7 B). This coincided with a period when there was no measurable loss of CFU (Figure 3.7 A). Comparison of eDNA production by all three variants by ANOVA over the time course revealed $p < 0.01$ between YB and WHT at 24 and 48 hours but no significant difference between WHT and YA at any point.

The source of eDNA in bacterial biofilms has been an issue of contention. Our data suggests that the source of eDNA - at least in *B. pseudomallei* YB biofilms was due extrusion and not lysis. Although YB did undergo a loss of CFU between 12 and 16 hours of approximately 7.96×10^7 CFU, this (assuming 7.826×10^{-15} g/genome for a 7.25×10^6 bp genome) equated to only 6.23×10^2 ng eDNA and yet we observed an increase in eDNA of 1.88×10^3 ng (the equivalent of 2.4×10^8 genomes) (Figure 3.7 B). The trend of increasing eDNA in YB continued from 12 hours until the end of the experiment at 48 hours and the majority of the eDNA accumulation occurred while there was no drop in CFU (Figure 3.8 A, B, and D). This rate was significant by ANOVA: YB compared to WHT over the time period of 12-24 hours gave $p < 0.001$.

If the observed eDNA were due to lysis, then the living bacteria in the system would have had to produce genomes and their accompanying cellular biomass purely for lysis at an astoundingly increasing rate as described by the exponential regression equation: $y = (5 \times 10^8)/x^{5.87}$ where y = minutes per extracellular genome and x =

minutes under hypoxia (after 12 hours) (r^2 = 0.982). Thus, the bacteria in the system would have needed to generate approximately 7 genomes, and the corresponding bacterial cells, per CFU per hour to produce the observed eDNA from lysis, and all without an apparent drop in live cell titers (Figure 3.8 D) – a feat not matched even by *B. pseudomallei* growing at a minimum doubling time of 63.6 minutes under optimum growth conditions when cell death is minimal.

However, the method used to assess bacterial number in this system had its limitations. Because the model growth system was predicated on settled growth without agitation, it allowed for the development of adherent bacterial communities. Tightly adherent bacterial communities can be very difficult to dissociate and accurately assess for cell number. It is then theoretically possible that the method used to measure live cell titers in Figure 3.8 did not accurately perform its function. However, if the actual CFU were significantly different from the measured CFU at any point, we would have expected large standard deviations in CFU readings between replicate measurements, which we did not observe (Figure 3.8 A). Furthermore, if the foundation of the bacterial community in this model was indeed DNA, pipetting the contents repeatedly (as was performed for the assay) would break the community apart, as DNA is highly sensitive to fragmentation by shearing. Alternative methods of bacterial quantification in microbial communities such as quantitative fluorescence microscopy have been employed by other researchers in different growth systems, but these methods were not available at the facility in which the experiments were performed.

Genes involved in the phenotype of eDNA production have not yet been identified and verified, but transcriptional analysis of yellow variant YB in the *in vitro*

stomach model revealed one gene annotated as a chromosome-partitioning ATPase lacking cis-associated cell division machinery that was up-regulated at 24 hours of growth. This gene, BPSL1137, is a *repA* homologue and was up-regulated almost 36-fold in YB relative to WHT (Table 3.2). BPSL1137 is an attractive target for a DNA-extruding pore, but requires further investigation before any claims can be made. Other genes associated with eDNA in bacterial biofilms are discussed in Chapter VI.

Properties of eDNA

Realizing that the mechanism of eDNA production would likely impact the properties of the eDNA, we sought to perform some preliminary characterization of yellow variant eDNA that would help narrow down possible mechanisms for eDNA production. Analysis of eDNA produced by all 3 forms — the white and two yellow forms — by PCR, showed several sites from both chromosomes present, indicating that eDNA was not polymerized randomly or from a single site in the chromosome. The efficiency of eDNA degradation with DNase I, and staining of eDNA with DAPI indicated the eDNA was double-stranded, as DNase I has extremely low efficiency for single-stranded DNA and DAPI is known to bind best in the minor groove of double-stranded DNA which would largely be absent if the eDNA were single-stranded. In addition to DAPI staining, staining of agarose gels containing eDNA with acridine orange showed fluorescence emission typical of double-stranded DNA and not single-stranded DNA (data not shown). These observations suggest that eDNA produced by yellow variants was both double-stranded, and not from any one specific template site on either chromosome.

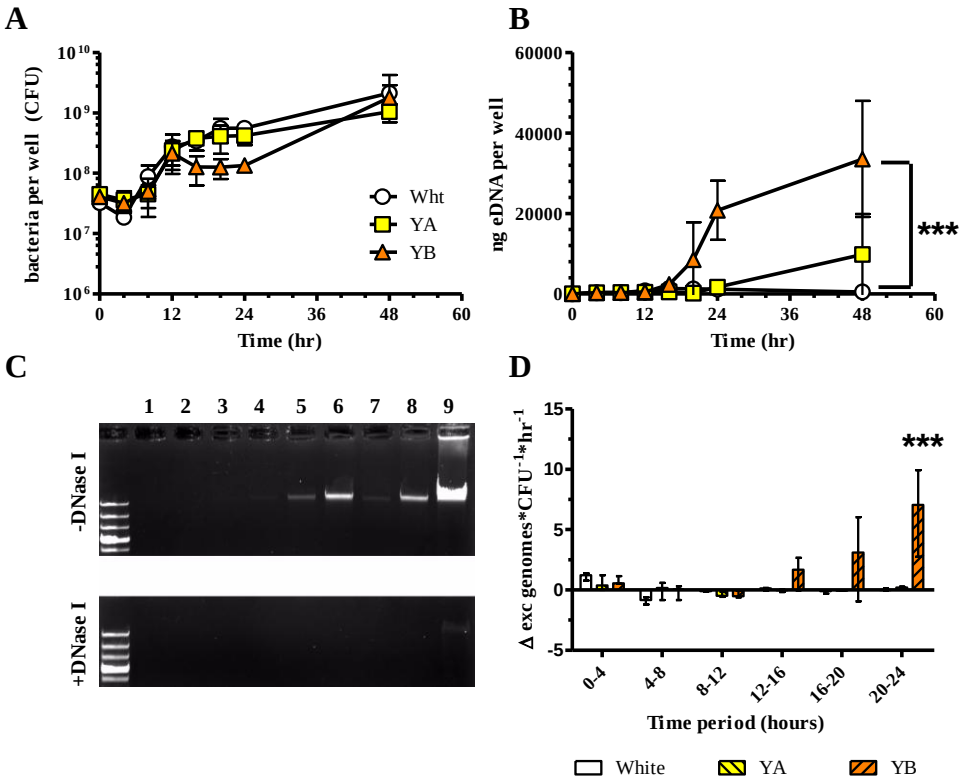

Figure 3.7 eDNA Production in an *in vitro* Stomach Model
Parental WHT (○), YA (□), or YB-type (△) bacteria were grown in an in vitro stomach model consisting of: a moderately acidic growth medium (LB pH 5.0), hypoxic atmospheric conditions (2.0% O_2), on mucin-coated plastic wells without agitation in a 24-well format. Bacterial viability and the presence of extracellular DNA were measured at 0, 4, 8, 12, 16, 20, 24, and 48 hours under hypoxia (A). eDNA from WHT, YA, and YB was quantified by in-gel quantification, staining with ethidium bromide. A representative gel of samples from WHT at 12, 24, and 48 hours (lanes 1, 4, and 7, respectively), YA (lanes 2, 5, and 8, respectively), and YB (lanes 3, 6, and 9, respectively) was stained with ethidium bromide (C); identification of bands staining with ethidium bromide as DNA was verified by digestion of the samples with DNase I for 30 minutes (C, lower panel). Quantities of eDNA were converted to theoretical genomes and the increase in extracellular genomes per CFU per hour was calculated for each time period in the time course (D). Statistical significance was determined of eDNA quantities was determined by ANOVA, n = 3. ***$p < 0.01$

Swimming Motility of Colony Variants

One common behavior conserved across bacterial species that form biofilms is the expression of flagella before attachment, to aid in reaching the surface; and after biofilm development, to aid in dispersal. *B. pseudomallei* is motile and has three distinct genomic regions dedicated to encoding flagellar apparati. We hypothesized that, if YB is indeed the sessile, biofilm-dwelling phase of *B. pseudomallei*, it would have diminished swimming motility under the combination of acid and hypoxia stress. Therefore, we chose to modify the standard motility assay to incorporate a hypoxic environment. Bacteria were placed at the bottom of 0.3% nutrient agar slurry using a hypodermic needle. In this hypoxic motility assay, YB had significantly diminished motility relative to WHT and even further diminished motility with additional acid stress (Figure 3.9 A). This behavior was statistically significant: comparison of WHT to YB swimming motility at pH 5, when stabbed, by the Student's T test yielded $p < 0.001$; and when comparing YB swimming motility at pH 5 and stabbed to pH 7 and spotted yielded $p = 0.0016$.

Transcriptional profiling of WHT and YB type variants in the *in vitro* stomach model revealed flagella and flagella-related genes to be down-regulated in YB almost universally across the genome (Table 3.3). Of the eight flagellar genes up-regulated in YB, only 3 were significantly up-regulated beyond 2-fold: BPSL0269 (*flgA*) (3.1 fold up-regulated), BPSL3293 (*flhF*) (6.3 fold up-regulated), and BPSS0860 (3.0 fold up-regulated) (Table 3.3). As expression of the entire flagellar operon is typically required for expression of functional flagella, it stands to reason that none of these three genes could nullify the hypothesis that motility of WHT and YA was flagella-mediated.

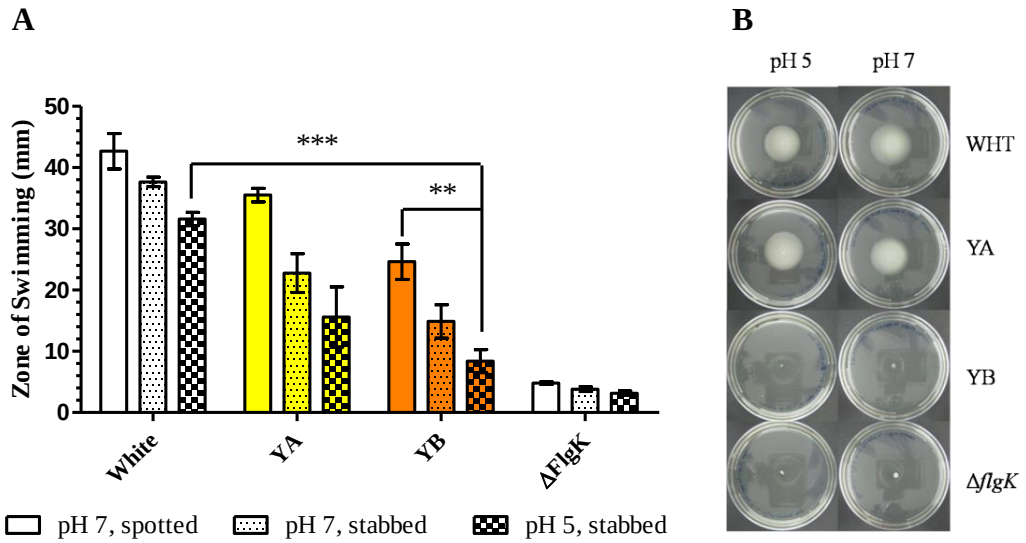

Figure 3.8 Swimming Motility of Colony Variants

Swimming motility of WHT-, YA-, YB-type colony variants, and a Δ*flgK* strain was determined by inoculating 10 cm Swimming Agar plates (0.3% LB Agar, pH 7.0 or pH 5.0) with overnight culture of each. Inoculation was performed either by spotting 2.0 µL of inoculum onto the surface of the plate (empty bars), or stabbing the inoculum to the bottom of the plate using a hypodermic needle (spotted bars for pH 7 agar, checkered bars for pH 5 agar). Plates were allowed to incubate at 37°C for 24 hours and zones of swimming were measured (A). Statistical significance of swimming motility was determined by the unpaired, two-tailed, Student's T test. ***$p < 0.001$, **$p = 0.0016$. Photographs were taken of representative zones of swimming for one of the more pronounced replicates immediately after measuring zones of swimming (B).

Protection from Strong Acid

YB exhibited enhanced protection from the cytopathic effects of Synthetic Gastric Fluid (SGF) when allowed to develop a microbial community (Figure 3.10). In the *in vitro* model of gastric colonization, YB exhibited a significant difference in survival in relation to the white type, exhibiting only a 19.1% loss in the population of viable cells ($p = 0.003$) in the presence of abundant strong acid (Figure 3.10) whereas YA and WHT lost 87.7% ($p = 0.018$) and 96.9% respectively (Figure 3.10). It is worth noting that, in developing the assay, it was observed that if agitated or otherwise disrupted in the presence of strong acid, YB actually had less resilience to acid stress than the other two variants (data not shown).

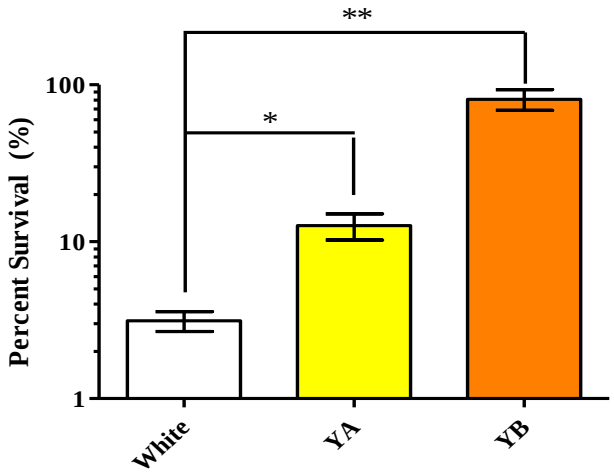

Figure 3.9 Percent Survival of Colony Variants in the Presence of Synthetic Gastric Fluid
Survival of WHT-, YA-, and YB-type colony variants was determined in the *in vitro* stomach model described for eDNA production. Except, at 24 hours of incubation, an equal volume (500 µL) of Synthetic Gastric Fluid (SGF), pH 2.0 was added to each well for 2.5 hours. After incubation in the presence of SGF, acid was neutralized by the addition of sterile bicarbonate and the titers of living bacteria were determined. Percent survival was calculated relative to known bacterial titers for this time point. Statistical significance determined by the unpaired, two-tailed Student's T test, comparing values for yellow variants against the value obtained for the white variant. *$p = 0.0175$, **$p = 0.003$, $n = 3$.

Table 3.2 Expression of Genes Potentially Involved in eDNA Production at 24 Hours of Growth in the *in vitro* Stomach Model Determined by RNAseq

Gene	Name	Product	YB:WHT (Std. Dev.)
FtsK/SpoIII E - like genes			
BPSL2604		DNA segregation ATPase	0.81 (0.01)
BPSL1109		FtsK/SpoIII E ATPase	2.2 (0.1)
Chromosome Partitioning ATPase Proteins			
BPSL1137	*repA*	Chromosome partitioning ATPase	36 (2.4)
BPSL3406	*parA*	Chromosome partitioning ATPase	1.4 (0.0)
Type IV Pilus genes			
BPSL1631		Type IV outer membrane protein	1.9 (0.1)
BPSL3262		plasmid conjugal transfer protein	0.91 (0.01)
BPSL3008		type IV pilus assembly protein	2.5 (0.2)
BPSL3009	*pilC*	type IV pilus assembly protein PilC	- (-)
BPSL3010	*gspO*	type IV prepilin leader peptide type M1	1.3 (0.1)
BPSS1593	*pilV*	type IV pilus biosynthesis protein	0.88 (0.13)
BPSS1594		pilM-like hypothetical protein	0.32 (0.01)
BPSS1595	*pilS*	major pilin subunit	2.8 (0.1)
BPSS1596	*pilR*	type IV pilus biosynthesis protein	1.5 (0.1)
BPSS1597	*pilQ*	type IV pilus biosynthesis protein	0.74 (0.11)
BPSS1599	*pilO*	type IV pilus biosynthesis protein	0.71 (0.06)
BPSS1600	*pilN*	type IV pilus biosynthesis protein	0.42 (0.03)
BPSS1601		type IV pilus biosynthesis protein	2.2 (0.1)
DNA Polymerases			
BPSL1117	*dnaE*	DNA polymerase III subunit alpha	1.1 (0.0)
BPSL0074	*dnaN*	DNA polymerase III subunit beta	1.2 (0.0)
BPSL0472	*dnaE2*	error-prone DNA polymerase	0.99 (0.17)
BPSL0966		DNA polymerase III subunit chi	1.1 (0.0)
BPSL1341	*dnaQ*	DNA polymerase III subunit epsilon	1.1 (0.1)
BPSL1437		DNA polymerase III subunit delta'	2.2 (0.1)
BPSL1498	*dnaX*	DNA polymerase III subunits gamma and tau	1.3 (0.0)
BPSL2306		DNA polymerase IV	0.84 (0.05)
BPSL2556		DNA polymerase/helicase	0.94 (0.01)
BPSL2936	*holA*	DNA polymerase III subunit delta	0.83 (0.01)
BPSS1770	*polA*	DNA polymerase I	2.3 (0.0)
BPSL2183		phage-related DNA polymerase	0.85 (0.01)

RNA was collected in triplicate from bacteria grown in the *in vitro* stomach model under hypoxia (2.0% O_2) at 24 hours of growth and analyzed by RNAseq**.** No values "-(-)" indicate insufficient YB or WHT reads to perform a valid ratio calculation (i.e. divide by zero). Data reported is the RPKM linear-normalized ratio of YB reads to WHT reads with the standard deviation in parentheses.

Table 3.3 Expression of swimming motility genes in the in vitro stomach model

Gene	Name	Product	YB:WHT (Std.Dev.)
BPSL0026	*fliL*	flagellar basal body protein FliL	1.9 (0.0)
BPSL0027	*fliM*	flagellar motor switch protein FliM	2.2 (0.1)
BPSL0028	*fliN*	flagellar motor switch protein	1.6 (0.0)
BPSL0029	*fliO*	flagellar protein	-(-)
BPSL0030	*fliP*	flagellar biosynthesis protein FliP	0.49 (0.03)
BPSL0031	*fliQ*	flagellar biosynthesis protein FliQ	0.78 (0.04)
BPSL0032	*fliR*	flagellar biosynthetic protein	1.7 (0.1)
BPSL0225		flagellar hook-length control protein	0.70 (0.06)
BPSL0226	*fliJ*	flagellar fliJ protein	0.43 (0.09)
BPSL0227	*fliI*	flagellum-specific ATP synthase	0.37 (0.11)
BPSL0228	*fliH*	flagellar assembly protein H	-(-)
BPSL0229	*fliG*	flagellar motor switch protein G	0.63 (0.04)
BPSL0230	*fliF*	flagellar MS-ring protein	0.28 (0.12)
BPSL0231	*fliE*	flagellar hook-basal body complex protein	0.83 (0.03)
BPSL0232	*fliS*	flagellar protein	0.77 (0.00)
BPSL0233		hypothetical protein	0.81 (0.02)
BPSL0267		flagella synthesis protein	0.29 (0.04)
BPSL0268		negative regulator of flagellin synthesis	0.22 (0.03)
BPSL0269	*flgA*	flagellar basal body P-ring biosynthesis protein FlgA	3.1 (0.0)
BPSL0270	*flgB*	flagellar basal-body rod protein FlgB	0.58 (0.07)
BPSL0271	*flgC*	flagellar basal body rod protein FlgC	0.64 (0.01)
BPSL0272	*flgD*	flagellar basal body rod modification protein	0.85 (0.11)
BPSL0273	*flgE*	flagellar hook protein FlgE	0.71 (0.01)
BPSL0274	*flgF*	flagellar basal body rod protein FlgF	0.46 (0.02)
BPSL0275	*flgG*	flagellar basal body rod protein FlgG	1.11 (0.03)
BPSL0276	*flgH*	flagellar basal body L-ring protein	0.58 (0.02)
BPSL0277	*flgI*	flagellar basal body P-ring protein	0.48 (0.04)
BPSL0278	*flgJ*	flagellar rod assembly protein/muramidase FlgJ	1.4 (0.0)
BPSL0280	*flgK*	flagellar hook-associated protein FlgK	0.62 (0.02)
BPSL0281	*flgL*	flagellar hook-associated protein FlgL	0.50 (0.03)
BPSL3291	*fliA*	flagellar biosynthesis sigma factor	1.5 (0.1)
BPSL3292	*flhG*	flagellar biosynthesis protein FlhG	0.35 (0.06)
BPSL3293	*flhF*	flagellar biosynthesis regulator FlhF	6.3 (0.5)
BPSL3294	*flhA*	flagellar biosynthesis protein FlhA	0.92 (0.06)
BPSL3295	*flhB*	flagellar biosynthesis protein FlhB	0.59 (0.00)
BPSL3308	*motB*	flagellar motor protein MotB	0.33 (0.01)
BPSL3309	*motA*	flagellar motor protein MotA	0.49 (0.01)

Gene	Name	Product	YB:WHT (Std.Dev.)
BPSL3319	*fliC*	flagellin	0.16 (0.00)
BPSL3320	*fliD*	flagellar hook-associated protein	0.42 (0.02)
BPSS0860		flagellar hook-associated protein	3.0 (0.0)

RNA was collected in triplicate from bacteria grown in the *in vitro* stomach model under hypoxia (2.0% O_2) at 24 hours of growth and analyzed by RNAseq**.** No values "-(-)" indicate insufficient YB or WHT reads to perform a valid ratio calculation (i.e. divide by zero). Data reported is the RPKM linear-normalized ratio of YB reads to WHT reads with the standard deviation in parentheses.

Discussion

Here we have demonstrated that colony variation — a phenomenon we observed under conditions of restricted respiration — is relevant during infection. The YB variant, derived *in vitro*, was competent for colonization of mouse stomachs when administered orally (Figure 3.5 B). Not only is the variant competent for gastric colonization, it was also fully virulent and capable of inducing fulminant disease: one YB-infected mouse died at day 15 and another at day 30 (Figure 3.5 A). Discovering that YB expressed several unique phenotypes allowed for a more complete explanation for the role of colony variation in gastric colonization. Diminished swimming motility was observed, as well as growth medium alkalization, a hypoxic growth advantage, and production of vast amounts of extracellular DNA.

Establishing a Focal Infection; Sessile and Motile Forms of B. pseudomallei

Persistent gastric colonization was achieved by development of focal bacterial communities in close association with the gastric glycoprotein: mucin (Figure 3.6). If development of a sessile bacterial community was essential to stomach colonization and was the tactic employed by YB to achieve that, we would have expected YB to not

exhibit swimming motility. That is exactly what was observed (Figure 3.8). YB had comparable swimming motility to the parent when inoculated on the surface of swimming agar but when inoculated below the surface of the agar which is a hypoxic environment, had reduced swimming motility. The YB form had even further reduced swimming motility under combination acid and hypoxia condition tested. Intriguingly, YA was not significantly different from the white type in expression of swimming motility under any condition measured (Figure 3.8), suggesting that YB may be the sessile, biofilm-inhabiting form and YA may be a transition form that functions to leave the gastric colony and seed the lower GI tract and eventually exit the body to return to the environment.

The Role of DNA in Developing Bacterial Communities

DNA possesses several properties that can aid in developing focal colonization of the gastric niche including its length, strength of covalent bonds, and adhesive properties. A more thorough discussion of the properties of eDNA and its potential role in gastric colonization is provided in Chapter VI.

Medium Alkalization and Gastric Colonization

Colonization of the gastric niche brings a requirement for addressing the challenges of strong acid. The two primary mechanisms for increasing extracellular pH by stomach tolerant bacteria involve production of ammonia either directly or via excretion of urease to make ammonia from endogenous urea.[99,100] Yellow variants did express genes that can be responsible for ammonia production: BPSL1743 (*arcA*), BPSL1745 (*arcC*), BPSL2925, and BPSS0628 (*glsA*) (Table B.1); but did not produce ammonia (Figure 3.4). It is possible that the *arcDABC* operon does not operate in yellow

variants in the canonical fashion to produce ammonia and perform substrate level phosphorylation of ADP, converting it into ATP. The enzymes of the *arcDABC* operon: carbamate kinase (*arcC*, E.C. 2.7.2.2), ornithine carbamoyltransferase (*arcB*, E.C. 2.1.3.3), and arginine deiminase (*arcA*, E.C. 3.5.3.6) are annotated by the Enzyme Commission as capable of bidirectional function. In this alternative scenario, the bidirectional *arcDABC* operon would function in reverse to transform ammonia into carbamoyl phosphate via BPSL1745 (*arcC*), and then conjugate carbamoyl phosphate to citrulline via BPSL1744 (*arcB*). Arginine would then be made from citrulline and ammonia via BPSL1743 (*arcA*). Arginine would then be converted into putrescine via BPSS0474 (*speB*) (Figure B.1) which was upregulated in both YA and YB (Table B.1). Putrescine as a final output of the urea and ammonia cycle in yellow variant *B. pseudomallei* is an attractive explanation for medium alkalization as it has a high pKa, and can bind DNA, neutralizing the negatively charged phosphate backbone, thus allowing for more compact conformations of eDNA. A polyamine would also not be measured by the ion-selective electrode used to measure ammonia in yellow variant supernatants, potentially explaining the increased culture pH in the absence of ammonia.

However, production of the substrate agmatine from asparagine requires expression of BPSL1003 (Figure B.1), which is not differentially regulated in the three variants (Table B.1), although it is still expressed (data not shown). These observations of gene expression and a lack of excreted ammonia by yellow colony variants warrant further investigation into the roles of polyamine biosynthesis and the *arcDABC* operon in the phenotypes of media alkalization and survival under hypoxic and acidic conditions. A more thorough discussion of acid resistance mechanisms is pursued in Chapter VI.

Stochastic Emergence of the Yellow Variant Phenotype

Emergence of the yellow variant phenotype appeared to be a stochastic event, as emergence kinetics varied with each biological but not technical replicate of the conversion rate experiment, sometimes as much as 48 hours or 72 hours (data not shown). There have been unpublished reports of *B. thailandensis* mutants in quorum sensing genes exhibiting phenotypes similar to YA and YB and to that end, some concern has been raised that expression of the yellow variants can be induced by a signaling event, or is dependent on culture density. The competition experiment (Figure 3.3) demonstrated that emergence of the yellow variant cannot be induced by a signaling event for if that were the case, *xylE*$^{+}$ colonies would present as yellow variants when in competition with YA or YB and that was not ever observed. Yellow variants of *xylE*$^{+}$ colonies could be isolated in competition with the white form, though, further underscoring the stochastic nature of the yellow variant expression.

CHAPTER IV

DIVERGENCE IN COLONY VARIANT PHYSIOLOGY

Introduction

Yellow colony variants of *B. pseudomallei* exhibited several additional physiological differences from their white, parental type than were described in the previous chapter. Investigation of yellow variant physiology using microscopy revealed differential cellular physiology in stationary phase. Yellow variants also strikingly developed toxicity in stationary phase. This toxicity was revealed to be metabolite-dependent. Investigation of this toxicity revealed a number of unique secreted products in yellow variant supernatants, some of which intriguingly possessed properties of UV fluorescence. Observation of these physiological differences in yellow variants revealed that yellow colony variants differed from white variant bacteria in far more than surface molecule expression.

Differential Microscopic Cellular Physiology in Yellow Variant Bacteria

Both yellow colony variants exhibited an alternative physiology in stationary phase: white form *B. pseudomallei* were observed to round up and develop a phase-bright appearance in stationary phase, while yellow form bacteria remained rod-shaped and free of phase-bright appearance (Figure 4.1). A phase-bright appearance is indicative of accumulation of the energy storage polymer β-polyhydroxybutyrate (PHB),[101] which is considered a hallmark of *B. pseudomallei*.[102,103] In addition to microscopic observations, transcriptional profiling of the white and yellow forms demonstrated genes responsible for production of PHB to be up-regulated in the white form and down-regulated in the yellow forms (Table B.2). Specifically, the genes responsible for PHB production: BPSL1535 (*phbA*), BPSL1536 (*phbB*), BPSS1916 (*phbB*), and BPSL534 (*phbC*) were all up-regulated in the WHT type relative to YA during planktonic growth in early stationary phase and all but BPSL1535 (*phbA*) and BPSL1534 (*phbC*) were up-regulated in WHT relative to YB in the *in vitro* stomach model (Table B.2) although the genes were still strongly expressed in WHT (data not shown). The observation of phase-bright appearance, in combination with decreasing surface area by rounding, indicated adoption of dormancy as a strategy by the white form for survival under typically growth-limiting conditions. Failure to accumulate PHB was indicative of alternative survival strategies for limiting growth conditions.

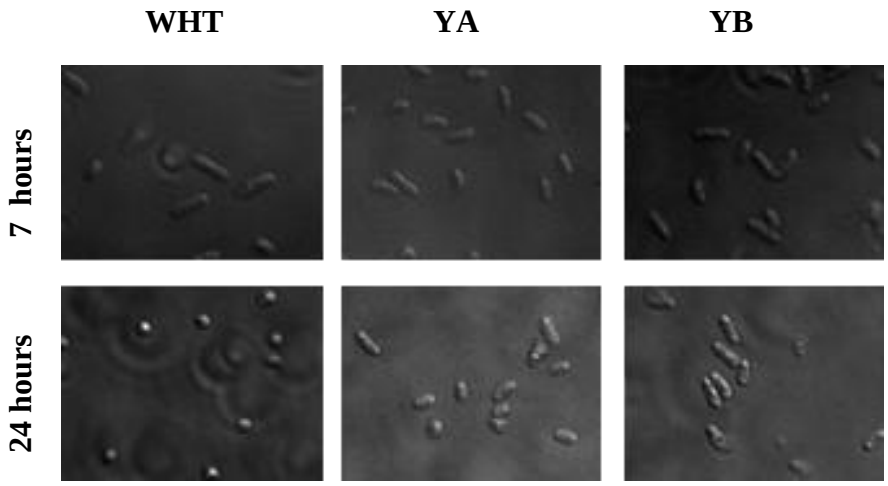

Figure 4.1 Phase Contrast Microscopy of Colony Variants in Logarithmic and Stationary Phase.
WHT- (left), YA- (center), and YB-variant (right) bacteria were sampled from growth rate cultures in logarithmic growth (upper panel) (7 hours) and stationary phase (lower panel) (24 hours). Samples were washed in PBS and applied to glass microscope slides coated with poly-L-Lysine using mounting media then visualized at 1000 x magnification, using an oil immersion lens and a phase contrast filter.

Toxic Effect of Yellow Variants

Yellow variants produced a toxic effect in stationary phase. This was first observed by a precipitous decrease in bacterial viability beginning at 14 hours and sometimes achieving complete sterilization by 48 hours (Figure 4.2). Toxicity was repeatedly observed in a number of different growth experiments but with a great deal of variability in the degree of bacterial death (data not shown).

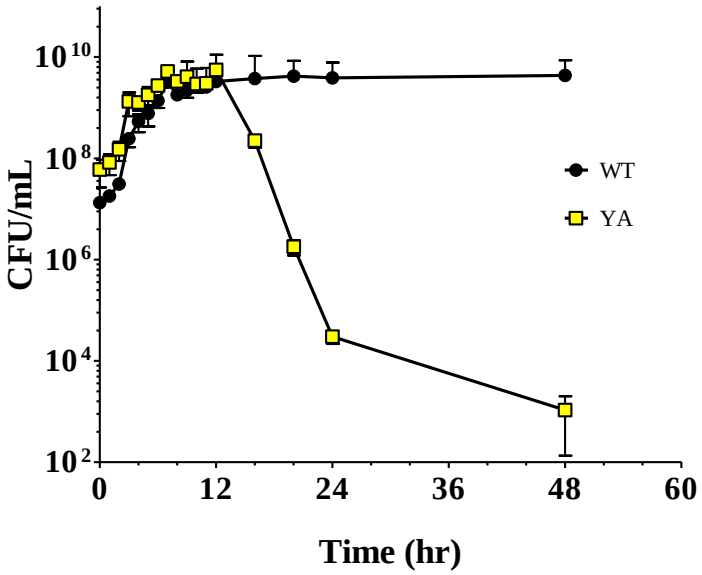

Figure 4.2 Production of Toxic Effect by Yellow Variants in Stationary Phase
Growth curves of WHT and YA-type bacteria were performed in LB by Amanda Stewart and Martin Voskuil. Bacteria were normalized to the same initial density then grown at 37°C with shaking. Cultures were sampled every hour for 24 hours and assayed for CFU/mL. Data reported is the average of two biological replicates, ± the standard deviation, n = 2.

Growth Medium Dependency of Yellow Variant Toxic Effect

In order to establish if the toxic effect of yellow variant *B. pseudomallei* was media-specific or a more general phenomenon, bacteria were grown in a variety of rich media. Toxicity was observed again in LB (Figure 4.3 A). Growth of yellow form bacteria in other rich, complex media: tryptic soy broth (TSB), brain-heart infusion broth (BHI), and liver infusion broth (LIB) also produced the toxic effect (Figure 4.3 B-D, respectively) indicating that the toxic effect was not an artifact of growth in LB.

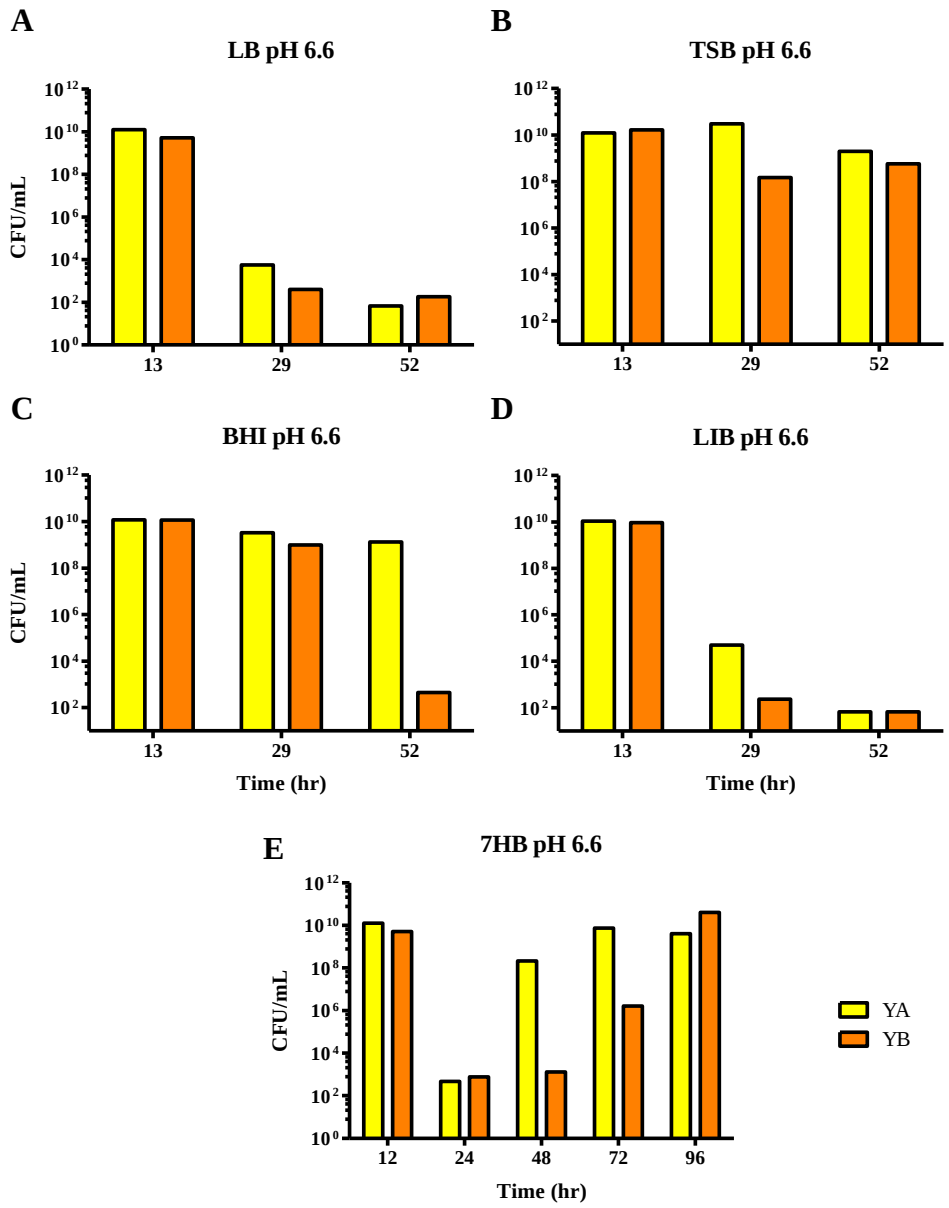

Figure 4.3 Growth Medium Dependency of Yellow Variant Toxicity
Yellow variants YA (yellow) and YB (orange) were grown in (A) Lennox Broth (LB), (B) Trypticase Soy Broth (TSB), (C) Heart-Brain Infusion (HBI) broth, (D), Liver Infusion Broth (LIB), or *Burkholderia*-adapted Middlebrook 7H9 (7HB), and assayed for CFU/mL at 13, 29, and 52 hours post-normalization of OD_{600} from logarithmically growing cells (n=1)

Interestingly, toxicity in TSB was not pronounced, did not reach sterilizing levels of toxicity, and yellow variants rebounded in viability. Manifestation of the toxic effect was also observed in the semi-defined medium, 7HB (Figure 4.3 E).

Stabilization and Ablation of Toxicity Production

Since toxicity of yellow variants was frequently observed to be variable, we sought to stabilize production of yellow variant toxic effects. Preliminary gene expression profiling of the YA variant revealed up-regulation of several genes involved in the tricarboxylic acid (TCA) cycle and one gene involved in gluconeogenesis (BPSL2547 (*fbp*)) (Tables B.3 and B.4). These observations suggested a strategy of glycolysis for energy production in white variant bacteria and TCA operation for energy production in yellow variant bacteria. Hypothesizing that these behaviors could be stabilized by addition of metabolites feeding directly into either pathway, we chose to add either a combination of glucose and glycerol, or a combination of pyruvate and succinate to bacterial cultures to determine if toxicity could be stabilized. Indeed, production of toxic effects of yellow colony variants was ablated with addition of glucose, or glycerol (Figure 4.4 A), and was enhanced and stabilized by addition of pyruvate and succinate (Figure 4.4 B), resulting in no countable colonies, even if an entire milliliter of culture was plated for CFU. In fact, addition of pyruvate and succinate consistently produced total sterilization of cultures under repeated trials (Figure 4.5) ($p < 0.001$, two-way ANOVA). Pigment production in planktonic cultures appeared to be ablated with addition of glucose or glycerol (not pictured).

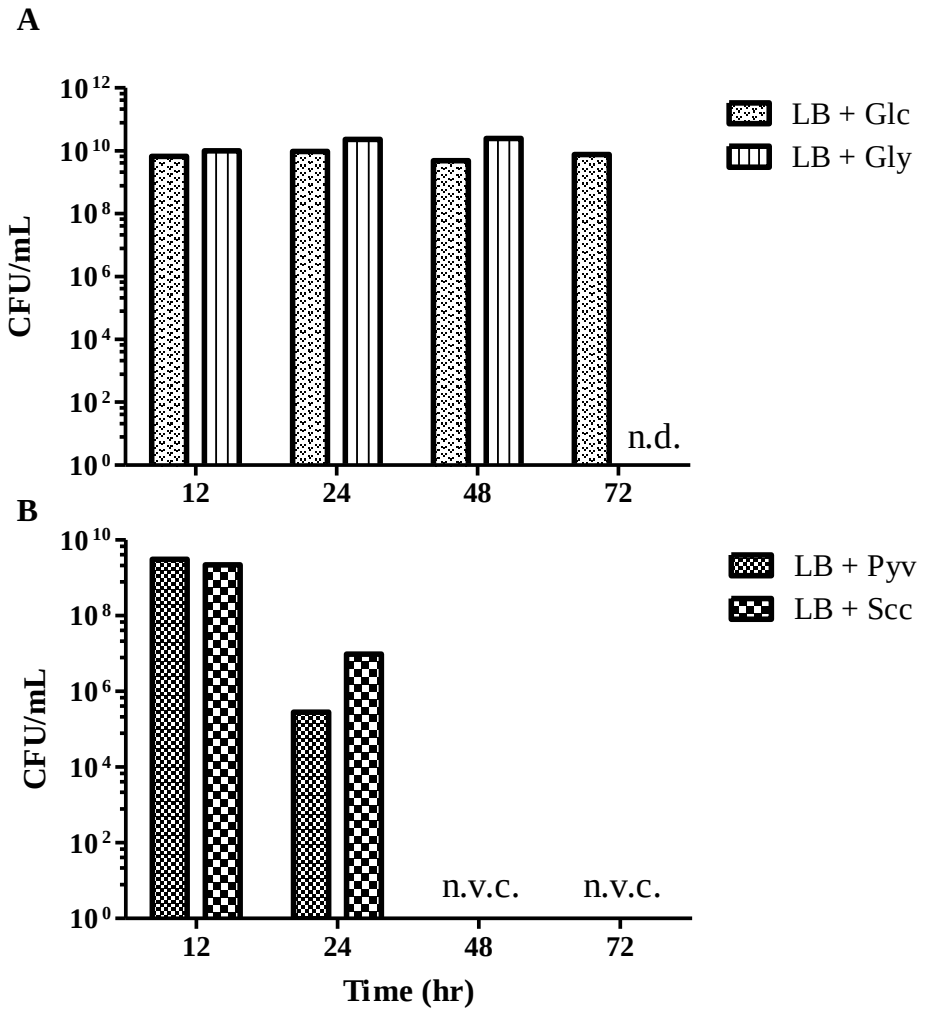

Figure 4.4 Addition of Glucose or Glycerol Ablated Toxic Effect; Addition of Pyruvate or Succinate Enhanced Toxic Effect

Yellow variant YA was grown in LB + 2% D-glucose (LB + Glc) or LB + 2% glycerol (LB + Gly) (A), in LB + 2% pyruvate (LB + Pyv) or LB + 2% succinate (LB + Scc) (B) using the same procedure described for observation of toxicity in other media. Viability of the bacteria was assessed by CFU at 12, 24, 48, and 72 hours for LB + Glc, LB + Pyv, and LB + Scc. Viability was assessed by CFU at 12, 24, and 48 hours for LB + Gly. "n.v.c." indicates no viable bacterial colonies were observed after plating 1.0 mL of culture on LB agar and incubation at 37°C for 48 hours.

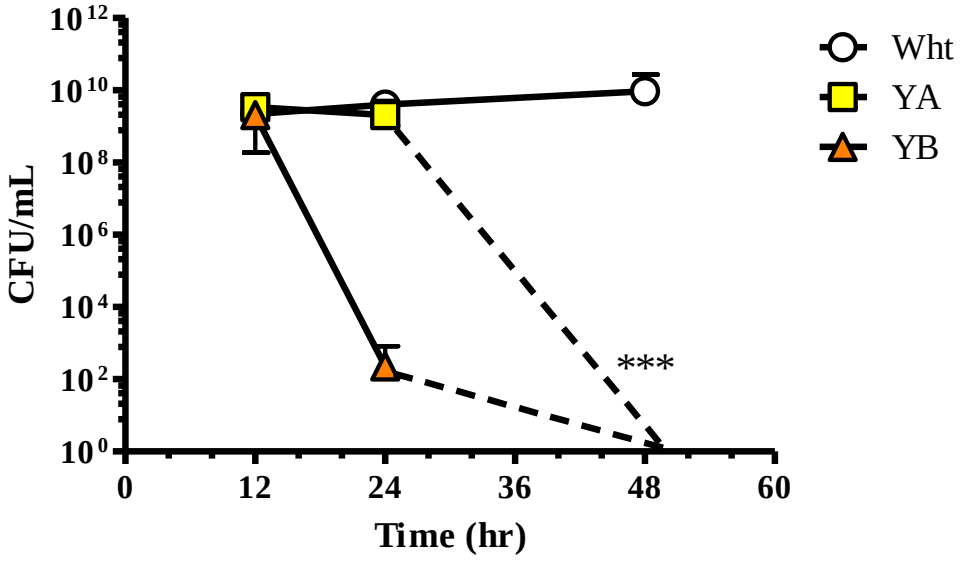

Figure 4.5 Addition of Pyruvate and Succinate Reliably Stabilized Toxic Effect of Yellow Colony Variants

WHT, YA, and YB-type colony variants were grown in LB with added pyruvate and succinate at 0.5% w/v and assayed for viability at 12, 24, and 48 hours post-normalization to an OD_{600} of 0.1 from logarithmically growing cells. At 48 hours, a full milliliter of YA and YB were each plated to increase the limit of detection of the CFU assay. The experiment was performed three times. Dashed lines indicate no viable counts for bacteria, even when plating 1 mL of culture. Data reported is the average of 3 replicates ± the 95% Confidence Interval. Statistical significance was determined using a two-way ANOVA with the Bonferroni post test for multiple comparisons. ***$p < 0.001$.

Contact-Dependence of Yellow Variant Toxicity

To determine if the toxic effect of yellow variant *B. pseudomallei* had activity against the white form, a model growth system was developed that allowed both forms to grow in the presence of each other simultaneously, separated by a semi-permeable membrane. Both YA and YB had toxic activity against WHT form bacteria (Figure 4.6), demonstrating that the toxic activity of yellow variant bacteria was contact-independent and diffusible. This difference in sensitivity to YA and YB variant supernatant was not statistically significant ($p = 0.23$) but the sensitivity to yellow variant supernatant was significant in comparison to sensitivity to WHT supernatant ($p = 0.004$).

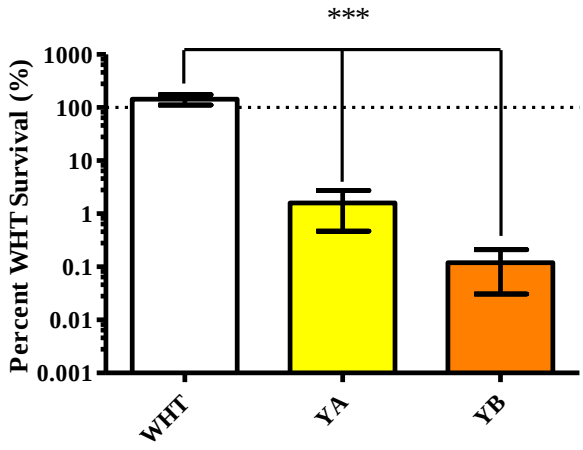

Figure 4.6 Toxic Effect of Yellow Variants was Active against White Variant Bacteria
White type *B. pseudomallei* were grown in the presence of WHT, YA, or YB type bacteria but were protected from physical contact by the presence of a semi-permeable membrane with a 10 KDa molecular weight cut-off. Viability of WHT type bacteria was assayed before exposure and after 24 hours of exposure, and percent survival was calculated. Data reported is the average of 5 biological replicates plus or minus the standard deviation. Statistical significance was determined using the unpaired, two-tailed, Student's T test. ***$p = 0.004$

Spectrum of Yellow Variant Toxicity

Since the yellow colony variants showed strong activity against the white form *B. pseudomallei*, we chose to investigate whether or not other strains and species of bacteria were susceptible to yellow variant toxicity. Because YB had the greatest effect, we chose to determine the toxicity of YB against *B. pseudomallei* strain 1026b, *B. thailandensis* strain E264, *P. aeruginosa* strain PAO1, *S. enterica* serovar Typhimurium strains 140285 and LT2, *B. cereus* strain MM1, and *E. coli* strain MG1655 sub-strain DH5α (Figure 4.7). YB colony variant showed toxic activity against all bacteria tested except *S. typhimurium* 140285 and *B. cereus* MM1 (Figure 4.7). Statistical significance was not determined because the experiment was only done once.

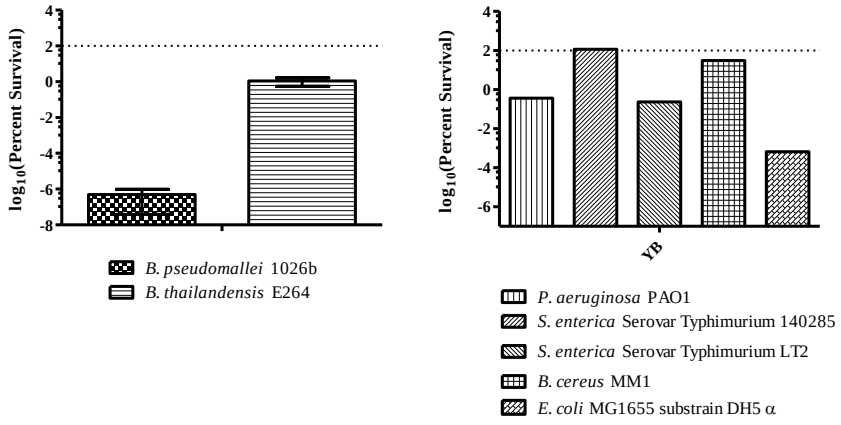

Figure 4.7 Toxic Effect of Yellow Variant YB Has Effect against Several Bacterial Species

Other bacterial species were grown in the presence of live YB in the same manner as described for WHT. Data reported for *B. pseudomallei* strain 1026b is the average of 3 repetitions, data reported for *B. thailandensis* strain E264 is the average of 4 repetitions ± the Standard Error of the Mean. Statistical comparison of data obtained for 1026b and E264 by the unpaired, two-tailed, Student's T test showed no statistically significant difference between the two. Data reported for *P. aeruginosa* PAO1, *B. cereus* MM1, *E. coli* MG1655 substrain DH5α *S. enterica* Serovar Typhimurium, 140825 and LT2, are the results of one experiment, no repetition.

Spectrum of Toxicity of Cell-Free Yellow Variant Supernatant

In order to determine if the toxic effect of yellow form *B. pseudomallei* required the presence of live cells, supernatant from yellow variant bacteria was harvested and applied to cells of several species of bacteria. Supernatant from yellow variants that was clarified of live cells by centrifugation and vacuum filtration was variably toxic to the same bacterial species that were sensitive to live yellow form cells (Figure 4.8), with total loss of viability for *B. thailandensis* but only minor loss of viability for *B. cereus* and no loss in viability for either *P. aeruginosa* or *S. enterica*.

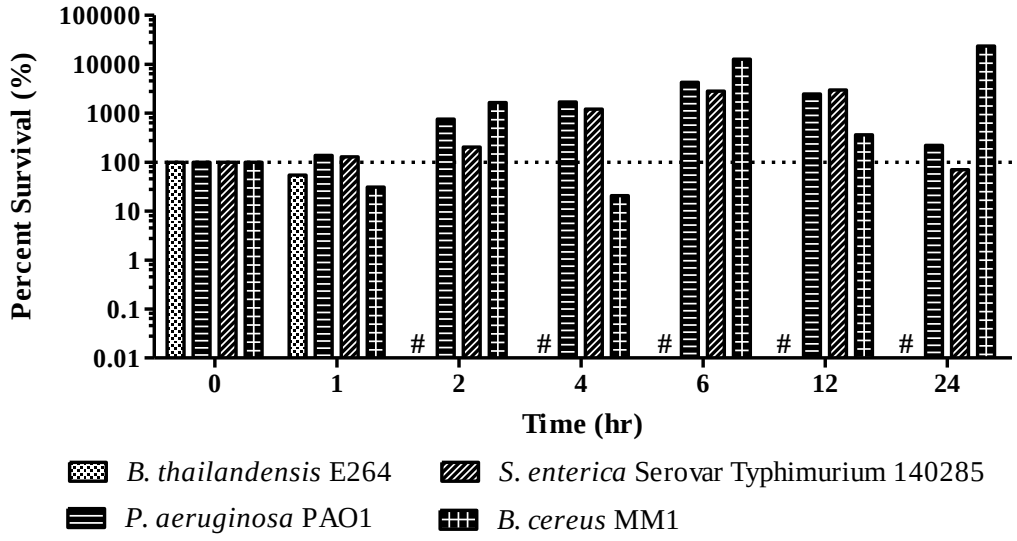

Figure 4.8 Spectrum of Activity of Clarified YA Supernatant
YA supernatant was harvested from YA cultures at 48 hours of growth in LB plus 0.5% pyruvate plus 0.5% succinate, mixed 1:1 with fresh LB and added to logarithmically growing cells of *B. thailandensis* E264, *P. aeruginosa* PAO1, *S. enterica* Serovar Typhimurium 140285, or *B. cereus* MM1 and viability was assessed at 0, 1, 2, 4, 6, 12, and 24 hours of exposure. Percent survival was calculated and data reported is the result of one experiment. "#" indicates no viable counts for *B. thailandensis* E264. Data reported is the result of one experiment.

Susceptibility of White Type and YA type bacteria to Yellow Variant Toxicity

White form *B. pseudomallei* were sensitive to yellow colony supernatant even in the absence of live yellow variant cells. When the same clarified yellow variant supernatant was applied to white form or YA form *B. pseudomallei* in increasing dilutions, the white form was clearly more susceptible to the toxic effects than the YA form (Figure 4.9).

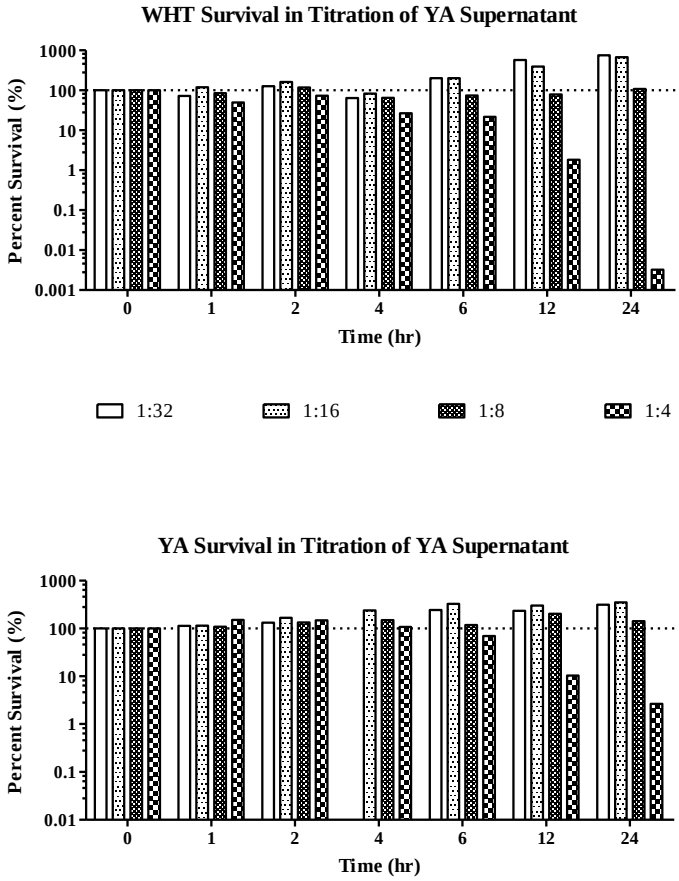

Figure 4.9 Toxic Effect of Yellow Variants is More Potent against WHT than YA
WHT and YA cells and YA SNT were prepared in the same manner as for determination of spectrum of YA toxicity except that YA SNT was diluted with fresh LB at 1:32, 1:16, 1:8, or 1:4 and viability of cells exposed to the mixture was measured at 0, 1, 2, 4, 6, 12, and 24 hours. Percent survival relative to pre-exposure was calculated. Data reported is the result of one experiment.

Both YA and YB Supernatant were Toxic to White form *B. pseudomallei* in Stationary Phase and in Logarithmic Growth Phase.

To verify that toxicity against the white form was not specific to YA, the experiment was repeated with YB form supernatant. YB supernatant was also observed to exhibit toxicity against the white form bacteria (Figure 4.10). Interestingly, logarithmically growing bacteria were somewhat less sensitive to the toxicity of yellow variants than cells in stationary phase (Figure 4.10).

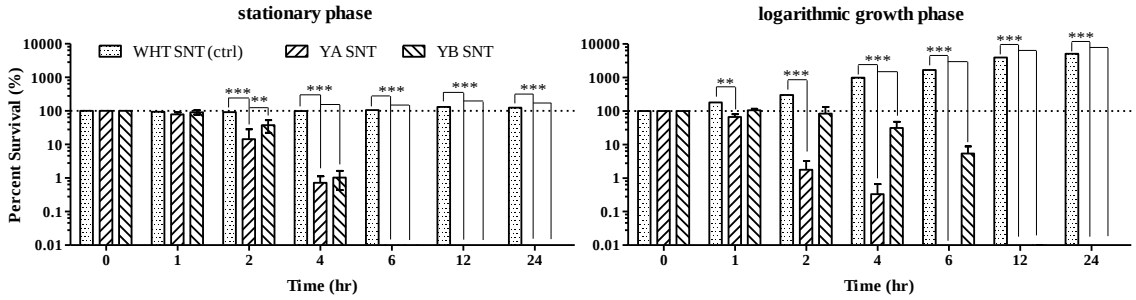

Figure 4.10 Survival of White Form Bacteria in Logarithmic or Stationary Phase in the Presence of YA and YB Supernatant
YB and YA SNT were prepared in the same manner as for the spectrum and titration effect experiments with the exception that, for stationary phase WHT *B. pseudomallei*, variant supernatant was mixed 1:1 with non-toxic WHT SNT from the same conditions and stationary phase WHT bacteria were collected from overnight cultures. Viability of the cells in variant supernatant was assessed at 0, 1, 2, 4, 6, 12, and 24 hours of exposure by CFU/mL. Percent survival was calculated. Data reported is the result of three biological replicates plus the standard error of the mean. Statistical significance was determined by two-way ANOVA with the Bonferroni post-test for multiple comparisons. $^{**}p < 0.01$; $^{***}p < 0.001$

Phenotypes of Toxicity Stabilization and Ablation Were Repeated in Semi-Defined Growth Media.

Due to the complexity of LB and the presence of numerous different molecules of all classes in it, it is not considered an ideal growth medium for chromatographic analysis of small molecules.. We planned to develop the yellow variant toxicity project to the point that a toxin could be identified and defined using chromatographic methods. In an attempt to develop a semi-defined medium for small molecule analysis, Middlebrook 7H9 (a completely defined medium) was adapted for use with *Burkholderia* species by addition of casein hydrolysate (7HB). This medium did support bacterial growth and toxin production (Figure 4.3 E), but the variability in toxin production was still seen. To determine if toxicity could be stabilized by addition of pyruvate and succinate, 7HBF was developed. This medium contained both pyruvate and succinate and did support the observation of toxicity (Figure 4.11 B). Interestingly, without the addition of casein hydrolysate (7HF), toxicity was not as pronounced, and the white form also exhibited loss of viability (Figure 4.11 A).

The addition of glucose and glycerol to 7H9 to make 7HG fully supported bacterial growth and did not support toxicity in any capacity (Figure 4.11 C). Combination of all five additives: casein hydrolysate, pyruvate, succinate, glucose, and glycerol to make 7HBFG moderately supported toxicity (Figure 4.11 D). Obviously, metabolite input and cellular metabolism had strong impacts upon the yellow variant toxicity phenotypes, suggesting, perhaps, a role for catabolite repression in control of at least some of the yellow variant phenotypes. However, delineating the impact and

interplay of metabolism on the various yellow variant phenotypes was beyond the scope of this project.

Molecular Characterization of Yellow Variant Toxicity

Molecular properties of yellow variant toxicity were investigated using a combination of approaches. Size fractionation of yellow variant supernatant gave variable results, however in totality; it was clear that toxicity could pass through any size filter (Figure 4.12). What was not pictured is the retentate after filtration; the retentate in all cases was dark yellow. It is unclear what the identity of the pigment is, or if it has any relation to the toxicity of the yellow variants.

We did observe that treatment of yellow variant supernatant with proteinase K did not ablate toxicity, either (Figure 4.12 suggesting that toxicity was not due to a proteinaceous source. Taken together, the results of Figure 4.12 indicate a molecular weight smaller than 3,000 Da for the toxic substance and that the toxic substance was not a polypeptide.

Attempts were made to isolate a toxin identified several unique small molecules present in the supernatant of yellow colony variants. Analysis of YA and YB supernatant using thin layer chromatography identified several differences in components of culture supernatants (Figure 4.13). At least one compound present in YA and YB supernatants but not in white supernatants has the property of UV fluorescence (Figure 4.14). Attempts made by rotation student Katherine Shives to determine if this unique compound had antibacterial activity failed, no loss of viability in bacteria exposed to the purified compound was observed (data not shown).

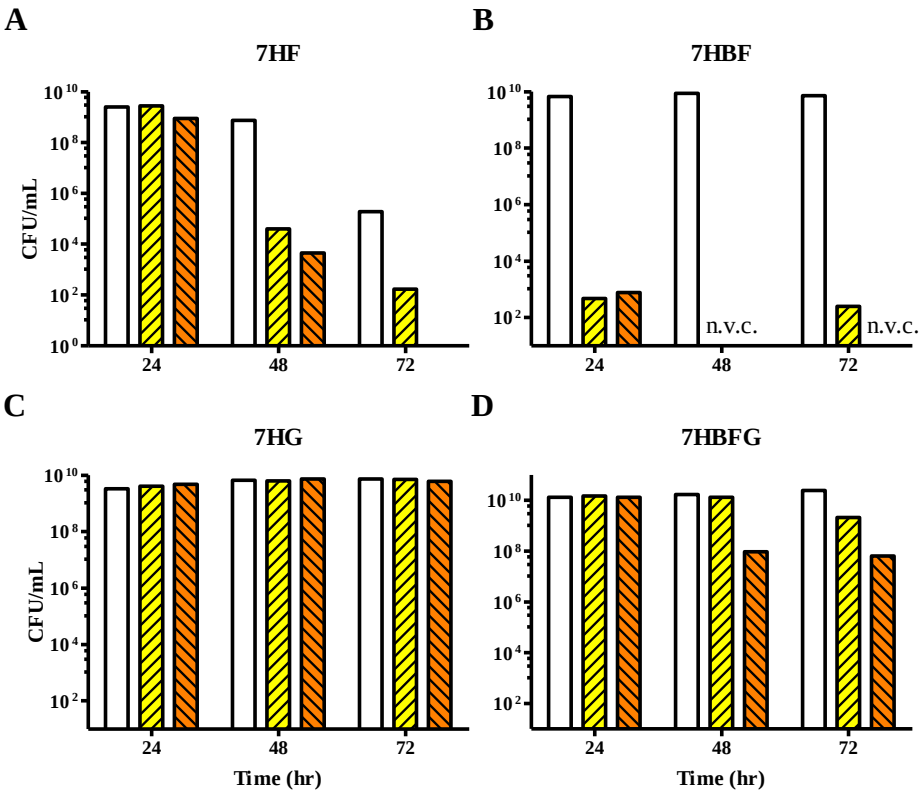

Figure 4.11 Toxicity Phenotypes Observed in LB were Replicated in a Semi-Defined Medium

Observations of toxin production and ablation by addition of pyruvate and succinate, or glucose and glycerol (respectively) were repeated in 7H9-based semi-defined media. Solute concentrations were balanced and normalized to 1.5% (Table 2.1). Bacteria were assayed for CFU/mL in each medium at 24, 48, and 72 hours post normalization to OD_{600} of 0.1. Cultures were grown at 37°C, with shaking. Data reported are the result of one experiment.

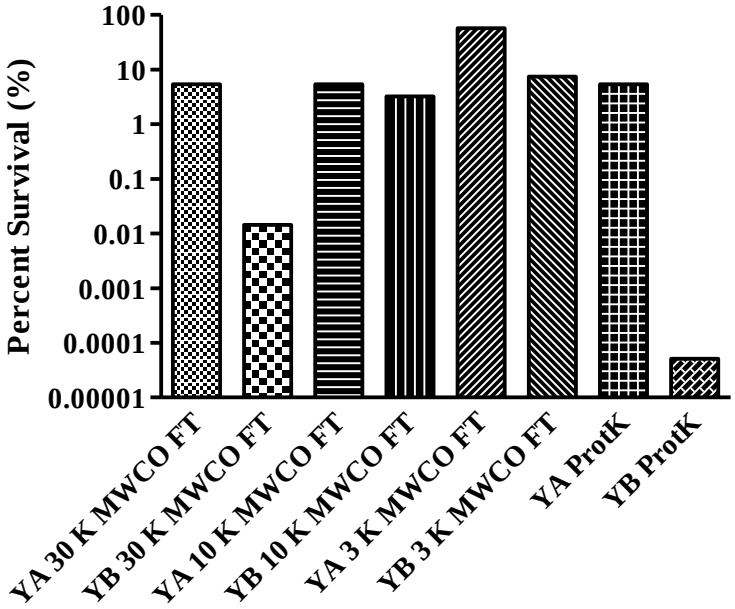

Figure 4.12 Size Fractionation and Proteolytic Analysis of Yellow Variant Toxicity
Yellow variant supernatant was prepared as for Figures 4.9 and 4.10 with the exception that variant SNT was treated before exposure to WHT form cells. Variant SNT was either passed through a 30 KDa or 3 KDa MWCO spin filtration device or treated with proteinase K for 30 minutes before addition to WHT cells.

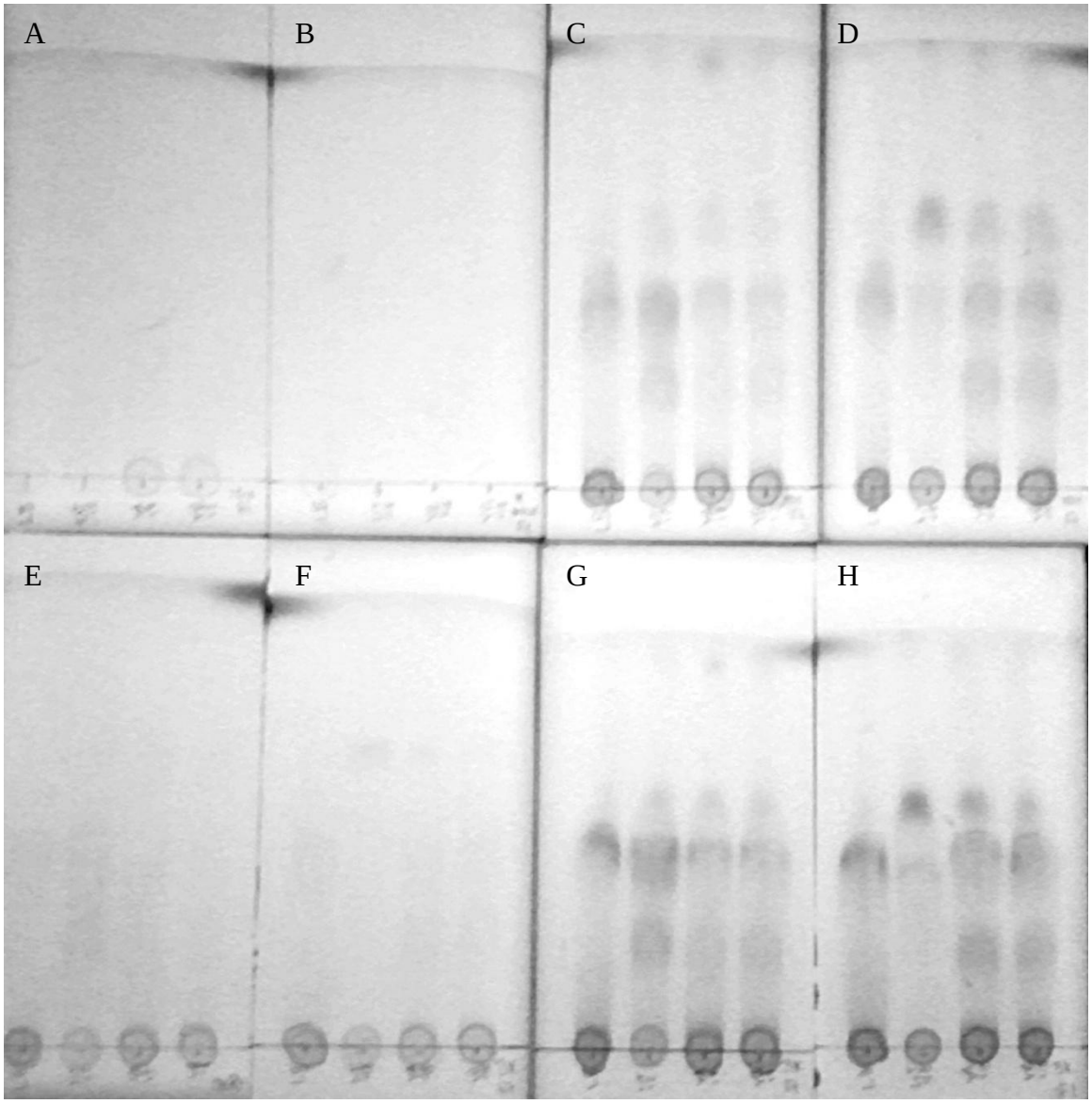

Figure 4.13 Thin Layer Chromatography of Variant Supernatant
WHT, YA, or YB supernatant was collected at 12 and 48 hours of growth in LB, size fractionated by passage through a 30 KDa or 3 KDa MWCO spin filtration device and either flow-through or retentate was spotted onto a TLC plate. Each TLC plate from left to right: media control (LB), 30µL each WHT, YA, YB per plate. Plate (A): 30K retentate, 12 hour samples. Plate (B): 30K retentate, 48 hour samples. Plate (C): 30K flow-through, 12 hour samples. Plate (D): 30K flow-through, 48 hour samples. Plate (E): 3K retentate, 12 hour samples, Plate (F): 3K retentate, 48 hour samples. Plate (G): 3K flow-through, 12 hour samples. Plate (H): 3K flow-through 48 hour samples. TLC plates were run in n-butanol: acetic acid (3:1), and UV exposed on TLC with integrated fluorophore. The resulting image was false-colored to black and white.

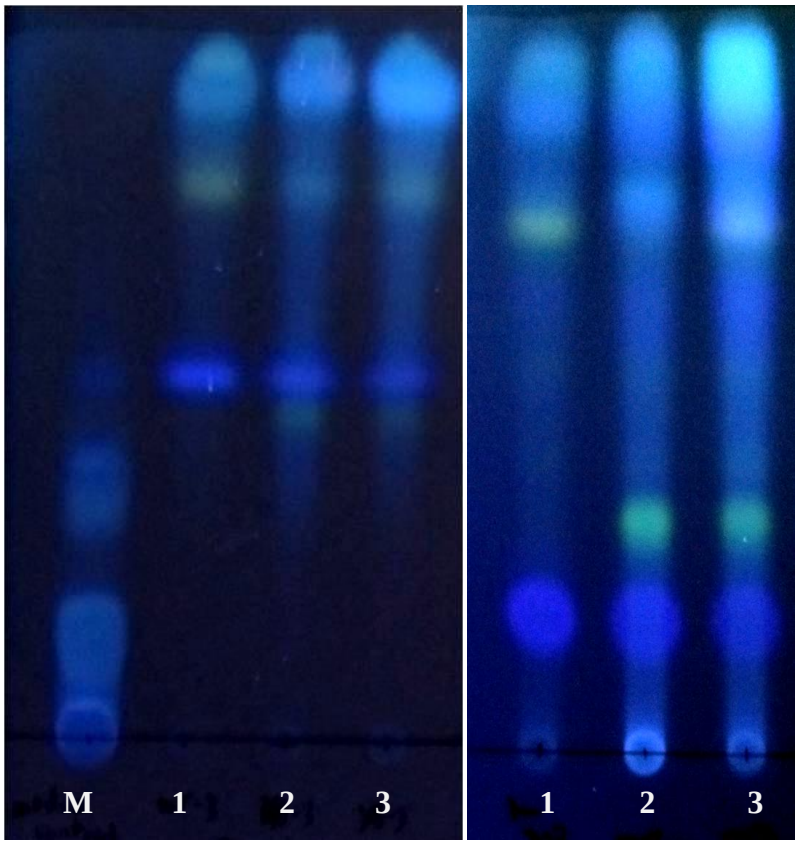

Figure 4.14 Ultra-Violet Fluorescence of Variant Supernatant
Yellow variant supernatant, white supernatant, or fresh media was collected as for the previous TLC assay but SNT was not size fractionated. Instead, SNT was lyophilized and resuspended in 1% the initial volume using water then extracted with Folch wash. The organic phase was separated and 20 µL of each extract was applied to each TLC (M: media, 1: WHT, 2: YA, 3: YB). TLCs were run in n-butanol: acetic acid: water (6:2:2) (left) or n-butanol: acetic acid (3:1) (right) then visualized with a UV lamp at 360 nm and images captured with a digital camera.

Transcriptional Analysis of Secondary Metabolite Operons

Based on gene annotation, *B. pseudomallei* K96243 possesses nine genomic regions potentially involved in production of secondary metabolites. Three of the nine were up-regulated in YB under settled, hypoxic conditions. RNAseq analysis of YB under settled growth conditions in hypoxia indicated that the genomic loci encompassing BPSS1165 to BPSS1174 and BPSS1175 to BPSS1187 were highly expressed in these cells (Table 4.1). This genomic region includes several non-ribosomal peptide/polyketide synthases, thioesterases, acetyltransferases, and transporters. Non-ribosomal peptide/polyketide synthase operons are responsible for synthesis of secondary metabolites such as pyoverdine, pyochelin, yersiniabactin, etc., and secondary metabolites frequently have antibacterial properties.[104,105] Secondary metabolites also frequently function as siderophores, and may also provide cells with the capacity for extracellular electron transfer (EET) – a strategy for respiration under oxygen-limiting conditions.[106–108] Although *B. pseudomallei* does not have homologues of the genes necessary for production of most known siderophores, it does have copies of the genes required to make the siderophore pyochelin. The genes responsible for production of the pyochelin were not upregulated in YA or YB under conditions in which global gene transcription were profiled (Table 4.1)

It is worth noting that the up-regulated genetic loci in YB did not include the locus for synthesis of malleobactin[109] and, to our knowledge, have not been described as responsible for any known secondary metabolites.[110,111] Attempts to isolate and identify unique small molecules produced by yellow variants did not yet bear fruit in most part because purified compounds were not observed to have antibacterial activity.

Table 4.1 Genomic Regions Encoding Pyochelin and Secondary Metabolite Production Upregulated in YB Variant

Gene	Product	YB:WHT† (Std.Dev.)	YA:WHT‡ (Std.Dev.)
Region 1			
BPSS1165	alpha-ketoglutarate-dependent taurine dioxygenase	6.2 (0.0)	1.8 (0.7)
BPSS1166	transport/efflux protein	7.7 (0.5)	1.1 (0.2)
BPSS1167	thioesterase	5.8 (0.3)	1.1 (0.1)
BPSS1168	acetyltransferase	4.0 (0.1)	0.79 (0.08)
BPSS1169	hypothetical protein	4.1 (0.0)	0.74 (0.11)
BPSS1170	non-ribosomal peptide synthase/polyketide synthase	4.4 (0.0)	0.93 (0.22)
BPSS1171	non-ribosomal peptide synthase/polyketide synthase	4.2 (0.0)	1.6 (0.8)
BPSS1172	non-ribosomal peptide synthase/polyketide synthase	4.9 (0.0)	1.3 (0.7)
BPSS1173	non-ribosomal peptide/polyketide synthase	6.2 (0.1)	1.4 (0.7)
BPSS1174	non-ribosomal peptide/polyketide synthase	9.6 (0.2)	4.9 (3.4)
Region 2			
BPSS1175	oligopeptidase A	6.8 (0.1)	4.7 (3.3)
BPSS1176	N-acyl-homoserine lactone dependent regulatory protein	3.7 (0.0)	4.8 (3.0)
BPSS1177	hypothetical protein	6.2 (0.0)	1.4 (0.8)
BPSS1178	transmembrane antiporter Na^+ or K^+/H^+ exchanger	13.9 (0.7)	1.2 (0.4)
BPSS1179	hypothetical protein	2.1 (0.0)	1.3 (0.6)
BPSS1180	N-acylhomoserine lactone synthase	9.1 (0.0)	1.6 (0.7)
BPSS1181	surfactin/non-ribosomally encoded peptide/polyketide synthase	4.5 (0.1)	1.5 (0.4)
BPSS1182	acyl carrier protein	4.4 (0.0)	0.91 (0.14)
BPSS1183	non-ribosomally encoded peptide/polyketide synthase	4.4 (0.0)	0.92 (0.16)
BPSS1184	hypothetical protein	4.4 (0.1)	1.2 (0.5)
BPSS1185a	hypothetical protein	2.3 (0.0)	1.3 (0.5)
BPSS1187	hypothetical protein	1.4 (0.0)	1.1 (0.1)
Region 3			
BPSS0299	fatty-acid CoA ligase	5.1 (0.3)	2.1 (1.2)
BPSS0300	malonyl CoA-ACP transacylase	3.8 (0.2)	2.5 (2.0)
BPSS0301	hypothetical protein	4.2 (0.1)	2.1 (0.9)
BPSS0302	fatty acid biosynthesis-related CoA ligase	2.8 (0.0)	2.3 (1.4)
BPSS0303	diaminopimelate decarboxylase	4.7 (0.3)	2.1 (0.7)
BPSS0304	hypothetical protein	1.3 (0.2)	2.0 (0.6)
BPSS0305	ketol-acid reductoisomerase	2.7 (0.0)	2.0 (0.6)
BPSS0306	multifunctional polyketide-peptide synthase	12.2 (5.7)	1.7 (1.2)
BPSS0307	gamma-aminobutyraldehyde dehydrogenase	7.9 (0.3)	1.6 (1.0)
BPSS0308	hypothetical protein	4.9 (0.1)	1.6 (1.0)
BPSS0309	peptide synthase regulatory protein	3.9 (0.1)	1.4 (0.8)
BPSS0310	hypothetical protein	10.5 (0.1)	1.6 (0.9)
BPSS0311	multifunctional polyketide-peptide synthase	10.1 (1.3)	1.7 (1.2)

Gene	Product		YB:WHT† (Std.Dev.)	YA:WHT‡ (Std.Dev.)
Pyochelin Production Region				
BPSS0581	*pchA*	salicylate biosynthesis isochorismate synthase	0.46 (0.05)	2.4 (0.6)
BPSS0582	*pchB*	isochorismate-pyruvate lyase	- (-)	1.4 (0.6)
BPSS0583	*pchC*	pyochelin biosynthetic protein	- (-)	2.1 (1.3)
BPSS0584	*pchD*	salicyl-AMP ligase	1.1 (0.0)	1.7 (0.7)
BPSS0585	*pchR*	AraC family transcriptional regulator	1.8 (0.0)	3.3 (2.7)
BPSS0586	*pchE*	pyochelin synthetase	0.29 (0.01)	2.3 (2.2)
BPSS0587	*pchF*	pyochelin synthetase	1.2 (0.8)	1.1 (0.1)
BPSS0588	*pchG*	pyochelin biosynthetic protein	- (-)	2.5 (0.9)
BPSS0589	*pchH*	ATP-binding component of ABC transporter	0.69 (0.18)	1.9 (1.2)
BPSS0590	*pchI*	ABC transporter ATP-binding protein	- (-)	1.7 (0.6)
BPSS0591	*fptA*	Fe(III)-pyochelin receptor	- (-)	1.4 (0.6)

†RNA was harvested in triplicate from bacteria grown in the *in vitro* stomach model under hypoxia (2.0% O_2) at 24 hours of growth and analyzed by RNAseq**.** ‡RNA was harvested in triplicate from YA and WHT bacteria grown planktonically for 12 hours (early in stationary phase) and analyzed by microarray. No values "-(-)" indicate insufficient YB or WHT reads to perform a valid ratio calculation (i.e. divide by zero). Data reported is the RPKM linear-normalized ratio of YB to WHT reads with the standard deviation in parentheses; and the ratio of normalized YA to WHT average signal intensities with the standard deviation in parentheses for microarray data.

Discussion

As demonstrated in Chapter III, yellow colony variants exhibited a broad spectrum of physiological differences relative to the white type. This chapter demonstrates that these differences are not just restricted to the surface of the cell or the extracellular space. These differences go to the core of how the bacteria grow, multiply, and respond to growth-limiting conditions.

The most striking of direct, microscopic observations was the lack of rounding and lack of phase-bright appearance in yellow variant cells (Figure 4.1). Phase-bright appearance has been attributed to accumulation of the large molecular weight polymer, β-polyhydroxybutyrate (PHB). Presumably, other low-density polymers or structures could

also produce the same microscopic phenomenon; however they have not been described. Furthermore, genes responsible for PHB production were down-regulated in yellow variant cells and up-regulated in white variant cells (Table B.2). PHB production and accumulation is a well-known behavior of *B. pseudomallei* and, for a time, was even proposed as a diagnostic criterion for identification of the organism.[103] Taken together and without empirical verification, we are tentatively suggesting that yellow variant cells fail to accumulate PHB, and white variant cells do accumulate PHB.

Accumulation of the energy storage polymer has been posited as strategy of preparation for growth-limiting conditions wherein the PHB-accumulating bacteria enter a state of non-replication and use the PHB stores to meet basal energy needs until environmental conditions again become favorable for growth. Presumably, unwillingness to accumulate the energy storage polymer indicates adoption of an alternative strategy for what would typically be understood as growth-limiting conditions. I have shown that yellow colony variants have a growth advantage under hypoxic conditions in Chapter III and therefore it is possible that yellow variants simply do not experience enough growth restriction to initiate PHB production, or that PHB production is mutually exclusive with yellow variant respiration.

Of the many different phenotypes and physiological differences of the yellow colony variants, the most readily apparent to the macroscopic observer was the dependency of pigment production and toxicity on the absence of glucose or glycerol (Figures 4.4 and 4.5). Full investigation of the impact of glucose or glycerol on metabolism and colony variation in *B. pseudomallei* was beyond the scope of this work. However, the prospect of metabolic influence on the regulation of other virulence factors

such as swimming motility, media alkalization, eDNA production, or hypoxic growth is intriguing. Of peculiar interest for a research project into colony variation in *B. pseudomallei* was the observation that Ashdown's medium (ASH), which was the medium of choice for previously published work in colony variation, consists of 4% glycerol and uses Trypticase Soy Broth (TSB) as its nutrient source[65] — the presence of both of which failed to support the yellow colony variant toxicity phenotype as shown here.

Converse to the observation that glucose and glycerol can suppress yellow variant toxicity and pigment was that addition of pyruvate or succinate enhanced the production of yellow variant toxicity (Figure 4.4 and 4.5). It was unclear how addition of these metabolites enhance toxicity of yellow variants, and it will be difficult to determine as they are both central in several metabolic pathways. However, some trends in production of toxic compounds are known. Secondary metabolites frequently have antibiotic properties.[112] Some secondary metabolites with antibiotic properties also have the capacity for accepting and donating electrons, such as pyocyanin[113] and are used in EET. Presumably, the antibiotic properties of electron-carrying secondary metabolites are due to spontaneous reduction of molecular oxygen to form toxic, reactive oxygen species. Three regions potentially responsible for secondary metabolites in YB variants were up-regulated in the *in vitro* gastric colonization model (Table 4.1): BPSS0299-0311, BPSS1165-1174, and BPSS1175-1187. Typically, organisms utilizing secondary metabolites for Extracellular Electron Transfer (EET) have specialized molecular mechanisms for capturing and repeatedly reducing electron carriers in the extracellular milieu. It is possible that the toxicity observed in the presence of live yellow variants

against other bacteria, but not in the presence of clarified supernatant, was due to burkholderia-specific machinery capable of repeatedly reducing a specialized electron carrier and the other bacterial species tested did not. This is supported by death of *B. pseudomallei* strains K96243 and 1026b and *B. thailandensis* but not other bacterial species under exposure to clarified supernatant. Unfortunately, efforts to purify and identify the toxin have not yielded definitive results.

Some speculation has been raised as to the identity of the yellow pigment. Some have suggested in personal communication that the pigment is riboflavin. Genes responsible for the production of riboflavin were observed to be up-regulated in YA (Table B.6) but not in YB at the time when transcriptional analysis was performed (Table B.6). Riboflavin is also very similar in its appearance to the yellow pigment. However, exact identification of the pigment has not been established. It is plausible that riboflavin is the toxin. Presumptive identification of the yellow pigment and yellow variant toxin as riboflavin is attractive for several reasons. One, riboflavin has antibacterial properties and has even been proposed for clinical use during bacterial infections.[114,115] Two, riboflavin is light-sensitive and can be deactivated by exposure to it; this would explain our futile attempts to determine antibacterial properties of purified unique products, as the purification process includes long exposures to light and oxygen. Three, riboflavin is UV fluorescent with an emission spectrum around 550 nm which roughly corresponds to the color green, which was the color of unique UV fluorescent compounds observed by TLC and UV exposure in variant supernatants (Figure 4.14).

Exact identification of the yellow pigment as riboflavin, and verification of its antibacterial properties would require further investigation. It would also require an

explanation for why toxicity passed through spin filtration devices but the yellow pigment was largely retained. Either the pigment was extraordinarily toxic, meaning the small, unconjugated fraction that passes through the filter was sufficient to sterilize several billion cells (even after dilution), or the toxic compound was altogether different from the pigment.

CHAPTER V

MOLECULAR REGULATION OF COLONY VARIATION IN *B. PSEUDOMALLEI* K96243

Introduction

To date, a molecular mechanism for control of colony variation in *B. pseudomallei* has not been described. Molecular control of colony or phase variation in other bacteria is usually due to the expression of genetic mutation, although examples of epigenetic control of colony morphology have also been described. Presuming that colony variation in *B. pseudomallei* was ultimately the expression of genetic mutations, a combination of molecular tools was used to investigate the molecular mechanism for colony variation including: transposon mutagenesis, whole-genome sequencing, and gene deletion and complementation analysis. This body of work suggests a non-genetic mechanism for control of colony variation in *B. pseudomallei*.

Transposon Mutagenesis

Mutagenesis of white-type, wild-type *B. pseudomallei* K96243 with the mobile genetic element known as the Mariner transposon borne on the plasmid pTBurk1 to a depth of approximately 25,000 mutants generated five mutants that were strikingly yellow after initial selection and 48 hours of growth. These mutants were streaked for isolation and observed to be rough and intensely pigmented. No mutants were isolated that were smooth and yellow as has been the observed phenotype for YA and YB-type colonies. Many more mutants were observed to be yellow after extended incubation past 48 hours but were not investigated due to possible amplification of pleiotropic effects that would be made evident by extended incubation of colonies. These yellow transposon mutants all also shared the property of exhibiting a toxic effect late in stationary phase that had been observed for YA and YB (Figure 5.1).

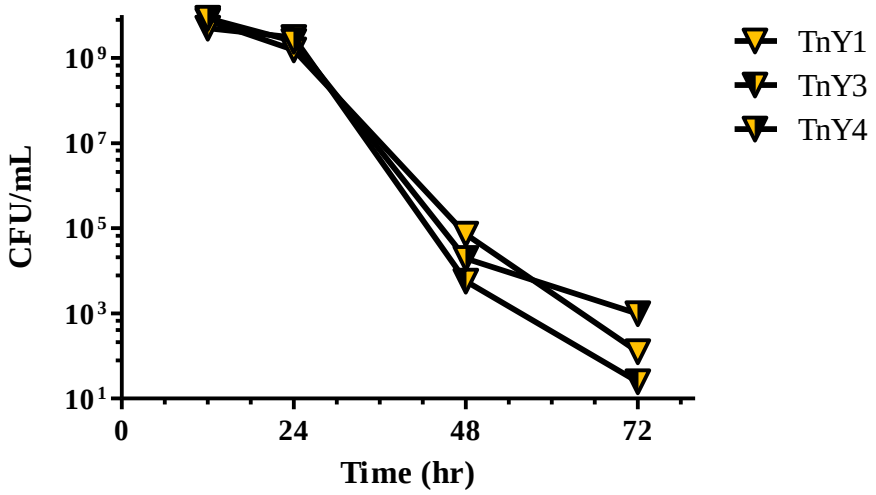

Figure 5.1 Toxicity of Yellow Transposon Mutants in LB
Yellow transposon mutants were streaked for isolation and then grown planktonically in LB and assayed for CFU/mL at 12, 24, 48, and 72 hours of growth. Data reported is the result of one experiment.

Determination of Transposon Insertion Sites

Determination of transposon insertion sites in yellow mutants identified BPSL1887 as a potential positive regulator of the yellow pigment production in *B. pseudomallei* K96243**.** Clonal isolates of yellow transposon mutants were investigated for sites of transposon insertion using pTBurk1-adapted ARB PCR (see Appendix A.1). Two of the five initial isolates were determined to be sisters to one of three unique transposon mutants. Each of the three unique transposon mutants had insertions within a 50 base-pair region immediately 5' to the gene BPSL1887 - a putative sigma54-dependent transcriptional regulator and all transposons were positioned in the same orientation. The proximity and orientation of the insertion suggested that these transposon mutants were not deficient in expression of a functional gene but were gain of function mutants that over-expressed BPSL1887.

Figure 5.2 Insertion Analysis of Isogenic Yellow Transposon Mutants
Insertion sites of each of the isogenic yellow transposons were determined by ARB PCR (see Appendix A). Sequencing results were compared to the published K96243 genome sequence and insertion sites mapped in red. Aquamarine arrows indicate putative -10 and -35 components of the promoter for BPSL1887.

Impact of YelR on Yellow Colony Phenotypes

When the coding sequence for BPSL1887 was inserted into the arabinose-inducible over-expression vector pHERD and transformed into the wild-type, white-type background, colonies isolated on LB + 200 µg/mL Kanamycin + 50 µg/mL Zeocin selection agar presented with the yellow colony morphology. This strain, which must be maintained with constant presence of kanamycin, alkalized media in the same manner as YA and YB - i.e., without ammonia production, but to a lesser degree (Figure 5.4 A and B). Intermediate phenotypes in the mutant strain were likely due to the removal of endogenous transcriptional control over BPSL1887 and substitution with pBAD-based control. The complemented strain also produced eDNA in the settled culture model (Figure 5.4 C), although to a lesser extent than YB. Since expression of this regulator induced yellow pigment production we propose to name the regulator "*yelR*" for yellow program regulator.

Deletion of *yelR* from a wild type background ablated emergence of yellow colony variants under normally permissive conditions, abolished alkalization of growth medium, production of eDNA, and restored ammonia production (Figure 5.4). When the coding sequence for *yelR* was removed from the white-type, wild-type background using an allelic exchange system, the knockout strain did not spontaneously develop altered colony morphology under hypoxia as occurred with the white-type wild-type strain. The knockout strain was also deficient in media alkalization but competent for ammonia production (Figure 5.4 A & B). The knockout strain also did not produce eDNA in the settled culture model (Figure 5.4 C).

Complementation of *yelR* in the knockout background restored the phenotypes of media alkalization without ammonia production, eDNA production and yellow colony morphology (Figure 5.3 and 5.4). Complementation of the knockout with the pHERD::*yelR* over-expression vector *in trans* restored the yellow colony morphology (Figure 5.3). Complementation of the knockout also moderately restored the media alkalization phenotype (Figure 5.4 A & B). Complementation also moderately but not completely restored eDNA production (Figure 5.4 C). Intermediate restoration of phenotypes in the complemented knockout strain was likely due to the complete loss of endogenous transcriptional control of *yelR*.

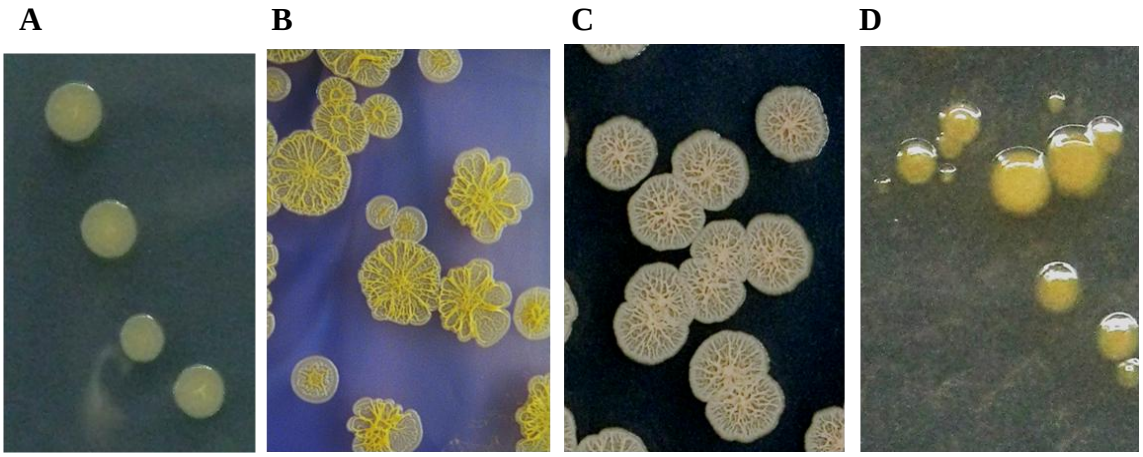

Figure 5.3 Appearance of YelR Mutants
The replicative plasmid pHERD::*yelR* was electroporated into white, wild type *B. pseudomallei* K96243 and successful transformations were selected on LB agar + 200 µg/mL Kanamycin + 50 µg/mL Zeocin and grown for 3-4 days. Plates were photographed with a digital camera (A). Yellow transposon mutant 1 was grown on LB agar for 48 hours and photographed with a digital camera (B). YelR deletion mutants were grown on LB agar for 48 hours and photographed with a digital camera (C). YelR deletion mutants complemented with the pHERD::*yelR* plasmid were transformed in the same manner as wild type bacteria and selected for in the same manner then grown for approximately 5 days on selection agar and photographed with a digital camera (D).

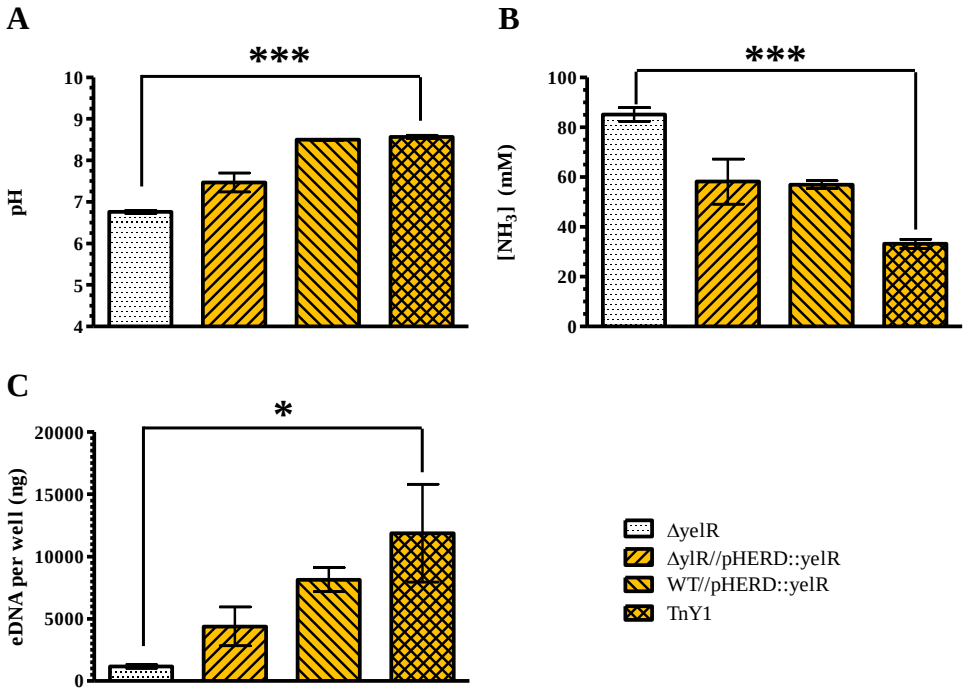

Figure 5.4 Fulfillment of Koch's Molecular Postulates for YelR as the regulator of the Yellow Colony Phenotype

The *yelR* deletion strain, complement strain, wild type complement strain, and one of the yellow transposon strains were assayed for pH (A) and ammonia (B) in the same manner as for yellow variants described in Figure 3.4 with growth in LB of initial pH of 5.0 for 48 hours. Determination of eDNA production (C) by deletion and complement strains was accomplished in the same manner as for Figure 3.7 by growth in the settled culture model for 48 hours and isolation of eDNA by centrifugation of well contents and extraction of SNT with phenol: chloroform: isoamyl alcohol. Data reported is the average of three biological replicates ± the standard deviation. Statistical significance was determined for pH and NH_3 by the unpaired, two-tailed Student's T test, ***$p < 0.001$. Statistical significance for eDNA was determined using one-way ANOVA, $p = 0.039$

HITS Analysis of Genes Important in Hypoxic Growth

All 25,000 plus mutants isolated during the transposon mutagenesis were collected and pooled. The pooled, random transposon library was placed in an anaerobic adaptation model,[85] and sampled immediately prior to massive selection from anaerobiosis (60 hr). The population's entire genomic landscape was surveyed by high-throughput sequencing and due to the transposon which derived from Himar1 and was selective for TA dinucleotides, insertion sites for each transposon and their relative abundance in the population could be tracked over the course of the adaptation to anaerobiosis. We unexpectedly observed enrichment for transposon mutants located 5' to the start codon of BPSL1887 (*yelR*). These mutants were enriched, on average, 7-fold from the initial distribution in the population (Table 5.1). The average transposon mutant, though, did not become enriched with an average fold enrichment of 1.0. It is worth observing that transposon mutants located within the coding sequence for *yelR* were diminished in their abundance during adaptation to hypoxia.

Another single transposon mutant was enriched during hypoxia. Its TA dinucleotide insertion site was in the 3' region for BPSL1018, a bottom-strand, putative transmembrane sugar phosphate permease. Although the location of this insertion site suggested that this particular transposon insertion disrupted function of the gene, other transposon mutants inserted at other points in the same gene were not enriched under hypoxia. The lack of an enrichment trend among transposon mutants inserted across the length of the gene suggested that there was a unique property to the enriched transposon and that loss of BPSL1018 function was not responsible for the transposon mutant enrichment. This insertion site was also 3' to both flanking genes and therefore the

insertion at TA_15404 was not likely causing polar gain of function mutations to neighboring genes.

High-Throughput, Next-Generation Sequencing of Yellow Colony Variants

High-throughput, next-generation sequencing of YA, YB and two white revertants of YA revealed no phenotype-associated Single Nucleotide Polymorphisms (SNPs). The genomes of YA, YB and two revertants of YA: YAr3.1 and YAr4.1 were sequenced on the Roche 4-5-4 high-throughput next generation sequencing platform. When tabulated and compared, no SNPs corresponded to the pattern of phenotypes observed for YA, YB, YAr3.1 and YAr4.1 revertants even if relaxed quality scores were considered. This is in agreement with a recently published study describing whole genome sequence for colony variants of another strain of *B. pseudomallei*: NCTC 13392, wherein the authors describe being unable to identify any SNPs correlating with colony variant phenotype.[116]

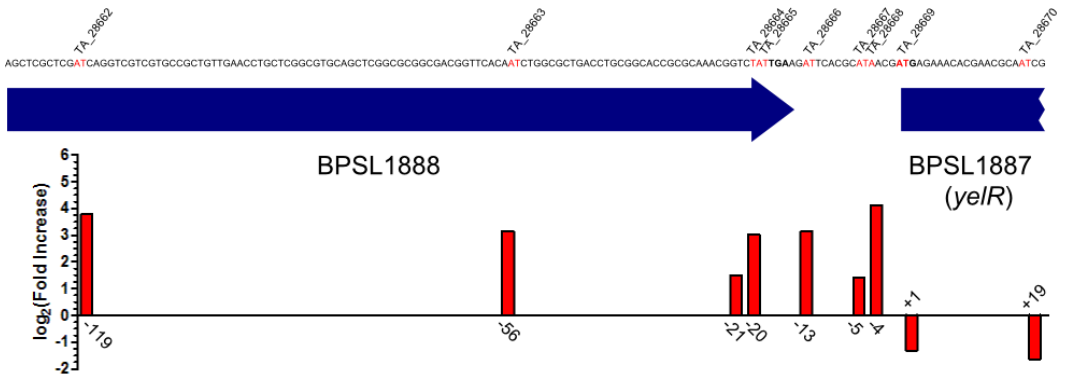

Figure 5.5 HITS Analysis of the Hypoxia-Enriched Transposon Mutant Family Immediately Upstream to BPSL1887
Analysis of transposon mutant populations was performed using HITS. Percent of total reads for each transposon insertion site was calculated after read normalization, and the fold increase between initial growth conditions and growth under hypoxia was calculated. Data reported above is the $\log_2$(Fold Increase) plotted with respect to the first nucleotide of the ATG start codon for BPSL1887. The TA number for each transposon insertion site is included for reference to Table 5.1.

Table 5.1 HITS Reads

TA Number	Initial Library (T_0)		Hypoxic Selection (T_f)		Fold Enrichment (T_f:T_0)
	reads	percent of total reads	reads	percent of total reads	
BPSL1887-8					
TA_28662	666	0.031%	1903	0.430%	13.71
TA_28663	838	0.039%	1553	0.351%	8.89
TA_28664	13758	0.65%	8124	1.836%	2.83
TA_28665	52680	2.48%	90130	20.365%	8.21
TA_28666	18412	0.87%	33949	7.671%	8.85
TA_28667	36708	1.73%	20677	4.672%	2.70
TA_28668	13654	0.64%	48731	11.011%	17.13
TA_28669	1754	0.083%	147	0.033%	0.40
TA_28670	164	0.0077%	11	0.0025%	0.32
TA_28671	48	0.0023%	0	0.00%	0.00
TA_28672	74	0.0035%	5	0.0011%	0.32
TA_28673	38	0.0018%	0	0.000%	0.00
TA_28674	22	0.0010%	0	0.000%	0.00
BPSL1018					
TA_15404	168	0.0079%	10646	2.4055%	304
TA_15405	8	0.00038%	1	0.00023%	0.60
TA_15406	12	0.00057%	1	0.00023%	0.40
TA_15407	8	0.00038%	0	0.00%	0.00
TA_15408	78	0.0037%	6	0.0014%	0.37
TA_15409	10	0.00047%	0	0.00%	0.00
TA_15410	4	0.00019%	0	0.00%	0.00
TA_15411	44	0.0021%	1	0.00023%	0.11
TA_15412	8	0.00038%	0	0.00%	0.00
TA_15413	14	0.00066%	1	0.00023%	0.34
TA_15414	20	0.00094%	1	0.00023%	0.24
TA_15415	48	0.0023%	2	0.00045%	0.20
TA_15416	20	0.00094%	0	0.00%	0.00
TA_15417	18	0.00085%	2	0.00045%	0.53
TA_15418	30	0.0014%	3	0.00068%	0.48

Discussion

Investigation of the molecular mechanism underlying colony variation in *B. pseudomallei* has proven to require a nuanced approach. Previously described paradigms of molecular control over colony variation are ultimately explained as expressions of genetic mutations. However, whole-genome sequencing of YA and YB revealed no statistically significant mutations correlating with phenotype. Transposon mutagenesis and deep sequencing of transposon mutant libraries did reveal one confirmed positive regulator of the phenotypes and two potential negative regulators of the phenotypes: BPSL1887 (*yelR*), BPSL1888, and BPSL1018, respectively.

These observations suggest two scenarios for control of *yelR*: in the first, BPSL1888 or BPSL1018 diminish activity of YelR; and repression of these genes allows for de-repression of *yelR* and induction of the yellow variant phenotypes. In the second scenario, *yelR* expression is either stochastic, or typically insufficient to induce and maintain expression of the phenotypes. Under rare or poorly understood conditions, *yelR* expression could become stabilized, allowing for manifestation of the yellow variant phenotypes.

The first scenario is attractive in that it mimics a paradigm described for expression of mucoidy in *P. aeruginosa*. However, no mutations were identified in yellow colony variants in the vicinity of BPSL1887 that would account for differential regulation of the gene. Furthermore, transposon mutants with insertions distal to BPSL1887 but within BPSL1888, and throughout the length of BPSL1018 were not enriched under hypoxic selection (Table 5.1) suggesting it was not disruption of those two gene products that provided a competitive advantage under hypoxia, i.e. they were

not negative regulators of *yelR*. Furthermore, a molecular model based on regulatory control over *yelR* predicts that expression of the phenotype, or de-repression of the regulator, is due to a specific environmental or cellular signal. However we have not observed any particular environmental stress to induce the yellow phenotype; we have only observed conditions that have allowed for its competitive emergence. The difference is nuanced, but important: regulatory control over the phenotype requires an inducing signal and a transcriptional response for the phenotypes to manifest; stochastic emergence of the phenotype allows a small proportion of the population to manifest the phenotypes before they are necessary.

The second scenario describes a phenomenon known as bistability or phenotypic heterogeneity which can be defined as maintenance of genetically identical but phenotypically diverse populations of bacteria.[117,118] This phenomenon is usually accomplished by accumulation of a master regulator that has the property of being auto-inducible. In most cells and under most circumstances, the regulator is unstable due to the activity of proteases or degradation of mRNA. However, in a minority of cells, the gene product can establish a steady-state concentration and autoregulation that allows for the maintenance of its own expression. Thus, when not degraded or titrated out by cellular division, the regulator epigenetically maintains inheritance of the phenotype(s) that it regulates.

Bistability is typically understood as a strategy for establishing sub-populations of bacteria that are predisposed for exploitation of harsh but not immediately available niches. This strategy is especially effective at providing a portion of a bacterial population a chance at surviving rapid and severe environmental changes, such as what

may be experienced by ingested bacteria that may not have an opportunity to mount a transcriptional response to the harsh gastric environment.

Bistability also predicts some behaviors that we have observed in yellow colony variants of *B. pseudomallei*: one, bistable populations arise randomly, or stochastically. We observed that yellow colony variants of *B. pseudomallei* appeared to be random in their emergence; although they had a distinct growth advantage under oxygen-limiting growth conditions (Figures 3.1 and 3.3). Second, a bistable population is always mixed because, by its very nature, it seeks to diversify the population to, in effect, prepare for harsh future conditions.[118] We observed that yellow variant populations always diversify to develop a population of mixed phenotypes (Table 3.1) where even under hypoxic conditions a near pure population of yellow variants will drift to approximately 50% yellow and 50% white culture (Figure 3.1).

It is unclear at this point, exactly which environmental or cellular conditions permit initial stability of YelR, if YelR can induce its own expression, or if y*elR* is under regulation by any other transcriptional regulator; the exact etiology of the gene's expression requires further investigation. It is also unclear if the phenotypes of medium alkalization, ammonia production, swimming motility, and eDNA production are under direct or indirect control of YelR. However, we do know that expression of *yelR* correlates with manifestation of the yellow variant phenotypes and that the yellow variants possess a growth advantage under hypoxia and exhibit protection from the cytopathic effects of strong acid.

CHAPTER VI

DISCUSSION

Roles and Functions of Colony Variation in *B. pseudomallei*

Colony variation has long been a bewildering property of *B. pseudomallei*. Its frequent observation in clinical isolates and not in environmental isolates has hinted at a role for the behavior in pathogenesis. However, clinical isolates have been mixed in colony type and not associated with any one specific host site (e.g. blood, sputum, etc.). In addition to these difficulties, the phenotypes are frequently unstable in a laboratory setting, discouraging investigation of the phenomenon, and suggesting to many that colony variation in *B. pseudomallei* is a random event - the investigation of which offers little insight into the organism's pathogenesis. To the contrary, we describe here a specific role in infection for colony variants of *B. pseudomallei*, we describe compelling

mechanisms potentially utilized by the organism to do so, and we provide a molecular mechanism for control of the phenomenon.

Colony Variation as a Strategy for Immune Evasion

In extremely generalized terms, a colony of bacteria is simply a very large number of cells arising from a single founder cell, stacked on top of each other, held in place because the growth surface does not permit them to readily move. As such, the system is highly artificial because very rarely in nature would a single bacterium have access to the nutrients or space to conduct such an operation, outside of an aquatic setting wherein the cells would not be restricted in their movements as they are on agar. However the relationship between each bacterium or the "packing" of bacteria in the colony is due in large part to the way their external surfaces interact. This, in turn, is due to the expression of proteins on the extracellular surface and/or lipid composition of the outer membrane. The human immune system initially recognizes bacterial invaders via their external surfaces, therefore bacteria from different colony types often produce variability in immune response.

Given the role of colony variation in immune evasion described for other species of bacteria, some investigators have suggested immune evasion as an explanation for colony variation in *B. pseudomallei*. Despite different lipopolysaccharide profiles existing for different strains of the organism,[119,120] the impact of this variability on colony morphology - if any, has not been described. Intriguingly, loss of PHB stores in infective *B. pseudomallei* has been correlated with differential serological profiles.[119] Unfortunately, the authors did not address the colonial appearance of PHB-deficient bacteria.

Colony Variation as an Altered Physiological State

One explanation for colony variation that isn't usually considered - typically because it occurs in extracellular contexts and is not often considered as a strategy for infection or immune evasion, is the excretion of vast quantities of substances from cells into the extracellular space that can alter the appearance of a colony. In this scenario, the resident cells of a colony are no longer packed membrane-to-membrane but are separated by an extracellular matrix and have the capacity to develop an ultrastructure[121–123] complete with channels and ordered structures.

The extracellular and opportunistic pathogen *P. aeruginosa*, for example, develops a mucoid colony phenotype. Mucoid colonies are so named because they excrete abundant amounts of an exopolysaccharide known as alginate and appear slimy or "mucoid" when grown on solid agar. However, *P. aeruginosa* only develops this phenotype when it has established a chronic infection in the lungs of Cystic Fibrosis patients. It is unclear at this point, exactly how expression of the mucoid phenotype serves to assist the bacteria in the context of chronic infection but it is undeniably a virulence factor of the organism and has major impacts on host colonization, virulence, and immune recognition.[79]

It is of paramount importance to understand that mucoid pseudomonads are not only producing alginate, the bacteria are also exhibiting several other unique phenotypes including (but not limited to): altered swarming motility, production of hydrogen cyanide,[124,125] and protease secretion[126] suggesting that the function of the mucoid phenotype reaches much farther than the surface of the cell. In a similar manner, we have shown that yellow colony variants of *B. pseudomallei* exhibit a vast array of unique

phenotypes. This plurality of phenotypes very clearly reveals that colony variation in *B. pseudomallei* is not simply variation of a few surface molecules to avoid immune detection, but is instead, an altered, cell-wide, physiological state.

Hypoxic Growth Advantage of Yellow Variant *B. pseudomallei*

We believe the primary purpose for the expression of this yellow colony morphology is the persistent colonization of hypoxic niches. We have shown here that these yellow colony variants are adept at growth under hypoxic conditions. Confirming how they accomplish this was beyond the scope of this work, but data gathered in pursuit of understanding these variants indicated a few possible mechanisms for efficient growth under hypoxia. These could include: synthesis of unique secondary metabolites with a possible role in EET and/or non-self selection (Chapter IV), and alternative expression of high-affinity cytochromes[127] (Table B.7).

Cytochrome c typically has a relatively weak affinity (high nanomolar) for molecular oxygen when compared to cytochrome b or cytochrome bd complexes (low nanomolar).[127] *B. pseudomallei* possess multiple copies of both kinds of genes (Table B.7). The majority of cytochrome genes up-regulated in YB in the *in vitro* stomach model are cytochrome c genes (Table B.7), however there is one cytochrome b gene that is up-regulated: BPSL0072, and two cytochrome d ubiquinol oxidases subunits up-regulated: BPSL0501 (*cydB*) and BPSL0502 (*cydA*) suggesting that there is still ample oxygen at a regulated 2.0% environmental O_2 to maintain standard cytochrome c function but that YB is responsive to the low oxygen tension and up-regulates the high-affinity cytochrome b and cytochrome d oxidase.

Extracellular electron transfer (EET) is a well-established paradigm for anaerobic growth and survival of environmental organisms *Shewanella oneidensis* and *Geobacter sulfurreducens*,[106] and EET has also been conclusively shown to be necessary for anaerobic growth and survival of *P. aeruginosa* in biofilms and dependent on the secondary metabolite, pyocyanin.[108] Given that even aerobically grown biofilms are anaerobic below a few microns in depth from the surface,[128,129] it is not outrageous to hypothesize that EET is a strategy for respiration in many different biofilms or microbial communities of any significant depth especially for an obligate respirer such as *B. pseudomallei*. Although electroactivity of *B. pseudomallei* cultures has not been empirically verified, we have observed yellow variants to excrete a unique substance with the property of UV fluorescence.

Fluorescence is best understood as the ability of a compound to emit absorbed energy with the emission occurring in the visible range of the electromagnetic spectrum. Although fluorescence frequently occurs in the visible range of the electromagnetic spectrum such as what is seen with the Green Fluorescent Protein, the phenomenon can also occur outside the visible spectrum as is the case with the electron carriers flavin adenine dinucleotide (FAD^+/H_2), nicotinamide adenine dinucleotide (NAD^+/H), or riboflavin (Vitamin B2) which fluoresce in the UV spectrum[130–132] or with members of the phenazine family.[133] All of these molecules are both electron carriers and UV fluorescent.

Hypoxic Niches in the Human Body

There are very few hypoxic niches in the healthy human body. Human beings are obligate aerobes and thus the human circulatory system is an excellent provider of

oxygen to all cells in all tissues throughout the body. The one exception to this rule in healthy individuals is the gastrointestinal (GI) tract. The interior of the GI tract is technically outside of the body and therefore does not require vascularization or oxygen delivery. In fact, the contents of the GI tract are largely hypoxic or anaerobic depending on the specific location. Beginning in the esophagus and stomach, ingested gases can be taken up by cells lining the organs or outgassed and expelled. Oxygen levels in the stomach have been measured at 25-30 mm Hg in pigs,[134] - which is 2.95% or approximately $^{1}/_{10}^{th}$ the concentration found in the atmosphere at sea level. An alternative electron acceptor, nitrate was measured at 105.3 ± 13 μM in human gastric mucosa.[135]

Acid Survival Mechanisms

Having established that yellow variants of *B. pseudomallei* are adept at growth under hypoxia and that the stomach is a hypoxic environment, surviving or even colonizing the stomach persistently requires more than a growth advantage under hypoxia. The stomach is famous for its extremely low pH: measured at 1.2 to 1.5 while resting and rising to pH 3 to 4 during a meal. Given the cytotoxic effects of extremely low pH environments, we would expect any stomach colonizer to have mechanisms for avoiding or abrogating the acid. We have shown that YB, and to a lesser extent, YA resisted the cytopathic effects of extremely acidic growth media (pH 2) (Figure 3.9) whereas the white form was sensitive to acid. The yellow variants did not, however, exhibit any protection from acid when grown planktonically (data not shown). Interestingly, diabetic patients - individuals most at risk for melioidosis can develop achlorhydria and/or gastroparesis and these conditions are associated with a higher

resting gastric pH and increased stomach emptying times.[45] Both of these pathologies would make colonization of the stomach less challenging for *B. pseudomallei*.

How the yellow variant bacteria achieve acid protection is not completely understood. We do know that YA and YB both alkalize an acidic growth medium and do so for as long as they are able to grow. Both yellow colony variants will shift the pH almost 3 and one half units up from 5 to 8.4 and the observed plateau in pH shift coincides with growth arrest (Figure 3.4). We also know they do this without the production of ammonia. This is extremely unusual as the majority of media-alkalizing bacteria will perform a pH shift via deamidation and then deamination of amino acid polymers which will liberate the amines from carbon backbones. The carbon skeletons of the molecules are then used in the tricarboxylic acid (TCA) cycle or the pentose phosphate pathway and the liberated amine groups are excreted as ammonia. This is the most efficient use of a polypeptide in terms of energy yield as it consumes the entire carbon backbone of the molecule using pathways that generate reducing equivalents and ATP.

A previous report on colony variants of *B. pseudomallei* observed that smooth colony variant cultures do produce ammonia and they produce it in toxic amounts.[136] It is difficult to determine if the authors were working on an equivalent to the yellow variant as they used Wahba growth medium which is very different from LB and includes dye, obscuring naturally produced pigments. However, the modified Kjeldahl method the authors used for quantification of ammonia releases amine groups from carbon backbones such as urea and, presumably, polyamines. In addition to this observation, the authors themselves admit observing increased measurements of ammonia with addition

of heat indicating thermolytic decay of nitrogen-containing compounds that are not ammonia. Finally, the authors noticed no significant difference in nitrogen levels between rough and smooth colonies, only variability in oxalic acid production which they presumed to be a balancing counter-ion to ammonia. Indeed, although they showed a combination of ammonia and high pH to be toxic, and a high pH alone to not be toxic, they did not show toxicity of neutral pH and ammonia which would be expected if ammonia were truly the toxic substance.

One alternative mechanism for dealing with acid stress is the expression of glutamate and arginine decarboxylases,[137] neither of which appear to be encoded in the *B. pseudomallei* genome. Another potential mechanism involved in acid tolerance is the inversion of membrane potential.[137] Genes implicated in this mechanism are not thoroughly described but are thought to be H^+/Cl^- antiporters (ClC).[137,138] However, there are no annotated proton/chloride antiporter genes or chloride transporter genes up-regulated in YB in the *in vitro* stomach model. A third alternative mechanism, and the one which *H. pylori* uses, is the utilization of endogenous urea in combination with production of an excreted urease,[139] which again, results in ammonia which we have not observed.

However, there are genes involved in polyamine production up-regulated in both YA and YB under planktonic and settled conditions, respectively (Table B.1, Figure B.1 and Chapter III Discussion). Polyamines are an attractive explanation for both medium alkalization and acid resistance as they have alkaline pKa's, can be held in the immediate vicinity of cells if bound to an eDNA substrate, and have been established as being necessary for development of bacterial biofilms in other paradigms.[140,141] The results

from this study are inconclusive in regards to the presence or role of polyamines in medium alkalization, acid resistance, or the development of structured communities; but the observations of *speB* expression and potential roles for the polyamines warrant further investigation.

eDNA Substrates for Microbial Communities

We have irrefutably shown that YB produces vast quantities of extracellular DNA (Figure 3.7 B). Extracellular DNA is known to be an essential component of *P. aeruginosa*,[142] *V. cholerae*, and *B. cereus*[143] biofilms and is exquisitely suited for use as a structural component of a microbial community.[144] It is long - often microns in length. This is especially true for large molecular weight polymers such as what we have observed in settled cultures of YB. DNA is also forged of covalent bonds which are resistant to acidic cleavage in environments above a pH of 1.0. In an aqueous environment, DNA is also typically well-hydrated, highly viscous and strongly adhesive.[143] These physical properties allow it to retain adherent cells and particles against mechanically dispersive forces such as peristalsis, which the stomach experiences within 2 to 3 hours after each meal. In addition to resisting mechanical clearance by peristalsis, resident microorganisms of the stomach must contend with constant turnover of the gastric mucin layer. For a well known stomach pathogen, *Helicobacter pylori*, the solution is simple: burrow through the mucin layer and attach to the epithelial/parietal cells below it. However, we observed YB colonization foci to be lumenal to the gastric mucin layer and to have down-regulated swimming motility under hypoxic and acidic conditions (Figure 3.8). These behaviors suggest the strategy employed for stomach colonization by YB is not cell surface attachment but development of a microbial colony

on the lumenal face of the gastric mucosa. The production of an exopolysaccharide matrix that protects the bacteria from the cytopathic effects of stomach acid would likely also protect the mucin layer below the community from acid hydrolysis as the intermolecular bonds that strengthen mucin glycoprotein polymers are acid-hydrolyzed.[145,146]

eDNA Source

Based on the rate of eDNA production relative to viable cells and the stability of live cell titers in YB cultures, we conclude that the source of eDNA in YB cultures is extrusion and not lysis. Molecular mechanisms for eDNA extrusion in biofilm formation have been proposed by other research groups interested in the topic. One study identified an FtsK/SpoIII-E - like pore involved in initial attachment of *Listeria monocytogenes* to abiotic surfaces and biofilm development.[147] Type IV pili have also been shown to be necessary for effective use of eDNA in *P. aeruginosa* biofilms.[142,148] Expression profiling of WHT and YB-type bacteria in the *in vitro* stomach model revealed no differential regulation of Type IV pili (Table 3.2), although this may be because at this point in the *in vitro* stomach model, attachment has already occurred. FtsK/SpoIII E genes were also not up-regulated in YB relative to WHT (Table 3.2), however a chromosome-partitioning ATPase, BPSL1137 — a *repA* homologue — was dramatically up-regulated by more than 36-fold (Table 3.2). DNA polymerase genes were not differentially regulated in YB relative to WHT at 24 hours in the *in vitro* stomach model (Table 3.2). One gene annotated as a DNA polymerase was up-regulated in YB over WHT: BPSS1770 (*polA*), however it was only up-regulated 2.3-fold. Expression of the error-prone DNA polymerase, DNA pol IV (BPSL2306) was not higher in YB than in

WHT but not more than 2-fold (Table 3.2), and the canonical DNA polymerase gene, *dnaE*, was also not differentially regulated (Table 3.2). Lack of differential expression of DNA polymerases at 24 hours is likely explained by the fact that the majority of eDNA production has already occurred by that point in the model (Figure 3.8 B and C) and eDNA production machinery are beginning to be down-regulated at that point.

Model of Infection and Molecular Control of Colony Variation

Considering that YB is capable of persistent gastric colonization but WHT and YA are not, and presuming that ingestion is the natural route of exposure to *B. pseudomallei*, the following integrated model for infection and molecular control of yellow colony variation is proposed: Presuming the expression of yellow variant phenotypes to be the result of a bistable mechanism, in the event that large numbers of *B. pseudomallei* are consumed orally, a small subpopulation of the ingested bacteria exist as the yellow variant phenotype.

Recalling that expression of the yellow phenotype results in the phenotypes of medium alkalization and acid tolerance, in this state of competence for colonization of the stomach, the ingested subpopulation expressing the yellow program could encounter the gastric mucin. Once in contact with the gastric mucin, expression of the yellow program would permit attachment and the extrusion of DNA.

We have observed that attachment is necessary for eDNA production (Chapter III), as growth of YB in uncoated plates failed to produce a highly viscous culture, indicative of eDNA presence. After a sufficient quantity of eDNA is accumulated, the underlying glycoprotein matrix could stabilize, and the cells could buffer local pH to avoid cytopathic effects of stomach acid. Then, once a small community or colony is

established, the YB-form, sessile members of the community would grow and reproduce without concern for the harsh environment of the stomach, utilizing their alternative respiratory mechanisms.

Once the YB form bacteria begin reproducing at significant rates, some could switch to YA. This would likely occur at low rates. We have observed both YB and YA switch away from their initial types to either the YA or WHT type (respectively) under conditions permitting growth. This is likely due to loss of sufficient YelR titers to maintain autoinduced expression. Loss of YelR could either be through dilution of the regulator itself during cellular division, degradation of the regulator by newly expressed proteases, or by dilution of its initially inducing signal if there is one.

The YA form can then swim away from the community - perhaps in the presence of a meal which will absorb some of the acid in the stomach and shift the pH up towards a neutral pH. It is worth remembering that YA is acid-tolerant as well. Once the escaped YA-type bacteria have passed the duodenum and entered a pH-neutral environment in the small intestine, YA can enter M cells that line the length of the intestinal tract and sample the intestinal contents on behalf of the immune system.

Once internalized in an M cell, the invading *B. pseudomallei* can engage its arsenal of intracellular survival techniques, spread via the lymphatic system and seed a constellation of systemic abscesses or progress to septicemia resulting in clinical presentation of melioidosis. Alternatively, the bacteria can exit the body from the intestinal tract and return to the environment to repeat the infection process. Exit from the GI tract or uptake into cells inside the body would bring YA into contact with well-

oxygenated environments and permit its rapid reversion to white-type variants, which are the type observed environmentally and most frequently in patient samples.

Conclusion

In conclusion, colony variation in *B. pseudomallei* strain K96243 is initially a stochastic event yet it confers a growth advantage under hypoxic growth conditions. Associated phenotypes of acid neutralization, acid resistance, production of eDNA, and decreased expression of swimming motility, likely confer the ability to persistently colonize the gastric niche environment which we have demonstrated for YB. The stochastic mechanism for initializing colony variation in *B. pseudomallei* is potentially epigenetic but involves the transcriptional regulator BPSL1887 (YelR). Identifying a colony variant of *B. pseudomallei* that selectively colonizes the stomach supports the theory that the natural route of exposure to *B. pseudomallei* is ingestion. Indeed, delineation of various phenotypes associated with colony variants reveals that not only is colony variation in *B. pseudomallei* actually phase variation, it is an intentional, programmed, cell-wide physiological change likely integral to the life cycle of the organism.

REFERENCES

1. Wuthiekanun, V., Smith, M. D., Dance, D. A. B. & White, N. J. Isolation of *Pseudomonas pseudomallei* from soil in north-eastern Thailand. *Trans. R. Soc. Trop. Med. Hyg.* **89,** 41–3 (1995).

2. Limmathurotsakul, D. *et al. Burkholderia pseudomallei* is spatially distributed in soil in Northeast Thailand. *PLoS Negl. Trop. Dis.* **4,** e694 (2010).

3. Vongphayloth, K. *et al. Burkholderia pseudomallei* detection in surface water in southern Laos using Moore's swabs. *Am. J. Trop. Med. Hyg.* **86,** 872–7 (2012).

4. Dance, D. A. B. Ecology of *Burkholderia pseudomallei* and the interactions between environmental *Burkholderia* spp. and human-animal hosts. *Acta Trop.* **74,** 159–68 (2000).

5. Inglis, T. J. J. & Sagripanti, J.-L. Environmental factors that affect the survival and persistence of *Burkholderia pseudomallei*. *Appl. Environ. Microbiol.* **72,** 6865–75 (2006).

6. Robertson, J., Levy, A., Sagripanti, J.-L. & Inglis, T. J. J. The survival of *Burkholderia pseudomallei* in liquid media. *Am. J. Trop. Med. Hyg.* **82,** 88–94 (2010).

7. Strauss, J. M., Groves, M. G., Mariappan, M. & Ellison, D. W. Melioidosis in Malaysia II. Distribution of *Pseudomonas pseudomallei* in soil and surface water. *Am. J. Trop. Med. Hyg.* **18,** 698–702 (1969).

8. Wuthiekanun, V. *et al.* The use of selective media for the isolation of *Pseudomonas pseudomallei* in clinical practice. *J. Med. Microbiol.* **33,** 121–6 (1990).

9. Suputtamongkol, Y. *et al.* The epidemiology of melioidosis in Ubon Ratchatani, northeast Thailand. *Int. J. Epidemiol.* **23,** 1082–90 (1994).

10. Antony, B. *et al.* Spectrum of melioidosis in the suburbs of Mangalore, S West coast of India. *Southeast Asian J. Trop. Med. Public Health* **41,** 169–174 (2010).

11. Whitmore, B. Y. A. An account of a Glanders-like disease occurring in Rangoon. *J. Hygeine* **13,** 1–35 (1913).

12. Chaowagul, W. *et al.* Melioidosis: a major cause of community-acquired septicemia in Northeastern Thailand. *J. Infect. Dis.* **159,** 890–899 (1989).

13. Dance, D. A. B. Melioidosis : the tip of the iceberg? *Clin. Microbiol. Rev.* **4,** 52–60 (1991).

14. Cheng, A. C. & Currie, B. J. Melioidosis: epidemiology, pathophysiology, and management. *Clin. Microbiol. Rev.* **18,** 383–416 (2005).

15. Currie, B. J., Dance, D. A. B. & Cheng, A. C. The global distribution of *Burkholderia pseudomallei* and melioidosis: an update. *Trans. R. Soc. Trop. Med. Hyg.* **102 Suppl,** S1–4 (2008).

16. Limmathurotsakul, D. & Peacock, S. J. Melioidosis: a clinical overview. *Br. Med. Bull.* 1–15 (2011).

17. Rolim, D. B. *et al.* Melioidosis, Northeastern Brazil. *Emerg. Infect. Dis.* **11,** 1458–60 (2005).

18. Leelarasamee, A. Epidemiology of melioidosis. *J. Infect. Dis. Antimicrob. Agents* **3,** 84–93 (1986).

19. Engelthaler, D. M. *et al.* Molecular investigations of a locally acquired case of melioidosis in Southern AZ, USA. *PLoS Negl. Trop. Dis.* **5,** e1347 (2011).

20. McCormick, J. & Weaver, R. Wound infection by an indigenous *Pseudomonas pseudomallei*-like organism isolated from the soil: case report and epidemiologic study. *J. Infect. Dis.* **135,** 103–107 (1977).

21. Pourtaghva, M., Dodin, A., Portovi, M., Teherani, M. & Galimand, M. [1st case of human pulmonary melioidosis in Iran]. *Bull. Soc. Pathol. Exot. Filiales* **70,** 107–9 (1977).

22. Dodin, A. & Galimand, M. [Origin, course and recession of an infectious disease, melioidosis, in temperate countries]. *Arch. Inst. Pasteur Tunis* **63,** 69–73 (1986).

23. Kao, A. Y. *et al.* Case 19-2005: a 17-year-old girl with respiratory distress and hemiparesis after surviving a tsunami. *N. Engl. J. Med.* **352,** 2628 (2005).

24. Currie, B. J., Ward, L. & Cheng, A. C. The epidemiology and clinical spectrum of melioidosis: 540 cases from the 20 year Darwin prospective study. *PLoS Negl. Trop. Dis.* **4,** e900 (2010).

25. Kanaphun, P. *et al.* Serology and carriage of *Pseudomonas pseudomallei*: a prospective study in 1000 hospitalized children in Northeast Thailand. *J. Infect. Dis.* **167,** 230–3 (1993).

26. Green, R. N. & Tuffnell, P. G. Laboratory acquired melioidosis. *Am. J. Med.* **44,** 599–605 (1968).

27. Schlech, W. F. *et al.* Laboratory-acquired infection with *Pseudomonas pseudomallei* (melioidosis). *N. Engl. J. Med.* **305,** 1133–5 (1981).

28. Kiertiburanakul, S., Sungkanuparph, S., Kositchiwat, S. & Vorachit, M. *Burkholderia pseudomallei*: abscess in an unusual site. *J. Postgrad. Med.* **48,** 124 (2002).

29. Inglis, T., Golledge, C., Clair, A. & Harvey, J. Case report: recovery from persistent septicemic melioidosis. *Am. J. Trop. Med. Hyg.* **65,** 76 (2001).

30. Apisarnthanarak, P., Apisarnthanarak, A. & Mundy, Li. M. Computed tomography characteristics of *Burkholderia pseudomallei*-associated liver abscess. *Clin. Infect. Dis.* **43,** 1618–1620 (2006).

31. Navaneethan, U., Ramesh Kumar, A. C. & Ravi, G. Multiple visceral abscess in a case of melioidosis. *Indian J. Med. Sci.* **60,** 68–70 (2006).

32. Lim, K. S. & Chong, V. H. Radiological manifestations of melioidosis. *Clin. Radiol.* **65,** 66–72 (2010).

33. Ahmad, S., Azura, L., Duski, S. & Aziz, M. Y. Melioidosis: a retrospective review of orthopaedic manifestations. *Malaysian Orthop. J.* **3,** 53–55 (2009).

34. Lath, R., Rajshekhar, V. & George, V. Brain abscess as the presenting feature of melioidosis. *Br. J. Neurosurg.* **12,** 170–2 (1998).

35. Krishnan, P. *et al.* Melioidosis. *J. Assoc. Physicians India* **56,** 636–640 (2008).

36. Dance, D. A. B. *et al.* Acute suppurative parotitis caused by *Pseudomonas pseudomallei* in children. *J. Infect. Dis.* **159,** 654–60 (1989).

37. Low, J. G. H., Quek, A. M. L., Sin, Y. K. & Ang, B. S. P. Mycotic aneurysm due to *Burkholderia pseudomallei* infection: case reports and literature review. *Clin. Infect. Dis.* **40,** 193–8 (2005).

38. Ip, M., Osterberg, L. G., Chau, P. Y. & Raffin, T. A. Pulmonary melioidosis. *Chest* **108,** 1420–1424 (1995).

39. Ngauy, V., Lemeshev, Y., Sadkowski, L. & Crawford, G. Cutaneous melioidosis in a man who was taken as a prisoner of war by the Japanese during World War II. *J. Clin. Microbiol.* **43,** 970–2 (2005).

40. Wong, K. T., Puthucheary, S. D. & Vadivelu, J. The histopathology of human melioidosis. *Histopathology* **26,** 51–55 (1995).

41. Piggott, J. A. & Hochholzer, L. Human melioidosis. A histopathologic study of acute and chronic melioidosis. *Arch. Pathol.* **90,** 101–111 (1970).

42. Goodyear, A., Bielefeldt-Ohmann, H., Schweizer, H. & Dow, S. Persistent gastric colonization with *Burkholderia pseudomallei* and dissemination from the gastrointestinal tract following mucosal inoculation of mice. *PLoS One* **7,** e37324 (2012).

43. Aangervall, L., Dotevall, G. & Lehmann, K.-E. The gastric mucosa in diabetes mellitus. *Acta Med. Scand.* **169,** 339–349 (1961).

44. Chey, W. Y., Kusakcioglu, O., Dinoso, V. & Lorber, S. H. Gastric secretion in patients with chronic pancreatitis and in chronic alcoholics. *Arch. Intern. Med.* **122,** 399–403 (1968).

45. Hasler, W. L. *et al.* Differences in intragastric pH in diabetic vs. idiopathic gastroparesis: relation to degree of gastric retention. *Am. J. Physiol. - Gastrointest. Liver Physiol.* **294,** G1384–91 (2008).

46. Telzak, E. E., Greenberg, M. S., Budnick, L. D., Singh, T. & Blum, S. Diabetes mellitus--a newly described risk factor for infection from *Salmonella enteritidis*. *J. Infect. Dis.* **164,** 538–41 (1991).

47. Stanton, A. T. & Fletcher, W. Melioidosis, a disease of rodents communicable to man. *Lancet* **205,** 10–13 (1925).

48. Mayo, M. *et al. Burkholderia pseudomallei* in unchlorinated domestic bore water, tropical Northern Australia. *Emerg. Infect. Dis.* **17,** 1283–5 (2011).

49. Baker, A. *et al.* Groundwater seeps facilitate exposure to *Burkholderia pseudomallei*. *Appl. Environ. Microbiol.* **77,** 7243–6 (2011).

50. Inglis, T. J. *et al. Burkholderia pseudomallei* traced to water treatment plant in Australia. *Emerg. Infect. Dis.* **6,** 56–9 (2000).

51. Currie, B. J. *et al.* A cluster of melioidosis cases from an endemic region is clonal and is linked to the water supply using molecular typing of *Burkholderia pseudomallei* isolates. *Am. J. Trop. Med. Hyg.* **65,** 177–9 (2001).

52. Dai, D., Chen, Y.-S., Chen, P.-S. & Chen, Y.-L. Case cluster shifting and contaminant source as determinants of melioidosis in Taiwan. *Trop. Med. Int. Heal.* **17,** 1005–13 (2012).

53. Heng, B. H., Goh, K. T., Yap, E. H., Loh, H. & Yeo, M. Epidemiological surveillance of melioidosis in Singapore. *Ann. Acad. Med. Singapore* **27,** 478–84 (1998).

54. Howe, C., Sampath, A. & Spotnitz, M. The *pseudomallei* group: a review. *J. Infect. Dis.* **124,** 598–606 (1971).

55. Yamamoto, T. *et al.* In vitro susceptibilities of *Pseudomonas pseudomallei* to 27 antimicrobial agents. *Antimicrob. Agents Chemother.* **34,** 2027–2029 (1990).

56. Vorachit, M., Chongtrakool, P., Arkomsean, S. & Boonsong, S. Antimicrobial resistance in *Burkholderia pseudomallei*. *Acta Trop.* **74,** 139–44 (2000).

57. Jenney, A. W., Lum, G., Fisher, D. A. & Currie, B. J. Antibiotic susceptibility of *Burkholderia pseudomallei* from tropical northern Australia and implications for therapy of melioidosis. *Int. J. Antimicrob. Agents* **17,** 109–13 (2001).

58. Rotz, L. D., Khan, A. S., Lillibridge, S. R., Ostroff, S. M. & Hughes, J. M. Public health assessment of potential biological terrorism agents. *Emerg. Infect. Dis.* **8,** 225–230 (2002).

59. Chantratita, N. *et al.* Biological relevance of colony morphology and phenotypic switching by *Burkholderia pseudomallei*. *J. Bacteriol.* **189,** 807–17 (2007).

60. Haussler, S., Rohde, M. & Steinmetz, I. Highly resistant *Burkholderia pseudomallei* small colony variants isolated in vitro and in experimental melioidosis. *Med. Microbiol. Immunol.* **188,** 91–7 (1999).

61. Lee, S.-H. *et al. Burkholderia pseudomallei* animal and human isolates from Malaysia exhibit different phenotypic characteristics. *Diagn. Microbiol. Infect. Dis.* **58,** 263–70 (2007).

62. Vietri, N. J. & DeShazer, D. in *Med. Asp. Biol. Warf.* (Dembeck, Z. F.) 147–166 (Borden Institute, Walter Reed Army Medical Center, 2008).

63. Howard, K. & Inglis, T. J. J. Novel selective medium for isolation of *Burkholderia pseudomallei*. *J. Clin. Microbiol.* **41,** 3312–3316 (2009).

64. Goodyear, A. *et al.* An improved selective culture medium enhances the isolation of *Burkholderia pseudomallei* from contaminated specimens. *Am. J. Trop. Med. Hyg.* (2013).

65. Ashdown, L. R. An improved screening technique for isolation of *Pseudomonas pseudomallei* from clinical specimens. *Pathology* **11,** 293–297 (1979).

66. Nigg, C., Ruch, J., Scott, E. & Noble, K. Enhancement of virulence of *Malleomyces pseudomallei*. *J. Bacteriol.* **71,** 530–41 (1956).

67. Van Der Woude, M. W. & Baumler, A. J. Phase and antigenic variation in bacteria. *Clin. Microbiol. Rev.* **17,** 581–611 (2004).

68. Weiser, J. N., Austrian, R., Sreenivasan, P. K. & Masure, H. R. Phase variation in pneumococcal opacity: relationship between colonial morphology and nasopharyngeal colonization. *Infect. Immun.* **62,** 2582–9 (1994).

69. Kim, J. O. & Weiser, J. N. Association of intrastrain phase variation in quantity of capsular polysaccharide and teichoic acid with the virulence of *Streptococcus pneumoniae*. *J. Infect. Dis.* **177,** 368–77 (1998).

70. Waite, R. D., Struthers, J. K. & Dowson, C. G. Spontaneous sequence duplication within an open reading frame of the pneumococcal type 3 capsule locus causes high-frequency phase variation. *Mol. Microbiol.* **42,** 1223–32 (2001).

71. Roche, R. J. & Moxon, E. R. Phenotypic variation of carbohydrate surface antigens and the pathogenesis of *Haemophilus influenzae* infections. *Trends Microbiol.* **3,** 187–190 (1995).

72. Haase, E. M., Zmuda, J. L. & Scannapieco, F. A. Identification and molecular analysis of rough-colony-specific outer membrane proteins of *Actinobacillus actinomycetemcomitans*. *Infect. Immun.* **67,** 2901–8 (1999).

73. Wang, Y., Liu, A. & Chen, C. Genetic basis for conversion of rough-to-smooth colony morphology in *Actinobacillus actinomycetemcomitans*. *Infect. Immun.* **73,** 3749–53 (2005).

74. Proctor, R. A. *et al.* Small colony variants: a pathogenic form of bacteria that facilitates persistent and recurrent infections. *Nat. Rev. Microbiol.* **4,** 295–305 (2006).

75. Kirisits, M. J., Prost, L., Starkey, M. & Parsek, M. R. Characterization of colony morphology variants isolated from *Pseudomonas aeruginosa* biofilms. *Appl. Environ. Microbiol.* **71,** 4809–21 (2005).

76. Onyango, L. A., Hugh Dunstan, R. & Roberts, T. K. Small colony variants of staphylococci: Pathogenesis and evolutionary significance in causing and sustaining problematic human infections. *J. Nutr. Environ. Med.* **17,** 56–75 (2008).

77. Deretic, V., Schurr, M. J. & Yu, H. *Pseudomonas aeruginosa*, mucoidy and the chronic infection phenotype in cystic fibrosis. *Trends Microbiol.* **3,** 351–356 (1995).

78. Zlosnik, J. E. a *et al.* Mucoid and nonmucoid *Burkholderia cepacia* complex bacteria in cystic fibrosis infections. *Am. J. Respir. Crit. Care Med.* 1–27 (2010).

79. Hauser, A. R., Jain, M., Bar-Meir, M. & McColley, S. A. Clinical significance of microbial infection and adaptation in cystic fibrosis. *Clin. Microbiol. Rev.* **24,** 29–70 (2011).

80. Holden, M. T. G. *et al.* Genomic plasticity of the causative agent of melioidosis, *Burkholderia pseudomallei*. *Proc. Natl. Acad. Sci. U. S. A.* **101,** 14240–5 (2004).

81. Van Zandt, K. E., Tuanyok, A., Keim, P. S., Warren, R. L. & Gelhaus, H. C. An objective approach for *Burkholderia pseudomallei* strain selection as challenge material for medical countermeasures efficacy testing. *Front. Cell. Infect. Microbiol.* **2,** 120 (2012).

82. *Biosafety in Microbiological and Biomedical Laboratories*. (U.S. Department of Health and Human Services, 2009).

83. Birge, E. A. *Bacterial and Bacteriophage Genetics*. 76–80 (Birkhäuser, 2006).

84. Hamad, M. A, Zajdowicz, S. L., Holmes, R. K. & Voskuil, M. I. An allelic exchange system for compliant genetic manipulation of the select agents *Burkholderia pseudomallei* and *Burkholderia mallei*. *Gene* **430,** 123–31 (2009).

85. Hamad, M. A. *et al.* Adaptation and antibiotic tolerance of anaerobic *Burkholderia pseudomallei*. *Antimicrob. Agents Chemother.* **55,** 3313–23 (2011).

86. Goodyear, A. *et al.* Protection from pneumonic infection with *Burkholderia* species by inhalational immunotherapy. *Infect. Immun.* **77,** 1579–88 (2009).

87. Rose, H., Baldwin, A., Dowson, C. G. & Mahenthiralingam, E. Biocide susceptibility of the *Burkholderia cepacia* complex. *J. Antimicrob. Chemother.* **63,** 502–10 (2009).

88. Mitsui, Y., Matsumura, K., Kondo, C. & Takashima, R. The role of mucin on experimental *Pseudomonas* keratitis in rabbits. *Invest. Ophthalmol.* **15,** 208–10 (1976).

89. Beumer, R. R., de Vries, J. & Rombouts, F. M. *Campylobacter jejuni* non-culturable coccoid cells. *Int. J. Food Microbiol.* **15,** 153–163 (1992).

90. Qiu, D., Damron, F. H., Mima, T., Schweizer, H. P. & Yu, H. D. PBAD-based shuttle vectors for functional analysis of toxic and highly regulated genes in *Pseudomonas* and *Burkholderia* spp. and other bacteria. *Appl. Environ. Microbiol.* **74,** 7422–6 (2008).

91. Don, R. H., Cox, P. T., Wainwright, B. J., Baker, K. & Mattick, J. S. "Touchdown" PCR to circumvent spurious priming during gene amplification. *Nucleic Acids Res.* **19,** 4008 (1991).

92. Warrens, A. N., Jones, M. D. & Lechler, R. I. Splicing by overlap extension by PCR using asymmetric amplification: an improved technique for the generation of hybrid proteins of immunological interest. *Gene* **186,** 29–35 (1997).

93. Liberati, N. T. *et al.* An ordered, nonredundant library of *Pseudomonas aeruginosa* strain PA14 transposon insertion mutants. *Proc. Natl. Acad. Sci.* **103,** 2833–2838 (2006).

94. Rholl, D. A., Trunck, L. A. & Schweizer, H. P. In vivo Himar1 transposon mutagenesis of *Burkholderia pseudomallei*. *Appl. Environ. Microbiol.* **74,** 7529–35 (2008).

95. Wong, S. M. S., Gawronski, J. D., Lapointe, D. & Akerley, B. J. High-throughput insertion tracking by deep sequencing for the analysis of bacterial pathogens. *Methods Mol. Biol.* **733,** 209–22 (2011).

96. Langmead, B. & Salzberg, S. L. Fast gapped-read alignment with Bowtie 2. *Nat. Methods* **9,** 357–9 (2012).

97. Li, H. *et al.* The Sequence Alignment/Map format and SAMtools. *Bioinformatics* **25,** 2078–9 (2009).

98. Jones-Carson, J. *et al.* Inactivation of [Fe-S] metalloproteins mediates nitric oxide-dependent killing of *Burkholderia mallei*. *PLoS One* **3,** e1976 (2008).

99. Foster, J. W. When protons attack: microbial strategies of acid adaptation. *Curr. Opin. Microbiol.* **2,** 170–174 (1999).

100. Cotter, P. D. & Hill, C. Surviving the acid test: responses of Gram-positive bacteria to low pH. *Microbiol. Mol. Biol. Rev.* **67,** 429–453 (2003).

101. Garton, N. J., Christensen, H., Minnikin, D. E., Adegbola, R. A. & Barer, M. R. Intracellular lipophilic inclusions of mycobacteria in vitro and in sputum. *Microbiology* **148,** 2951–8 (2002).

102. Levine, H. B. & Wolochow, H. Occurrence of poly-β-hydroxybutyrate in *Pseudomonas pseudomallei*. *J. Bacteriol.* **79,** 305 (1960).

103. Redfearn, M. S., Palleroni, N. J. & Stanier, R. Y. A comparative study of *Pseudomonas pseudomallei* and *Bacillus mallei*. *J. Gen. Microbiol.* **43,** 293–313 (1966).

104. Dorrestein, P. C. & Kelleher, N. L. Dissecting non-ribosomal and polyketide biosynthetic machineries using electrospray ionization Fourier-Transform mass spectrometry. *Nat. Prod. Rep.* **23,** 893–918 (2006).

105. Donadio, S., Monciardini, P. & Sosio, M. Polyketide synthases and nonribosomal peptide synthetases: the emerging view from bacterial genomics. *Nat. Prod. Rep.* **24,** 1073–109 (2007).

106. Hernandez, M. E. & Newman, D. K. Extracellular electron transfer. *Cell. Mol. Life Sci.* **58,** 1562–1571 (2001).

107. Newman, D. K. & Kolter, R. A role for excreted quinones in extracellular electron transfer. *Nature* **405,** 94–7 (2000).

108. Wang, Y., Kern, S. E. & Newman, D. K. Endogenous phenazine antibiotics promote anaerobic survival of *Pseudomonas aeruginosa* via extracellular electron transfer. *J. Bacteriol.* **192,** 365–9 (2010).

109. Alice, A. F., López, C. S., Lowe, C. A., Ledesma, M. A. & Crosa, J. H. Genetic and transcriptional analysis of the siderophore malleobactin biosynthesis and transport genes in the human pathogen *Burkholderia pseudomallei* K96243. *J. Bacteriol.* **188,** 1551–66 (2006).

110. Biggins, J. B., Liu, X., Feng, Z. & Brady, S. F. Metabolites from the induced expression of cryptic single operons found in the genome of *Burkholderia pseudomallei*. *J. Am. Chem. Soc.* 1638–1641 (2011).

111. Ishida, K., Lincke, T., Behnken, S. & Hertweck, C. Induced biosynthesis of cryptic polyketide metabolites in a *Burkholderia thailandensis* quorum sensing mutant. *J. Am. Chem. Soc.* **132,** 13966–8 (2010).

112. Hranueli, D. *et al.* Molecular biology of polyketide biosynthesis. *Food Technol. Biotechnol.* **39,** 203–213 (2001).

113. Dietrich, L. E. P., Teal, T. K., Price-Whelan, A. & Newman, D. K. Redox-active antibiotics control gene expression and community behavior in divergent bacteria. *Science (80).* **321,** 1203–1206 (2008).

114. Martins, S. A. R. *et al.* Antimicrobial efficacy of riboflavin/UVA combination (365 nm) in vitro for bacterial and fungal isolates: a potential new treatment for infectious keratitis. *Invest. Ophthalmol. Vis. Sci.* **49,** 3402–8 (2008).

115. Reddy, H. L. *et al.* Toxicity testing of a novel riboflavin-based technology for pathogen reduction and white blood cell inactivation. *Transfus. Med. Rev.* **22,** 133–53 (2008).

116. Vipond, J., Kane, J., Hatch, G., Mccorrison, J. & Nierman, W. C. Sequence determination of *Burkholderia pseudomallei* strain NCTC 13392 colony morphology variants. *Genome Announc.* **1,** 6–7 (2013).

117. Dubnau, D. & Losick, R. Bistability in bacteria. *Mol. Microbiol.* **61,** 564–72 (2006).

118. Veening, J.-W., Smits, W. K. & Kuipers, O. P. Bistability, epigenetics, and bet-hedging in bacteria. *Annu. Rev. Microbiol.* **62,** 193–210 (2008).

119. Nanagara, R., Vipulakorn, K., Suwannaroj, S. & Schumacher Jr, H. R. Atypical morphological characteristics and surface antigen expression of *Burkholderia pseudomallei* in naturally infected human synovial tissues. *Mod. Rheumatol.* **10,** 0129–0136 (2000).

120. Anuntagool, N. *et al.* Short report: lipopolysaccharide heterogeneity among *Burkholderia pseudomallei* from different geographic and clinical origins. *Am. J. Trop. Med. Hygeine* **74,** 348–352 (2006).

121. Lam, J., Chan, R., Lam, K. & Costerton, J. W. Production of mucoid microcolonies by *Pseudomonas aeruginosa* cystic fibrosis. *Infect. Immun.* **28,** 546–556 (1980).

122. Shapiro, J. A. Scanning electron microscope study of *Pseudomonas putida* colonies. *J. Bacteriol.* **164,** 1171–81 (1985).

123. Tetz, V. V., Rybalchenko, O. V. & Savkova, G. A. Ultrastructural features of microbial colony organization. *J. Basic Microbiol.* **30,** 597–607 (1990).

124. Lizewski, S. E. *et al.* Identification of AlgR-regulated genes in *Pseudomonas aeruginosa* by use of microarray analysis. *J. Bacteriol.* **186,** 5672–84 (2004).

125. Carterson, A. J. *et al.* The transcriptional regulator AlgR controls cyanide production in *Pseudomonas aeruginosa*. *J. Bacteriol.* **186,** 6837–44 (2004).

126. Firoved, A. M. & Deretic, V. Microarray analysis of global gene expression in mucoid *Pseudomonas aeruginosa*. *J. Bacteriol.* **185,** 1071–1081 (2003).

127. Morris, R. L. & Schmidt, T. M. Shallow breathing: bacterial life at low O_2. *Nat. Rev. Microbiol.* **11,** 205–12 (2013).

128. Borriello, G. *et al.* Oxygen limitation contributes to antibiotic tolerance of *Pseudomonas aeruginosa* in biofilms. *Antimicrob. Agents Chemother.* **48,** 2659 (2004).

129. Walters, M. C., Roe, F., Bugnicourt, A., Franklin, M. J. & Stewart, P. S. Contributions of antibiotic penetration, oxygen limitation, and low metabolic activity to tolerance of *Pseudomonas aeruginosa* biofilms to Ciprofloxacin and Tobramycin. *Antimicrob. Agents Chemother.* **47,** 317–323 (2003).

130. Casutt, M. S. *et al.* Localization and function of the membrane-bound riboflavin in the Na^+-translocating NADH:quinone oxidoreductase (Na^+-NQR) from *Vibrio cholerae*. *J. Biol. Chem.* **285,** 27088–99 (2010).

131. Yamashita, M., Rosatto, S. S. & Kubota, L. T. Electrochemical comparative study of riboflavin, FMN and FAD immobilized on the silica gel modified with zirconium oxide. *J. Braz. Chem. Soc.* **13,** 635–641 (2002).

132. Oster, G., Bellin, J. S. & Holmstrom, B. Photochemistry of riboflavin. *Experientia* **18,** 249–253 (1962).

133. Cox, C. D. & Graham, R. Isolation of an iron-binding compound from *Pseudomonas aeruginosa*. *J. Bacteriol.* **137,** 357–64 (1979).

134. Kivilaakso, E. *et al.* Gastric blood flow, tissue gas tension and microvascular changes during hemorrhage-induced stress ulceration in the pig. *Am. J. Surg.* **143,** 322–30 (1982).

135. McKnight, G. M. *et al.* Chemical synthesis of nitric oxide in the stomach from dietary nitrate in humans. *Gut* **40,** 211–4 (1997).

136. Rogul, M. & Carr, S. R. Variable ammonia production among smooth and rough strains of *Pseudomonas pseudomallei*: resemblance to bacteriocin production. *J. Bacteriol.* **112,** 372–380 (1972).

137. Foster, J. W. *Escherichia coli* acid resistance: tales of an amateur acidophile. *Nat. Rev. Microbiol.* **2,** 898–907 (2004).

138. Richard, H. & Foster, J. W. *Escherichia coli* glutamate- and arginine-dependent acid resistance systems increase internal pH and reverse transmembrane potential. *J. Bacteriol.* **186,** 6032–41 (2004).

139. Weeks, D. L. A H^+-gated urea channel: the link between *Helicobacter pylori* urease and gastric colonization. *Science (80-.).* **287,** 482–485 (2000).

140. Shah, P. & Swiatlo, E. A multifaceted role for polyamines in bacterial pathogens. *Mol. Microbiol.* **68,** 4–16 (2008).

141. Patel, C. N. *et al.* Polyamines are essential for the formation of plague biofilm. *J. Bacteriol.* **188,** 2355–63 (2006).

142. Van Schaik, E. J. *et al.* DNA binding: a novel function of *Pseudomonas aeruginosa* Type IV pili. *J. Bacteriol.* **187,** 1455–64 (2005).

143. Das, T., Sharma, P. K., Busscher, H. J., van der Mei, H. C. & Krom, B. P. Role of extracellular DNA in initial bacterial adhesion and surface aggregation. *Appl. Environ. Microbiol.* **76,** 3405–8 (2010).

144. Flemming, H.-C. & Wingender, J. The biofilm matrix. *Nat. Rev. Microbiol.* **8,** 623–33 (2010).

145. Allen, A. & Garner, A. Mucus and bicarbonate secretion in the stomach and their possible role in mucosal protection. *Gut* **21,** 249–262 (1980).

146. Celli, J. *et al.* Viscoelastic properties and dynamics of porcine gastric mucin. *Biomacromolecules* **6,** 1329–33 (2005).

147. Chang, Y., Gu, W., Zhang, F. & McLandsborough, L. Disruption of *lmo1386*, a putative DNA translocase gene, affects biofilm formation of *Listeria monocytogenes* on abiotic surfaces. *Int. J. Food Microbiol.* **161,** 158–63 (2013).

148. Barken, K. B. *et al.* Roles of type IV pili, flagellum-mediated motility and extracellular DNA in the formation of mature multicellular structures in *Pseudomonas aeruginosa* biofilms. *Environ. Microbiol.* **10,** 2331–43 (2008).

APPENDIX A

PROTOCOLS

A.1 - Arbitrary PCR (ARB PCR)

ARB PCR is modified from a protocol received from the Vasil laboratory to work with the transposon pTBurk1 and is as follows:

1. Isolate total DNA of verified transposon mutant in purity using the DNeasy Blood & Tissue Kit (QIAGEN) with the following minor modifications:
2. Resuspend bacteria collected for total DNA harvest in enzymatic lysis buffer (filter-sterile 20 mM Tris*Cl pH 8.0, 2mM EDTA, 1.2% Triton X-100 plus 1.0 mg/mL fresh lysozyme in 10mM Tris-HCl added directly before use)
3. Incubate at 37°C for 60 min
4. Follow the DNeasy Blood & Tissue protocol for Gram-negative bacteria exactly for the remainder of the DNA isolation
5. Before PCR, digest 5µL of the purified total DNA with BamHI or EcoRI in a 10µL reaction (total volume)
6. In the first PCR reaction, prepare the following mixture:

Table A.1 ARB PCR1 Reaction

Volume (μL)	Reagent	Initial Concentration
1.0	pTBurk1 ARB1	1 μg/μL
1.0	pTBurk1 ARB2	1 μg/μL
1.0	pTBurk1 ARB3	1 μg/μL
1.0	pTBurk1 ARB4	1 μg/μL
10.0	Phusion Buffer HF	5x
2.0	dNTP mix	2.5 mM each, 10 mM total
25.5	sterile, distilled, nuclease-free H_2O	-
2.5	Dimethylsulfoxide (DMSO)	100%
1.0	Phusion Polymerase	-
5.0	digested total DNA	-
(50)	Total volume	

7. Then subject the mixtures to the following cycling parameters:

Table A.2 ARB PCR1 Cycling Parameters

Stage	Temperature	Duration
A	94°C	2 min
B (5 cycles)	94°C	30 sec
	42°C -1°C per cycle	30 sec
	72°C	3 min
C (25 cycles)	94°C	2 min
	65°C	30 sec
	72°C	3 min
D	4°C	indefinitely

8. Purify PCR products from buffer, reagents, and enzyme using the PCR Cleanup Kit (QIAGEN) and elute in 50 μL sterile, distilled, nuclease-free H_2O
9. In the second PCR, use:

Table A.3 ARB PCR2 Reaction

Volume (μL)	Reagent	Initial Concentration
1.0	pTBurk1 ARB5	1 μg/μL
1.0	pTBurk1 ARB6	1 μg/μL
10.0	Phusion Buffer HF	5x
2.0	dNTP mix	2.5 mM each, 10 mM total
1.0	$MgCl_2$	25mM
30.5	sterile, distilled, nuclease-free H_2O	-
2.5	Dimethylsulfoxide (DMSO)	100%
1.0	Phusion Polymerase	-
1.0	PCR1 product	-
(50)	Total volume	

10. Then subject the reactions to the following cycling parameters:

Table A.4 ARB PCR2 Cycling Parameters

Stage	Temperature	Duration
A	94°C	2 min
B (30 cycles)	94°C	30 sec
	57°C	30 sec
	72°C	3 min
C	72°C	5 min
D	4°C	indefinitely

11. Check PCR products by agarose gel electrophoresis; expect a smear or a ladder
12. Purify PCR products with the PCR Cleanup Kit (QIAGEN), elute in 40 μL sterile, distilled, nuclease-free H_2O
13. Sequence the PCR products by submitting the following mixture to the University of Colorado Cancer Center DNA Sequencing Core: 1.0 μL final PCR product, 1.0 μL pTBurk1 ARBSeq, 18.0 μL sterile, nuclease-free H_2O for a total volume of 20 μL. Indicate that the template is a PCR product when submitting the samples.

APPENDIX B

TRANSCRIPTIONAL PROFILING DATA

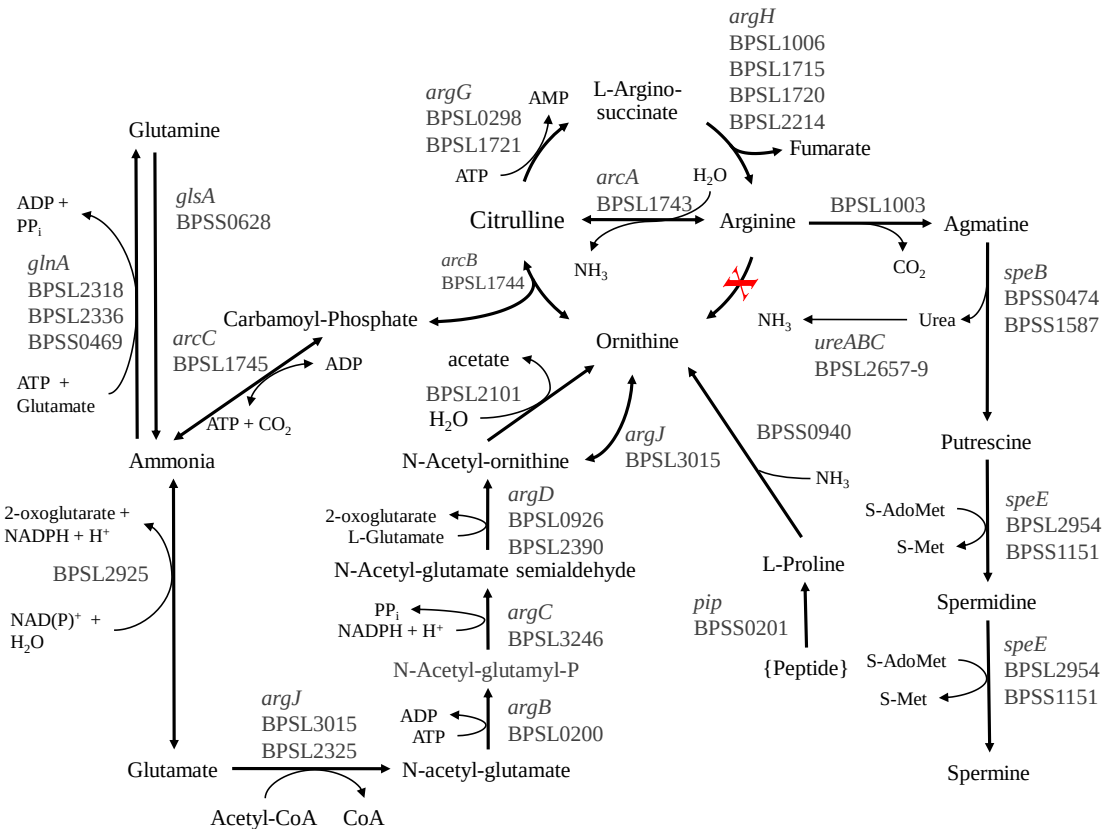

Figure B.1 Polyamine and Urea Metabolism in *B. pseudomallei* K96243
Metabolic reactants, products, enzyme names, genes, and enzymatic reactions for ammonia, urea, and polyamine metabolism were retrieved from the Kyoto Encyclopedia of Genes and Genomes (KEGG) as annotated for *B. pseudomallei* K96243. Multiple genes containing the same Enzyme Commission (E.C.) categorization were grouped together alongside the same reaction arrow. The "**X**" indicates an enzyme missing from the canonical Urea Cycle in *B. pseudomallei* K96243.

Table B.1 Transcriptional Profiling of Polyamine and Urea Metabolism Genes

Gene	Name	Product	YB:WHT† (Std.Dev.)	YA:WHT‡ (Std.Dev.)
BPSL0200	*argB*	acetylglutamate kinase	0.95 (0.0)	0.91 (0.4)
BPSL0298	*argG*	argininosuccinate synthase	0.99 (0.0)	0.72 (0.3)
BPSL0926	*argD*	acetylornithine transaminase	0.86 (0.0)	1.1 (0.2)
BPSL1003		ornithine decarboxylase	0.99 (0.0)	1.0 (0.4)
BPSL1006	*argH*	argininosuccinate lyase	1.6 (0.0)	1.3 (0.4)
BPSL1556	*potG*	putrescine transport ATP-binding protein	1.7 (0.0)	1.1 (0.2)
BPSL1715		argininosuccinate lyase	0.26 (0.03)	1.9 (0.8)
BPSL1720		argininosuccinate lyase	0.08 (0.0)	1.3 (0.3)
BPSL1721		argininosuccinate synthase	0.13 (0.0)	1.2 (0.3)
BPSL1742	*arcD*	arginine/ornithine antiporter	3.7 (0.0)	1.1 (0.1)
BPSL1743	*arcA*	arginine deiminase	2.8 (0.0)	2.6 (2.0)
BPSL1744	*arcB*	ornithine carbamoyltransferase	2.2 (0.0)	1.7 (0.8)
BPSL1745	*arcC*	carbamate kinase	2.5 (0.0)	1.3 (0.8)
BPSL2101		acetylornithine deacetylase	0.83 (0.01)	2.3 (1.6)
BPSL2318	*glnA*	glutamine synthetase	0.67 (0.0)	1.1 (0.4)
BPSL2325		N-acetylglutamate synthase	1.1 (0.0)	3.1 (2.3)
BPSL2336		glutamine synthetase	1.8 (0.0)	1.2 (0.3)
BPSL2390	*argD*	bifunctional N-succinyldiaminopimelate-aminotransferase/acetylornithine transaminase	0.79 (0.0)	2.0 (1.4)
BPSL2925		glutamate dehydrogenase	1.2 (0.0)	0.16 (0.1)
BPSL2954	*speE*	spermidine synthase	1.2 (0.0)	1.7 (0.6)
BPSL3015	*argJ*	bifunctional ornithine acetyltransferase/N-acetylglutamate synthase	2.0 (0.0)	1.8 (0.9)
BPSL3246	*argC*	N-acetyl-gamma-glutamyl-phosphate reductase	0.60 (0.0)	1.3 (0.4)
BPSS0201	*pip*	prolyl iminopeptidase	0.96 (0.03)	1.7 (0.8)
BPSS0469		glutamine synthetase	1.0 (0.0)	1.9 (1.0)
BPSS0474	*speB*	agmatinase	2.4 (0.2)	4.3 (2.7)
BPSS0628	*glsA*	glutaminase	2.5 (0.1)	1.8 (0.3)
BPSS0940		ornithine cyclodeaminase	3.0 (0.2)	2.4 (1.3)
BPSS1151		spermidine synthase	8.8 (0.5)	3.3 (2.5)
BPSS1587	*speB*	agmatinase	0.65 (0.05)	1.1 (0.3)
BPSL2656	*ureD*	UreD-family accessory protein	2.4 (0.0)	1.8 (1.1)
BPSL2657	*ureA*	urease, gamma subunit	1.4 (0.1)	1.4 (0.7)
BPSL2658	*ureB*	urease beta subunit	1.1 (0.0)	0.81 (0.08)
BPSL2659	*ureC*	urease alpha subunit	0.88 (0.03)	1.5 (1.0)
BPSL2660	*ureE*	urease accessory protein	- (-)	2.1 (1.3)
BPSL2661	*ureF*	Urease accessory protein	1.4 (0.0)	1.1 (0.1)

Gene	Name	Product	YB:WHT† (Std.Dev.)	YA:WHT‡ (Std.Dev.)
BPSL2662	*ureG*	Urease accessory protein	1.5 (0.1)	1.8 (1.0)

†RNA was collected in triplicate from bacteria grown in the *in vitro* stomach model under hypoxia (2.0% O_2) at 24 hours of growth and analyzed by RNAseq**.** ‡RNA collected in triplicate from YA and WHT bacteria grown planktonically for 12 hours (early in stationary phase) and analyzed by microarray. No values "-(-)" indicate insufficient YB or WHT reads to perform a valid ratio calculation (i.e. divide by zero). Data reported is the RPKM linear-normalized ratio of YB to WHT reads with the standard deviation in parentheses for RNAseq data; and the ratio of normalized YA to WHT average signal intensities with the standard deviation in parentheses for microarray data.

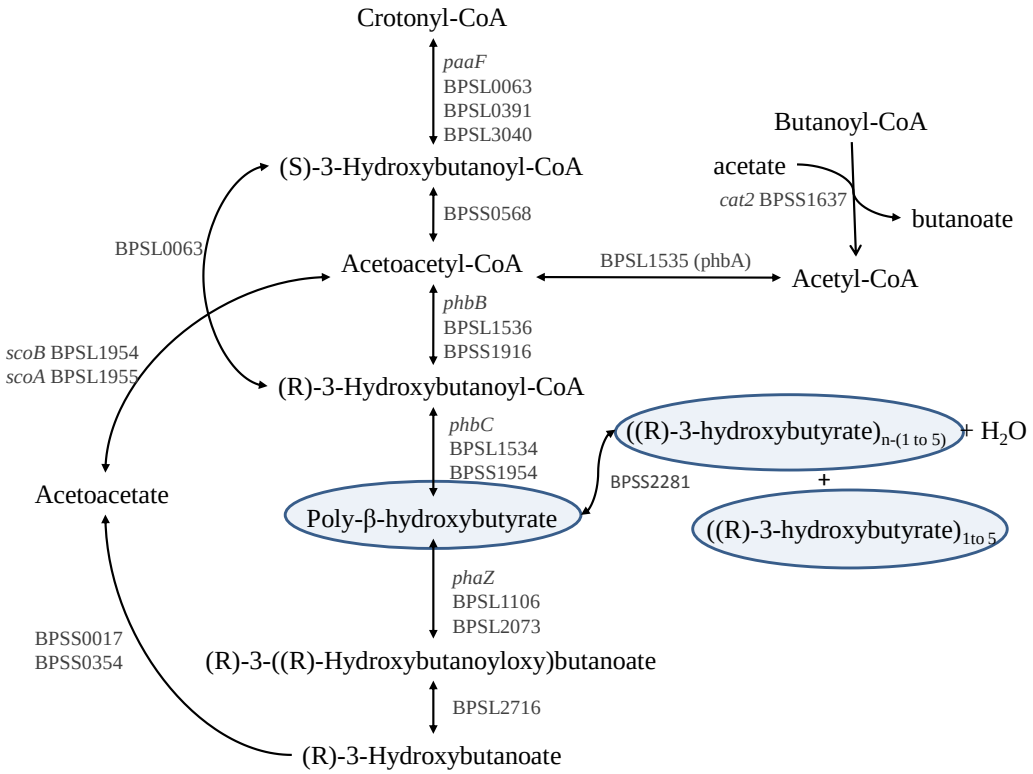

Figure B.2 β-poly-hydroxybutyrate (PHB) Metabolism in *B. pseudomallei* K96243
Metabolic reactants, products, enzyme names, genes, and enzymatic reactions for β-poly-hydroxybutyrate (PHB) and butanoate metabolism were retrieved from KEGG as annotated for *B. pseudomallei* K96243. Multiple genes containing the same E.C. categorization were grouped together alongside the same reaction arrow. Light blue filled circles indicate PHB polymer.

Table B.2 Transcriptional Profiling of β-PHB Production and Use Genes

Gene	Name	Product	YB:WHT† (Std.Dev.)	YA:WHT‡ (Std.Dev.)
BPSL3040	*paaF*	enoyl-CoA hydratase	0.79 (0.0)	1.1 (0.8)
BPSL0063		fatty oxidation complex subunit alpha	1.7 (0.1)	1.1 (0.2)
BPSL0391		enoyl-CoA hydratase	1.1 (0.0)	3.4 (2.3)
BPSS0568		3-hydroxybutyryl-CoA dehydrogenase	0.8 (0.05)	1.5 (0.7)
BPSL1535	*phbA*	acetyl-CoA acetyltransferase	1.4 (0.0)	0.21 (0.10)
BPSL1536	*phbB*	acetyacetyl-CoA reductase	0.89 (0.0)	0.28 (0.10)
BPSS1916	*phbB*	acetoacetyl-CoA reductase	0.54 (0.0)	0.17 (0.07)
BPSL1534	*phbC*	poly-beta-hydroxybutyrate polymerase	1.2 (0.0)	0.19 (0.07)
BPSS2281		PHB depolymerase	0.92 (0.13)	1.2 (0.6)
BPSL2073	*phaZ*	poly(3-hydroxybutyrate) depolymerase	0.87 (0.02)	0.05 (0.01)
BPSL1106		depolymerase/histone-like protein	1.7 (0.0)	1.8 (1.0)
BPSL2716		exported hydrolase	1.1 (0.0)	1.2 (0.3)
BPSS0017		3-hydroxybutyrate dehydrogenase	1.4 (0.0)	0.92 (0.34)
BPSS0354		3-hydroxybutyrate dehydrogenase	0.81 (0.0)	§
BPSL1954	*scoB*	succinyl-CoA:3-ketoacid-coenzyme A transferase subunit B	0.40 (0.0)	0.52 (0.50)
BPSL1955	*scoA*	succinyl-CoA:3-ketoacid-coenzyme A transferase subunit A	0.52 (0.0)	0.06 (0.04)

†RNA was collected in triplicate from bacteria grown in the *in vitro* stomach model under hypoxia (2.0% O_2) at 24 hours of growth and analyzed by RNAseq**.** ‡RNA collected in triplicate from YA and WHT bacteria grown planktonically for 12 hours (early in stationary phase) and analyzed by microarray. Data reported is the RPKM linear-normalized ratio of YB to WHT reads with the standard deviation in parentheses for RNAseq data; and the ratio of normalized YA to WHT average signal intensities with the standard deviation in parentheses for microarray data. § indicates no unique microarray probe for indicated gene

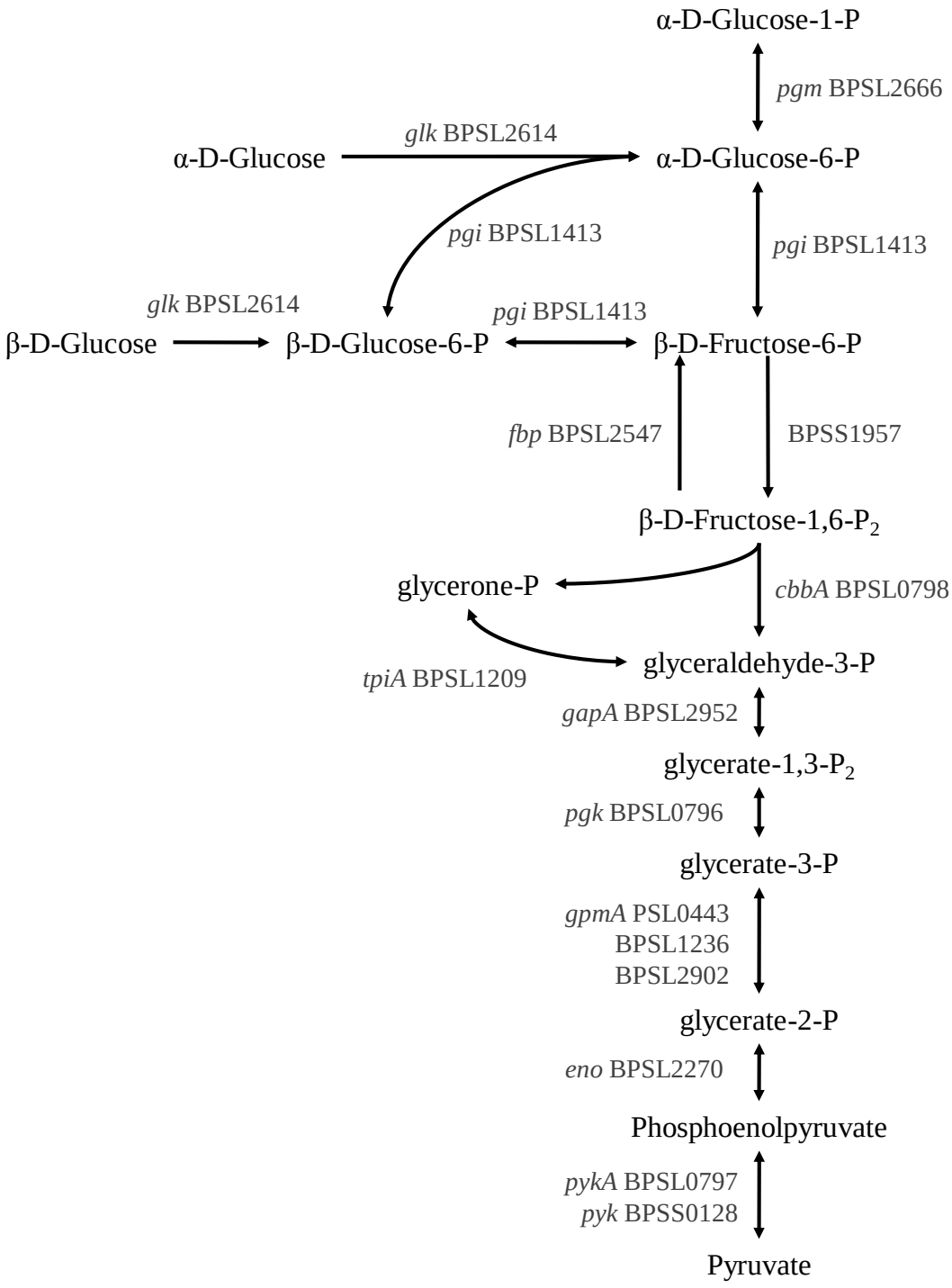

Figure B.3 Glycolysis and Gluconeogenesis in *B. pseudomallei* K96243
Metabolic reactants, products, enzyme names, genes, and enzymatic reactions for glycolysis and gluconeogenesis were retrieved from KEGG as annotated for *B. pseudomallei* K96243. Multiple genes containing the same E.C. categorization were grouped together alongside the same reaction arrow.

Table B.3 Transcriptional Profiling of Glycolysis and Gluconeogenesis Genes

Gene	Name	Product	YB:WHT† (Std.Dev.)	YA:WHT‡ (Std.Dev.)
BPSL2666	*pgm*	phosphoglucomutase	1.1 (0.0)	0.67 (0.30)
BPSL1413	*pgi*	glucose-6-phosphate isomerase	0.77 (0.01)	0.65 (0.19)
BPSL2614	*glk*	bifunctional glucokinase/RpiR family transcriptional regulator	0.72 (0.0)	1.6 (0.9)
BPSL2547	*fbp*	fructose-1,6-bisphosphatase	0.84 (0.0)	2.8 (1.9)
BPSS1957		6-phosphofructokinase	2.1 (0.1)	2.0 (1.3)
BPSL0798	*cbbA*	fructose-1,6-bisphosphate aldolase	0.98 (0.0)	0.26 (0.05)
BPSL1209	*tpiA*	triosephosphate isomerase	1.3 (0.0)	0.99 (0.20)
BPSL2952	*gapA*	glyceraldehyde 3-phosphate dehydrogenase 1	1.0 (0.0)	0.34 (0.27)
BPSL0796	*pgk*	phosphoglycerate kinase	0.81 (0.0)	0.67 (0.08)
BPSL0443	*gpmA*	phosphoglyceromutase	0.81 (0.0)	1.6 (0.8)
BPSL1236		phosphoglycerate mutase	0.66 (0.02)	1.5 (0.8)
BPSL2902		phosphoglycerate mutase	0.50 (0.08)	1.0 (0.5)
BPSL2270	*eno*	phosphopyruvate hydratase	0.87 (0.0)	0.73 (0.07)
BPSL0797	*pykA*	pyruvate kinase	0.638 (0.0)	2.1 (1.7)
BPSS0128	*pyk*	pyruvate kinase	0.88 (0.15)	1.5 (0.7)

†RNA was collected in triplicate from bacteria grown in the *in vitro* stomach model under hypoxia (2.0% O_2) at 24 hours of growth and analyzed by RNAseq**.** ‡RNA collected in triplicate from YA and WHT bacteria grown planktonically for 12 hours (early in stationary phase) and analyzed by microarray. Data reported is the RPKM linear-normalized ratio of YB to WHT reads with the standard deviation in parentheses for RNAseq data; and the ratio of normalized YA to WHT average signal intensities with the standard deviation in parentheses for microarray data.

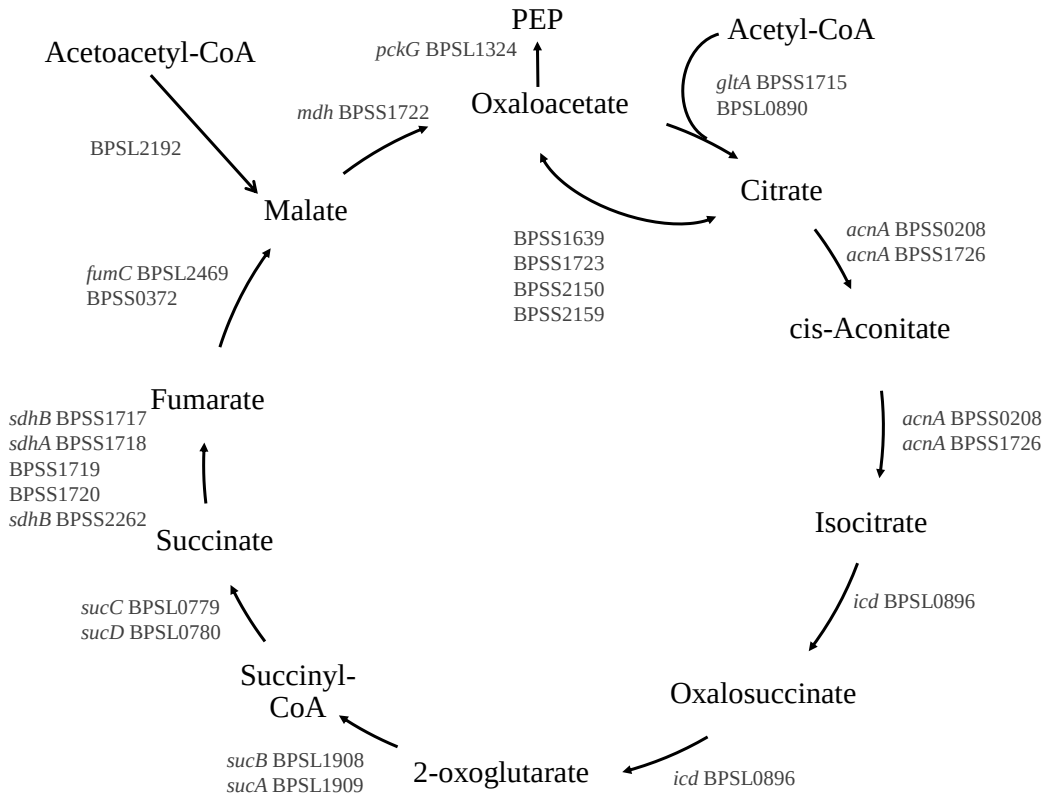

Figure B.4 Tricarboxylic Acid (TCA) Cycle in *B. pseudomallei* K96243
Metabolic reactants, products, enzyme names, genes, and enzymatic reactions for the Tricarboxylic Acid (TCA) cycle were retrieved from KEGG as annotated for *B. pseudomallei* K96243. Multiple genes containing the same E.C. categorization were grouped together alongside the same reaction arrow.

Table B.4 Transcriptional Profiling of TCA Cycle Genes

Gene	Name	Product	YB:WHT† (Std.Dev.)	YA:WHT‡ (Std.Dev.)
BPSS1715	*gltA*	type II citrate synthase	0.82 (0.0)	1.5 (0.8)
BPSL0890		citrate synthase	- (-)	1.5 (0.7)
BPSS0208	*acnA*	aconitate hydratase	1.2 (0.0)	1.4 (0.3)
BPSS1726	*acnA*	aconitate hydratase	1.1 (0.0)	0.62 (0.32)
BPSL0896	*icd*	isocitrate dehydrogenase	1.1 (0.0)	1.1 (0.9)
BPSL1908	*sucB*	dihydrolipoamide succinyltransferase	0.98 (0.0)	1.6 (1.2)
BPSL1909	*sucA*	2-oxoglutarate dehydrogenase E1	0.90 (0.0)	0.38 (0.09)
BPSL0779	*sucC*	succinyl-CoA synthetase subunit beta	1.4 (0.0)	1.2 (0.3)
BPSL0780	*sucD*	succinyl-CoA synthetase subunit alpha	0.74 (0.0)	0.89 (0.66)
BPSS1717	*sdhB*	succinate dehydrogenase iron-sulfur subunit	0.64 (0.0)	0.42 (0.22)
BPSS1718	*sdhA*	succinate dehydrogenase flavoprotein subunit	0.71 (0.0)	0.82 (0.28)
BPSS1719		succinate dehydrogenase	1.5 (0.0)	1.4 (1.3)
BPSS1720		succinate dehydrogenase cytochrome b-556 subunit	1.3 (0.0)	2.7 (3.2)
BPSS2262	*sdhB*	succinate dehydrogenase iron-sulfur subunit	1.0 (0.0)	0.80 (0.30)
BPSL2469	*fumC*	fumarate hydratase	2.0 (0.2)	1.3 (0.3)
BPSS0372		fumarate hydratase	1.1 (0.0)	1.0 (0.0)
BPSL2192	*aceB*	malate synthase	0.61 (0.0)	0.72 (0.55)
BPSS1722	*mdh*	malate dehydrogenase	0.93 (0.0)	0.32 (0.13)
BPSL1324	*pckG*	phosphoenolpyruvate carboxykinase	0.96 (0.0)	4.5 (4.1)
BPSS1639		citrate lyase subunit beta	0.47 (0.02)	1.1 (0.1)
BPSS1723		lyase	1.6 (0.1)	1.1 (0.6)
BPSS2150		citrate lyase	0.69 (0.03)	2.1 (1.7)
BPSS2159		citrate lyase subunit beta	1.1 (0.1)	1.6 (0.4)

†RNA was collected in triplicate from bacteria grown in the *in vitro* stomach model under hypoxia (2.0% O_2) at 24 hours of growth and analyzed by RNAseq**.** ‡RNA collected in triplicate from YA and WHT bacteria grown planktonically for 12 hours (early in stationary phase) and analyzed by microarray. No values "-(-)" indicate insufficient YB or WHT reads to perform a valid ratio calculation (i.e. divide by zero). Data reported is the RPKM linear-normalized ratio of YB to WHT reads with the standard deviation in parentheses for RNAseq data; and the ratio of normalized YA to WHT average signal intensities with the standard deviation in parentheses for microarray data.

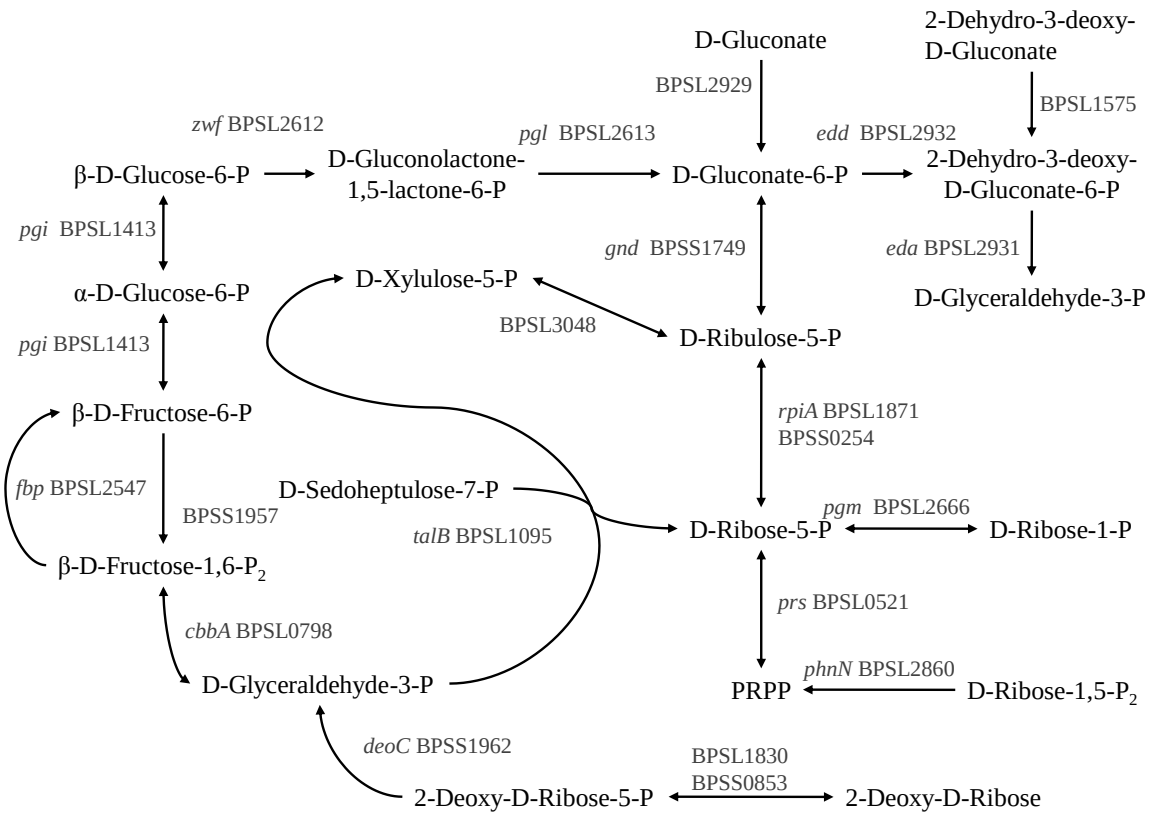

Figure B.5 Pentose Phosphate Pathway in *B. pseudomallei* K96243
Metabolic reactants, products, enzyme names, genes, and enzymatic reactions for the pentose phosphate pathway were retrieved from KEGG as annotated for *B. pseudomallei* K96243. Multiple genes containing the same E.C. categorization were grouped together alongside the same reaction arrow.

Table B.5 Transcriptional Profiling of Pentose Phosphate Pathway Genes

Gene	Name	Product	YB:WHT† (Std.Dev.)	YA:WHT‡ (Std.Dev.)
BPSL1830		ribokinase	0.47 (0.01)	1.5 (0.5)
BPSS0853		ribokinase	0.85 (0.06)	1.0 (0.1)
BPSS1962	*deoC*	deoxyribose-phosphate aldolase	0.85 (0.06)	1.4 (0.4)
BPSL1095	*talB*	transaldolase B	0.89 (0.0)	0.89 (0.16)
BPSL0798	*cbbA*	fructose-1,6-bisphosphate aldolase	0.98 (0.0)	0.26 (0.05)
BPSL2547	*fbp*	fructose-1,6-bisphosphatase	0.84 (0.0)	2.8 (1.9)
BPSS1957		6-phosphofructokinase	2.1 (0.1)	2.0 (1.3)
BPSL1413	*pgi*	glucose-6-phosphate isomerase	0.77 (0.01)	0.65 (0.19)
BPSL2612	*zwf*	glucose-6-phosphate 1-dehydrogenase	0.83 (0.0)	5.5 (4.6)
BPSL2613	*pgl*	6-phosphogluconolactonase	0.88 (0.05)	2.8 (2.0)
BPSL2929		thermoresistant gluconokinase	0.65 (0.0)	13.5 (5.8)
BPSL2932	*edd*	phosphogluconate dehydratase	0.63 (0.01)	2.1 (1.0)
BPSL1575		sugar kinase	1.3 (0.2)	1.6 (0.6)
BPSL2931	*eda*	KHG/KDPG aldolase	1.2 (0.0)	1.1 (0.3)
BPSS1749	*gnd*	6-phosphogluconate dehydrogenase	0.76 (0.01)	1.0 (0.2)
BPSL1871	*rpiA*	ribose-5-phosphate isomerase A	1.1 (0.0)	1.3 (0.4)
BPSS0254		ribose 5-phosphate isomerase	2.8 (0.1)	1.5 (0.9)
BPSL2666	*pgm*	phosphoglucomutase	1.1 (0.0)	0.67 (0.30)
BPSL0521	*prs*	ribose-phosphate pyrophosphokinase	1.9 (0.0)	20 (19)
BPSL2860	*phnN*	ATP-binding protein PhnN	-(-)	1.0 (0.4)

†RNA was collected in triplicate from bacteria grown in the *in vitro* stomach model under hypoxia (2.0% O_2) at 24 hours of growth and analyzed by RNAseq**.** ‡RNA collected in triplicate from YA and WHT bacteria grown planktonically for 12 hours (early in stationary phase) and analyzed by microarray. No values "-(-)" indicate insufficient YB or WHT reads to perform a valid ratio calculation (i.e. divide by zero). Data reported is the RPKM linear-normalized ratio of YB to WHT reads with the standard deviation in parentheses for RNAseq data; and the ratio of normalized YA to WHT average signal intensities with the standard deviation in parentheses for microarray data.

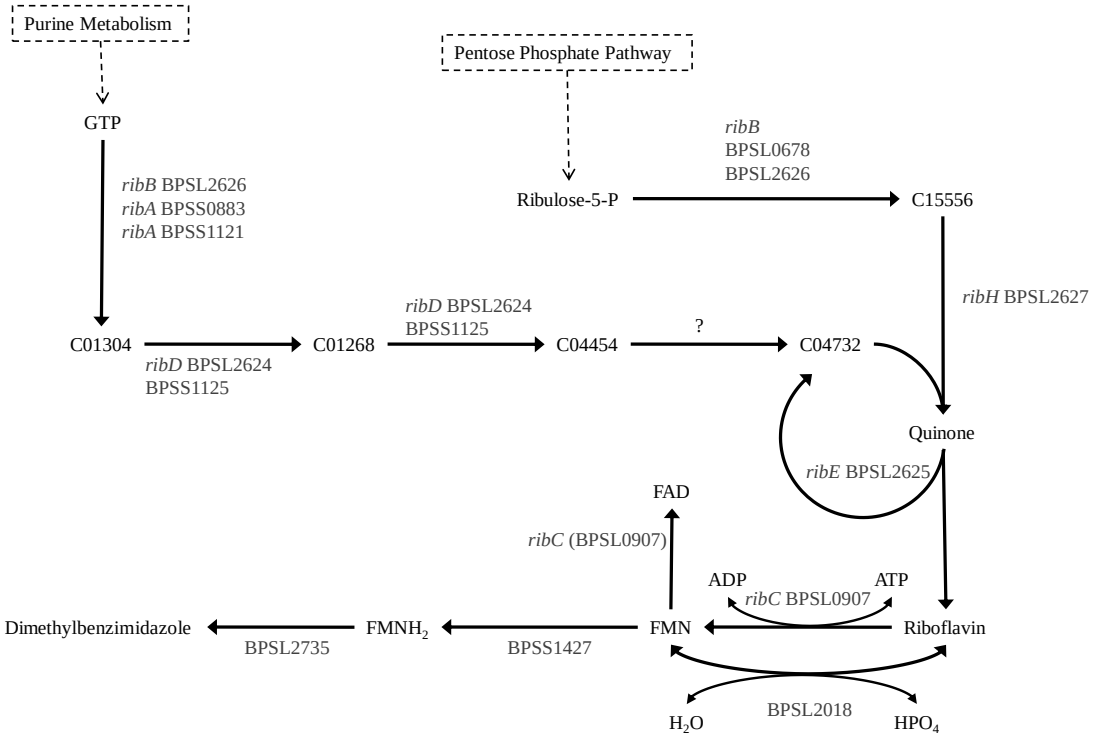

Figure B.6 Riboflavin Metabolism Genes in *B. pseudomallei* K96243
Metabolic reactants, products, enzyme names, genes, and enzymatic reactions for riboflavin metabolism were retrieved from KEGG as annotated for *B. pseudomallei* K96243. Multiple genes containing the same E.C. categorization were grouped together alongside the same reaction arrow. C01304: 2,5-Diamino-6-(5-phospho-D-ribosyl-amino)pyrimidin-4(3H)-one. C01268: 5-Amino-6-(5'-phospho-ribosylamino)uracil. C04454: 5-Amino-6-(5'-phospho-D-ribitylamino)-uracil. C04732: 5-Amino-6-(1-D-ribitylamino)uracil. C15556: L-3,4-Dihydroxy-butan-2-one 4-phosphate. "?" Indicates a missing step for the conversion of GTP to quinone in *B. pseudomallei* K96243

Table B.6 Transcriptional Profiling of Riboflavin Metabolism Genes

Gene	Name	Product	YB:WHT† (Std.Dev.)	YA:WHT‡ (Std.Dev.)
BPSL0678	ribB	3,4-dihydroxy-2-butanone 4-phosphate synthase	0.79 (0.05)	1.7 (0.8)
BPSL0907		bifunctional riboflavin kinase/FMN adenylyltransferase	0.99 (0.0)	1.5 (1.0)
BPSL2018		acid phosphatase	0.94 (0.03)	0.92 (0.46)
BPSL2624	ribD	multifunctional riboflavin biosynthetic protein [deaminase, reductase	1.1 (0.0)	1.9 (0.7)
BPSL2625	ribE	riboflavin synthase subunit alpha	1.0 (0.0)	7.7 (6.0)
BPSL2626	ribB	bifunctional 3,4-dihydroxy-2-butanone 4-phosphate synthase/GTP cyclohydrolase II-like protein	1.2 (0.0)	1.4 (0.7)
BPSL2627	ribH	6,7-dimethyl-8-ribityllumazine synthase	0.58 (0.0)	0.26 (0.10)
BPSL2628	nusB	transcription antitermination protein NusB	0.85 (0.03)	0.19 (0.07)
BPSL2735		oxidoreductase	1.3 (0.0)	1.3 (0.5)
BPSS0883	ribA	GTP cyclohydrolase II	1.2 (0.0)	2.3 (0.7)
BPSS1121	ribA	GTP cyclohydrolase II	- (-)	2.0 (2.1)
BPSS1125		riboflavin biosynthesis protein	1.2 (0.0)	1.7 (1.1)
BPSS1427		hypothetical protein	0.79 (0.05)	1.5 (0.7)

†RNA was collected in triplicate from bacteria grown in the *in vitro* stomach model under hypoxia (2.0% O_2) at 24 hours of growth and analyzed by RNAseq**.** ‡RNA collected in triplicate from YA and WHT bacteria grown planktonically for 12 hours (early in stationary phase) and analyzed by microarray. No values "-(-)" indicate insufficient YB or WHT reads to perform a valid ratio calculation (i.e. divide by zero). Data reported is the RPKM linear-normalized ratio of YB to WHT reads with the standard deviation in parentheses for RNAseq data; and the ratio of normalized YA to WHT average signal intensities with the standard deviation in parentheses for microarray data.

Table B.7 Expression of Cytochrome Genes under Settled Conditions

Gene	Name	Product	YB:WHT (Std.Dev.)
BPSL1261		cytochrome c-like protein	6.3 (0.5)
BPSL1256		cytochrome c	4.4 (0.1)
BPSL1260		cytochrome c oxidase subunit 1	4.2 (0.0)
BPSL0501	cydB	cytochrome d ubiquinol oxidase subunit II	4.0 (0.0)
BPSL0502	cydA	cytochrome d ubiquinol oxidase subunit I	3.9 (0.0)
BPSS0673		cytochrome c oxidase subunit III protein	3.5 (0.0)
BPSL1257		cytochrome c	3.2 (0.0)
BPSL1454		cytochrome C oxidase	3.1 (0.1)
BPSL0072		type-b cytochrome	2.9 (0.0)
BPSL1259		cytochrome c oxidase subunit II-like protein	2.5 (0.0)
BPSL0697		periplasmic cytochrome c protein	2.2 (0.0)
BPSL1100		cytochrome C -like protein	2.0 (0.0)
BPSL1099		cytochrome C -like protein	1.7 (0.0)
BPSL3271		cytochrome c-551	1.3 (0.0)
BPSS0977		cytochrome c subunit II	1.3 (0.04)
BPSL0453		cytochrome c oxidase	1.2 (0.0)
BPSL0458		cytochrome c oxidase subunit III	1.2 (0.0)
BPSL0696		periplasmic cytochrome c containing protein	1.2 (0.0)
BPSS0086		cytochrome C oxidase-related protein	1.2 (0.0)
BPSL0722		cytochrome c oxidase subunit I	1.1 (0.1)
BPSS1729		cytochrome C	1.1 (0.00)
BPSL3122	petB	cytochrome b	0.99 (0.00)
BPSL3181		cytochrome C	0.99 (0.00)
BPSL3121	petC	cytochrome c1	0.97 (0.00)
BPSL3354		cytochrome	0.96 (0.01)
BPSL0454	ctaD	cytochrome c oxidase polypeptide I	0.91 (0.00)
BPSL3123	petA	ubiquinol-cytochrome c reductase iron-sulfur subunit	0.89 (0.00)
BPSL0968		cytochrome c protein	0.88 (0.01)
BPSS0235		cytochrome oxidase subunit I	0.78 (0.01)
BPSS0234		cytochrome oxidase subunit II	0.72 (0.01)
BPSS1377		ubiquinol cytochrome c cyanide insensitive terminal oxidase	0.53 (0.04)
BPSL0723		cytochrome c oxidase polypeptide II	- (-)

RNA was collected in triplicate from bacteria grown in the *in vitro* stomach model under hypoxia (2.0% O_2) at 24 hours of growth and analyzed by RNAseq**.** No values "-(-)" indicate insufficient YB or WHT reads to perform a valid ratio calculation (i.e. divide by zero). Data reported is the RPKM linear-normalized ratio of YB to WHT reads with the standard deviation in parentheses.

APPENDIX C

OLIGONUCLEOTIDES

Oligonucleotides were purchased from Integrated DNA Technologies (IDT) (Coralville, IA) and received as lyophilized, pure nucleotides. Lyophilized nucleotides were suspended in certified sterile, nuclease-free water at 100 mM then frozen at -80°C. For use, each oligonucleotide solution was thawed and diluted 1:10 in certified sterile, nuclease-free water for a 10x solution of reagent. Oligonucleotide sequences and names are listed in table C.1.

Table C.1 Oligonucleotides Used in This Study

Primer Name	Nucleotide Sequence
Probe Bpm427	5’-CCACTCCGGGTATTAGCCAGA-3’
Probe Bpm95	5’-CGCCCAACTCTCATCGGG-3’
Probe Eub338	5’- GCTGCCTCCCGTAGGAGT-3’
Probe Non338	5’- ACTCCTACGGGAGGCAGC-3’
Kan_F2-BsrGI	5’-TGTACACGTGATACGCCTATTTTTATAGG-3’
Kan_R3-AclI	5’- AACGTTATCGTTTCCTCCTGTGCAGC-3’
BPSL1887OEX_F1-EcoRI	5’-AGAATTCGATGAGAAACACGAACGC-3’
BPSL1887OEX_R1-HindIII	5’-CAAGCTTGCTTTCATTCGCTTTCC-3’
BPSS1519_USF1-ApaI	5’- GCATAGGGCCCCCAGGGCACAGTAG-3’
BPSS1519_USR1-NheI	5’-CCAAGCTAGCGCCGGATGCGCCGGTAC-3’
BPSS1519_DSF3-BamHI	5’-CTTGGATCCGCATTCCGCCCAGTATTGC-3’
BPSS1519_DSR2-XbaI	5’-GTATCTAGACTGGAGCGAGCCGTGTTTC-3’
BPSL1887KOF1	5’-TCGGCGGCGGGACATTCAG-3’
BPSL1887KOR2	5’-TCATTCGCTTTCCCGCGCCTCAGGTTCGATTGCGTTCGTGTTTCTCAT-3’
BPSL1887KOF3	5’-ATGAGAAACACGAACGCAATCGAACCTGAGGCGCGGGAAAGC-3’
BPSL1887 KOR4	5’-CCGCTCGCTTTTCTGCTCCC-3’
pMrT7F	5’-GTATACCGTCAGACCCCGTAGAAAAG-3’
pMrT7R	5’-GTCGACTGGGACGCTGATACAGTGTC-3’
pMrT7IntF	5’CAGTGGCGATAAGTCGTG-3’
pMrT7IntR	5’-CTGCTCACGCAATGGGAC-3’

Primer Name	Nucleotide Sequence
pTBurk1ARB1	5’-GATATTGCTGAAGAGCTTGGCG-3’
pTBurk1 ARB2	5’-GGCCACGCGTCGACTAGTACNNNNNNNNNNGATAT-3’
pTBurk1 ARB3	5’-GGCCACGCGTCGACTAGGTACNNNNNNNNNNACGCC-3’
pTBurk1 ARB4	5’-GGCCACGCGTCGACTAGTACNNNNNNNNNNAGAG-3’
pTBurk1 ARB5	5’-CCTTCTTGACGAGTTCTTCTGAGC-3’
pTBurk1 ARB6	5’-GGCCACGCGTCGACTAGTAC-3’
pTBurk1 ARBseq	5’-GCTCTTGAAGGGAACTATGTTGC-3’
Read 1 Adapter	5'- AATGATACGGCGACCACCGAGATC TACACTCTTTCCCTACACGACGCTCTTCCGATC* T-3'
Read 2 Adapter	5'- P- G*ATCGG AAGAGCACACGTCTGAACTCCAGTCA-3'
PE PCR 1.0	5'-AATGATACGGCGACCACCGAGATCTACACTCTTTCCCTACACGACGCTCTTCCGATCT-3'
HITS PCR 2.0-Indexx1	5'-CAAGCAGAAGACGGCATACGAGAT**ATCACG**CGGTCTCGGCATTCCTGCTGAACCGCTCTTCCGATCT AGACCGGGGACTTATCAGCCAACC-3’
HITS PCR 2.0-Indexx2	5'-CAAGCAGAAGACGGCATACGAGAT**CGATAT**CGGTCTCGGCATTCCTGCTGAACCGCTCTTCCGATCT AGACCGGGGACTTATCAGCCAACC-3’
HITS PCR 2.0-Indexx3	5'-CAAGCAGAAGACGGCATACGAGAT**TTAGGC**CGGTCTCGGCATTCCTGCTGAACCGCTCTTCCGATCT AGACCGGGGACTTATCAGCCAACC-3’
HITS PCR 2.0-Indexx4	5'-CAAGCAGAAGACGGCATACGAGAT**TGACCA**CGGTCTCGGCATTCCTGCTGAACCGCTCTTCCGATCT AGACCGGGGACTTATCAGCCAACC-3’
HITS PCR 2.0-Indexx5	5'-CAAGCAGAAGACGGCATACGAGAT**ACAGTG**CGGTCTCGGCATTCCTGCTGAACCGCTCTTCCGATCT AGACCGGGGACTTATCAGCCAACC-3’

* Indicates phosphorothioate bond. Nucleotide sequences in **bold** are index sequences. “N” indicates random nucleotide